Western Graduate&PostdoctoralStudies

Western University
Scholarship@Western

Electronic Thesis and Dissertation Repository

7-17-2013 12:00 AM

Effects of niacin in human vascular endothelial cells during lipotoxicity

Jennifer M. Hughes-Large, *The University of Western Ontario*

Supervisor: Dr. Nica Borradaile, *The University of Western Ontario*

A thesis submitted in partial fulfillment of the requirements for the Master of Science degree in Physiology

© Jennifer M. Hughes-Large 2013

Follow this and additional works at: https://ir.lib.uwo.ca/etd

 Part of the Cardiovascular Diseases Commons

Recommended Citation

Hughes-Large, Jennifer M., "Effects of niacin in human vascular endothelial cells during lipotoxicity" (2013). *Electronic Thesis and Dissertation Repository*. 1350.
https://ir.lib.uwo.ca/etd/1350

This Dissertation/Thesis is brought to you for free and open access by Scholarship@Western. It has been accepted for inclusion in Electronic Thesis and Dissertation Repository by an authorized administrator of Scholarship@Western. For more information, please contact wlswadmin@uwo.ca.

EFFECTS OF NIACIN IN HUMAN VASCULAR ENDOTHELIAL CELLS DURING LIPOTOXICITY

(Thesis format: Monograph)

by

Jennifer Hughes-Large

Graduate Program in Physiology

A thesis submitted in partial fulfillment
of the requirements for the degree of
Master of Science

The School of Graduate and Postdoctoral Studies
The University of Western Ontario
London, Ontario, Canada

© Jennifer Hughes-Large 2013

Abstract

Nicotinic acid (NA) can improve vascular function and regeneration independent of correcting dyslipidemia. NA, as a potential biosynthetic precursor for NAD^+, may elicit these vascular benefits through SIRT-mediated NAD^+-dependent responses. We hypothesized that NA improves endothelial cell function under lipotoxic conditions through NAD^+-dependent pathways. Angiogenic function in excess palmitate was assessed by tube formation assay following treatment of human microvascular endothelial cells (HMVEC) with NA or nicotinamide mononucleotide (NMN; a direct NAD^+ precursor). Both NA and NMN improved HMVEC angiogenic function during palmitate overload. Only NMN increased cellular NAD^+ and SIRT1 activity, while both compounds activated SIRT2/3. By microarray, NA did not induce expression of known SIRT-regulated genes. However, we found that HMVEC robustly express NA receptor GRP109A, whose specific activation recapitulated NA-induced improvements in angiogenic function. We conclude that NA improves in vitro HMVEC angiogenic function under lipotoxic conditions, perhaps through GPR109A, but likely unrelated to NAD^+ biosynthesis and SIRT activation.

Keywords

Nicotinic acid, nicotinamide mononucleotide, endothelial cells, lipotoxicity, obesity, angiogenesis, sirtuins, GPR109A

Co-Authorship Statement

Three replicates of the HMVEC tube formation assay in Figure 3.1, as well as the growth rate assays in Figures 3.3F and 3.4F were performed by Debra Robson and Pak Chan.

The 2 mM AICAR treatment for the palmitate oxidation assay in Figure 3.8C was performed by Dominic Pang.

The microarray GeneChip analysis in Table 3.1 was performed by Dr. David Carter and the London Regional Genomics Centre.

Acknowledgments

Firstly, I would like to sincerely thank my supervisor, Dr. Nica Borradaile. Nica, I am so appreciative that you gave me the opportunity to be part of your lab, and for all your patience, understanding, support and guidance along the way. I really cannot thank you enough for everything you've done for me! You have been a wonderful mentor and are truly a credit to Western and to this department!

Thank you to the past and present members of the Borradaile lab, Alex Stoianov, Dominic Pang, and Alex Hetherington, and to the members of the Urquhart lab for the lab camaraderie. You all definitely made lab work a more enjoyable experience! To Alex S in particular, thank you for making me feel welcome when I joined the lab; it has been great getting to know you! Thank you also to our lab technicians Debbie Robson and Cindy Sawyez for your help and guidance with experiments.

Thank you to my advisory committee members, Drs. John Di Guglielmo, Tim Regnault, and Lina Dagnino, for your suggestions and guidance as I progressed through this project.

Thank you to Dr. Kristin Chadwick for your guidance with flow cytometry, and to the members of the Pickering, Bhattacharya, and Di Guglielmo laboratories for generously allowing me to use your microscopes.

Finally, I would like to thank my family and friends who were supportive of me throughout my graduate work. Your encouragement and understanding have been so helpful in my pursuit of this degree. I'm so lucky to have people like you in my life!

Table of Contents

List of Tables

List of Figures

Abbreviations and Symbols

ABC	ATP-binding cassette
AC	Adenylyl cyclase
ADP	Adenosine diphosphate
AICAR	5-aminoimidazole-4-carboxamide-1-β-4-ribofuranoside
AMPK	5' adenosine monophosphate-activated protein kinase
ANOVA	Analysis of variance
Apo	Apolipoprotein
ATP	Adenosine triphosphate
Bax	Bcl-2-associated X protein
BCA	Bicinchoninic acid
BMI	Body mass index
BSA	Bovine serum albumin
cDNA	Complementary DNA
CHO	Chinese hamster ovary
CYP4Z1	Cytochrome P450, family 4, subfamily Z, polypeptide 1
DAPI	4',6-Diamidino-2-phenylindole
DGAT	Diacylglycerol acyltransferase
DMSO	Dimethyl sulfoxide
DNA	Deoxyribonucleic acid

EC	Endothelial cell
EDTA	Ethylenediaminetetraacetic acid
EFCAB4B	EF-Hand Calcium Binding Domain 4B
eNOS	Endothelial nitric oxide synthase
ER	Endoplasmic reticulum
Eto	Etomoxir
FOXO	Forkhead Box O
GAPDH	Glyceraldehyde 3-phosphate dehydrogenase
GO	Gene ontology
GPR109A	G-protein coupled receptor
H_2O_2	Hydrogen peroxide
HAEC	Human aortic endothelial cell
HCl	Hydrogen chloride
HDL	High density lipoprotein
HEK	Human embryonic kidney
HIFα	Hypoxia inducible factor-alpha
HMVEC	Human microvascular endothelial cell
HRP	Horseradish peroxidise
HUVEC	Human umbilical vein endothelial cell
LCAD	Long-chain acyl-CoA dehydrogenase

LDL	Low density lipoprotein
LSB	Laemmli sample buffer
LXR	Liver X receptors
MUFA	Monounsaturated fatty acids
NA	Nicotinic acid
NAD^+	Nicotinamide adenine dinucleotide [oxidized form]
NADH	Nicotinamide adenine dinucleotide [reduced form]
NADPH	Nicotinamide adenine dinucleotide phosphate [reduced form]
NAFLD	Non-alcoholic fatty liver disease
NAM	Nicotinamide
NAMN	Nicotinic acid mononuleotide
Nampt	Nicotinamide phosphoribosyltransferase
NaOH	Sodium hydroxide
NAP1L2	Nucleosome assembly protein 1 like 2
Napt	Nicotinic acid phosphoribosyltransferase
NEFA	Non-esterified fatty acids
NF-κB	Nuclear factor kappa-light-chain-enhancer of activated B cells
NMN	Nicotinamide mononucleotide
Nmnat	Nicotinamide/nicotinic acid mononucleotide adenylyltransferase
NO	Nitric oxide

NR	Nicotinamide riboside
Nrk	Nicotinamide riboside kinase
OA	Oleate
Opti-MEM	Opti-minimum essential medium
OR13C8	Olfactory receptor 13C8
PA	Palmitate
PAD	Peripheral artery disease
PAGE	Polyacrylamide gel electrophoresis
PBS	Phosphate-buffered saline
PGC-1α	Peroxisome proliferator-activated receptor-γ coactivator 1α
PI	Propidium iodide
PKA	Protein kinase A
PKC	Protein kinase C
Pnp	Purine nucleoside phosphorylase
PPARα	Peroxisome proliferator-activated receptor-α
PVDF	Polyvinylidene difluoride
qRT-PCR	Quantitative real-time polymerase chain reaction
rcf	Relative centrifugal force
RIPA	Radioimmunoprecipitation assay
RNA	Ribonucleic acid

ROS	Reactive oxygen species
RQ	Relative quantification
SCD1	Stearoyl CoA desaturase 1
SDS	Sodium dodecyl sulfate
SEM	Standard error of mean
SIGLEC5	Sialic acid-binding IgG-like lectin 5
SIRT	Sirtuin
SNORD13P1	Small Nucleolar RNA, C/D Box 13 Pseudogene 1
T2DM	Type 2 diabetes mellitus
TCA	Trichloroacetic acid
TG	Triglycerides
TGFβ	Transforming growth factor beta
TSA	Trichostatin A
VLDL	Very low density lipoprotein

Chapter 1

1 Introduction

1.1 Vascular Disease during Obesity and Metabolic Syndrome

The prevalence of obesity and its complications is increasing globally at an alarming rate. According to 2008 estimates by the World Health Organization, over 10% of adults worldwide are obese, and the rates of childhood obesity are also increasing dramatically (World Health Organization, 2013). Although obesity was once associated with affluence, it is now increasing in low- and middle-income countries as well (World Health Organization, 2013). The increase in obesity over the last half-century can be attributed to a gastronomic revolution in the Western world promoting the consumption of large portions of food with high fat and sugar content, combined with an increasingly sedentary lifestyle (Unger and Scherer, 2010).

Obesity is defined as the accumulation of abnormal or excessive adipose tissue which may cause impairments to health, and which develops due to an energy imbalance in calories consumed versus calories expended (World Health Organization, 2013). Quantitatively, a body mass index (BMI= weight [kg] / height^2 [m^2]) of >30 kg/m^2 is considered obese, although waist/ hip ratio is also used as a measure of abdominal obesity. Abdominal obesity is a risk factor for the development of metabolic syndrome. The current unified criteria for metabolic syndrome take into account definitions from several international organizations (Alberti et al., 2009). These criteria are abdominal obesity (increased waist circumference) plus two of the following characteristics: elevated plasma triglycerides (≥1.7 mmol/L), elevated fasting blood glucose (≥5.6 mmol/L), decreased high-density lipoprotein (HDL) cholesterol (<1.03 mmol/L), and elevated blood pressure (≥130/85) (Alberti et al., 2009).

Adipocytes are specialized cells which have evolved to store lipid as an energy source for use by non-adipocytes during starvation. Under normal physiological conditions, diet-derived plasma lipids are taken up by adipocytes and stored as triglycerides (TG), and are

later released by lipolysis for use by tissues during fasting (Unger and Scherer, 2010). In response to increased lipid availability, adipose tissue undergoes adipogenesis and adipocyte hypertrophy to maximize lipid storage capacity (Bays et al., 2008). Coincident with adipose expansion is the increased secretion of leptin by adipocytes, which is proportional to adipose mass and targets the hypothalamus to reduce food intake (Mattu and Randeva, 2013). Leptin also acts to reduce non-adipocyte lipid accumulation by activating fatty acid β-oxidation pathways (Unger and Scherer, 2010). However, the capacity of adipose tissue to expand in response to fatty acid uptake is limited.

Under conditions of caloric surplus, once the capacity of the adipose tissue to store excess lipid has been exceeded, adipocytes become dysfunctional and uncontrolled TG lipolysis ensues, releasing non-esterified fatty acids (NEFAs) into the bloodstream. The resulting chronic hyperlipidemia generates insulin resistance in the liver, restricting the ability of insulin to regulate hepatic production of very low density lipoproteins (VLDL)(Sparks et al., 2012). As a result, VLDL production and flux from the liver increases. Increased plasma concentrations of NEFAs and VLDL induce ectopic accumulation in tissues not metabolically programmed to store large amounts of excess lipid, including the pancreas, skeletal muscle, cardiac tissue, and the vasculature, causing tissue damage and generating a low-grade inflammatory state (Nikolopoulou and Kadoglou, 2012; Odegaard and Chawla, 2013). The development of metabolic syndrome is summarized in Figure 1.1.

Unfortunately, obesity and metabolic syndrome greatly increase the risk of premature mortality, as well as a broad range of chronic co-morbidities, representing a large-scale public health crisis. Obesity has been linked to an increased risk of many types of cancer (Vucenik and Stains, 2012), type 2 diabetes mellitus (T2DM) (Shao et al., 2013), liver disease (Masuoka and Chalasani, 2013), osteoarthritis (Zhuo et al., 2012), and reproductive issues (Lim et al., 2013; O'Reilly and Reynolds, 2013). However, some of the most widespread consequences of obesity are seen in its detriment to the vasculature. Vascular complications due to hyperlipidemia present in multiple vascular beds. Atherosclerotic plaque formation occurs in large- to medium-sized arteries (Talayero and Sacks, 2011). Plaques can occlude arteries, increasing blood pressure, and are also in

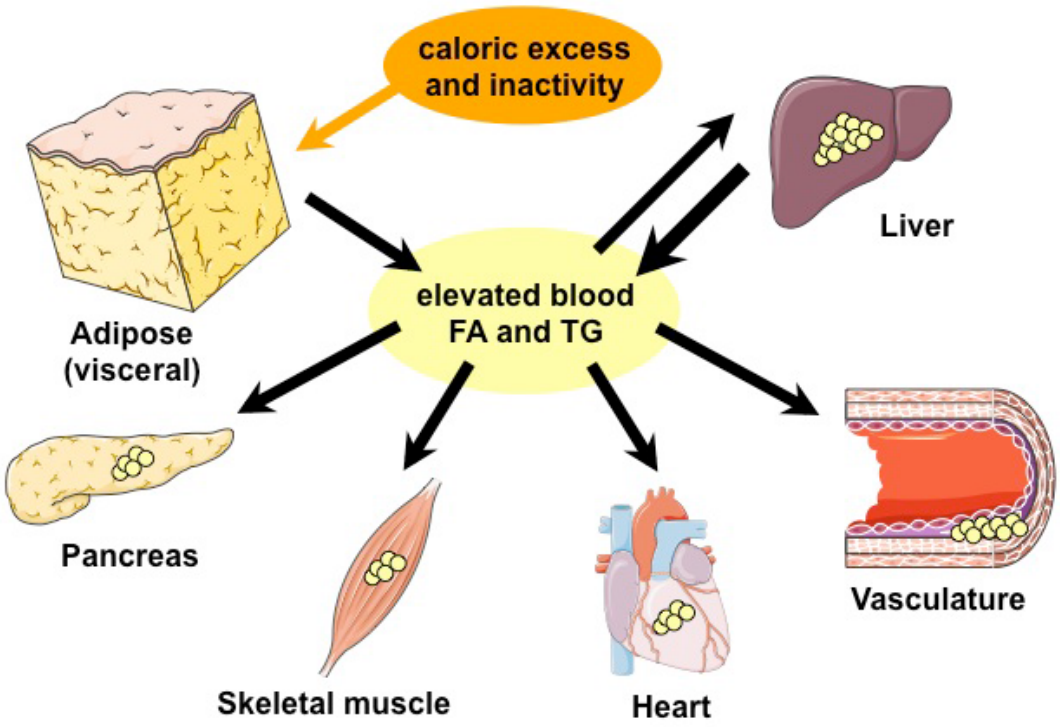

Figure 1.1. Organs affected during obesity and metabolic syndrome.

In the setting of caloric surplus coupled with a sedentary lifestyle, elevated circulating fatty acid levels eventually exceed the storage capacity of adipose tissue, resulting in the uncontrolled flux of non-esterified fatty acids (NEFAs) into the bloodstream and the development of a chronic hyperlipidemic state. Hyperlipidemia causes hepatic insulin resistance, which increases hepatic production and flux of very low density lipoprotein (VLDL) into the circulation. Increased plasma concentrations of NEFAs and VLDL result in ectopic lipid accumulation (yellow circles) in the pancreas, skeletal muscle, cardiac tissue, and the vasculature, causing tissue dysfunction. Adapted from Muoio and Newgard (2006).

danger of rupture, which can generate thromboemboli capable of causing a myocardial infarction (Manduteanu and Simionescu, 2012). Hyperlipidemia can also cause peripheral artery disease (PAD), a condition involving restricted blood flow to peripheral tissues and extremities. In 1-2% of cases, PAD progresses to critical limb ischemia, requiring amputation of the affected limb (Teodorescu et al., 2013). Similarly, hyperlipidemia is also a strong risk factor for chronic kidney disease. Especially with co-morbid hypertension and poor glycemic control, obesity has been linked to nephropathy due to glomerular dysfunction, which can progress to end-stage kidney disease and renal failure (Maric and Hall, 2011). Given the serious morbidity and mortality associated with vascular disease in obesity, therapeutic interventions to attenuate vascular damage warrant further study.

1.2 Endothelial Damage during Metabolic Disease

Endothelial cells (EC) serve many important physiological functions. Through balancing the production and secretion of vasodilators and vasoconstrictors, EC regulate vascular tone, ensuring appropriate perfusion of associated tissues. EC also regulate blood fluidity, secreting factors to decrease blood viscosity, or to initiate platelet aggregation and clotting following injury. The inflammatory process can also be modulated by EC through the production of cytokines and adhesion molecules to allow for homing and recruitment of immune cells (Widlansky et al., 2003). Furthermore, EC are responsible for regeneration and repair of vascular tissue following injury, as well as the maintenance of vascularization through angiogenesis. Considering these vital roles, EC dysfunction can be detrimental to surrounding tissues.

EC dysfunction is defined as a broad change in EC phenotype that may contribute the clinical development or expression of vascular disease (Levine et al., 1995). In particular, this condition is characterized by a decreased availability of the EC-produced vasodilator nitric oxide (NO), and increased activity of proatherogenic and vasoconstrictor factors (Campia et al., 2012). Endothelial dysfunction was first reported in association with obesity by Steinberg et al. (1996), as measured by blunted vasodilation in the legs of obese patients in response to infusion of a vasodilator. Endothelial dysfunction has since been established as a precursor to vascular disease, and a key process in the development

of vascular aspects of metabolic syndrome. In keeping with this, Bigornia et al. (2010) showed that endothelial function, measured as flow-mediated dilation of the brachial artery, was improved in obese patients who lost weight. EC functional improvement, however, was independent of weight loss and most strongly correlated with serum glucose levels, suggesting that EC dysfunction is mediated by metabolic abnormalities associated with obesity, and not directly with obesity itself. Conversely, the maintenance of proper endothelial function potently opposes the development of the atherosclerotic and thrombotic phenotypes associated with metabolic syndrome (Xu and Zou, 2009).

The development of EC dysfunction is a gradual process. When exposed to an insult, such as hyperlipidemia or hyperglycemia, EC will first modify their constitutive functions in an attempt to adapt to the altered microenvironment. If the insult persists, EC will undergo dysfunction, which will eventually lead to injury and cell apoptosis (Simionescu, 2007). Initial EC modifications in response to hyperlipidemia include increased trafficking of low density lipoprotein (LDL) and VLDL through the endothelium as a result of increased circulating cholesterol concentrations, and conversion of EC to a secretory phenotype. The shift to a secretory phenotype is accompanied by increased secretion of chemotactic factors and alterations in expression of adhesion molecules, resulting in monocyte recruitment and the development of a chronic inflammatory state (Simionescu, 2007).

Endothelial cells throughout the body are heterogeneous, resulting in different pathological responses to a given stimulus based on blood vessel type and associated tissue (Simionescu et al., 1975; Simionescu et al., 1976). In response to chronic hyperlipidemia, larger arteries develop atherosclerosis. Atherosclerotic plaques develop in the intima of vessel walls, initiated by endothelial functional changes. Plaques expand and become fibrotic through the accumulation of LDL cholesterol and the activities of infiltrating immune and smooth muscle cells. Plaques can eventually become unstable, leading to rupture and thrombotic vascular occlusion resulting in myocardial infarction or stroke (Manduteanu and Simionescu, 2012). Despite uniform exposure of the vascular tree to circulating insults, atherosclerotic plaques preferentially develop at sites

experiencing disturbed flow or altered shear stress, including vessel branch points, bifurcations and curvatures (VanderLaan et al., 2004).

The presentation of microvascular dysfunction in patients with PAD was identified several decades ago by Matsen et al. (1980), who observed decreased transcutaneous oxygen tension in patients' extremities. EC dysfunction in microvessels likely develops through mechanisms similar to those that occur in large vessel EC, but results in impaired blood flow and vasoreactivity rather than atherosclerotic plaque formation (Abularrage et al., 2005). Notably, EC dysfunction in the microvasculature is evident long before atherosclerotic symptoms develop, serving as an early marker of vascular disease (Verma et al., 2003). If left untreated, microvascular dysfunction can progress to critical limb ischemia and lead to the necessity for limb amputation.

1.3 Lipotoxicity in Endothelial Cells

Lipotoxicity is the process by which excess fatty acids and their metabolites influence membrane structure, intracellular signaling, and energy homeostasis within the cell, leading to cell dysfunction and death (Brookheart et al., 2009). In the setting of obesity and metabolic syndrome, endothelial cells are especially vulnerable to lipotoxicity because they are continuously and directly exposed to high concentrations of fatty acids. Moreover, studies in human umbilical vein EC (HUVEC) have indicated that EC predominantly generate ATP by aerobic glycolysis, and are therefore inefficient at metabolizing fatty acids through β-oxidation or esterification into triglycerides (TG) (Dagher et al., 1999; Dagher et al., 2001; Helies-Toussaint et al., 2006). This inability of EC to process large quantities of lipid through oxidative or TG storage pathways results in the channeling of excess lipid toward pathways that lead to metabolic stress and cell dysfunction. Pathways contributing to lipotoxicity in EC are summarized in Figure 1.2, and are discussed in detail below.

It is well established that unsaturated fatty acids, but not saturated fatty acids, are well tolerated by cells, and may even protect against damage induced by saturated fatty acids. In human EC, and several other cell types, saturated fatty acids such as palmitate induce apoptosis, whereas unsaturated fatty acids do not (Ciapaite et al., 2007; Staiger et al.,

2006). These results have been recapitulated in vivo, where animals fed a high saturated fat, Western-style diet develop symptoms of metabolic disorder, including atherosclerosis and peripheral vascular disease (Breslow, 1996; Nishina et al., 1990; Schreyer et al., 1998; Wang et al., 2009). Clinically, intake of saturated fatty acids increases plasma LDL and decreases HDL cholesterol concentrations, resulting in a proatherogenic environment (Kris-Etherton and Yu, 1997). By contrast, monounsaturated or polyunsaturated fatty acids, such as those found in plant and fish oils, are either neutral or antiatherogenic (Carrero and Grimble, 2006; Vecka et al., 2012).

Saturated FA can lead to ceramide production in the mitochondria via the actions of serine palmitoyltransferase and ceramide synthase. Ceramides are intracellular lipid second messengers involved in initiating apoptosis in response to injurious stimuli (Claria, 2006). Treatment of HUVEC with palmitate has been shown to cause de novo synthesis of ceramide and inhibit endothelial nitric oxide synthase (eNOS), reducing NO production by EC and generating a dysfunctional phenotype (Xiao-Yun et al., 2009). Mugabo et al. (2011) provided further evidence for the role of ceramide in palmitate toxicity, as treatment of human aortic EC (HAEC) with ceramide mimicked the intracellular signaling events elicited by treatment with palmitate, including decreased AMPK activation, and increased protein kinase C (PKC) and NADPH activation, leading to reactive oxygen species (ROS) production upstream of eNOS inhibition. Similarly, ceramide has been shown to impair microvascular EC function. Treatment of human microvascular EC (HMVEC) with ceramide analogues decreased cell proliferation and migration and induced apoptosis, while ceramide-treated mice showed reduced tumour angiogenesis (Bocci et al., 2012). Therefore, ceramide synthesis from palmitate may be one mechanism that contributes to EC dysfunction during lipid overload.

Based on in vivo data, a key mechanism in the development of EC lipotoxicity appears to be increased ROS production (Chinen et al., 2007). However, ceramide synthesis does not appear to be the only pathway that elicits oxidative stress during palmitate overload (Listenberger et al., 2001). PKC-dependent ROS generation in EC can also be elicited by palmitate induced diacylglycerol production (Inoguchi et al., 2000). Moreover, data from rat cardiomyocytes suggests that palmitate is incorporated into phospholipids in the inner

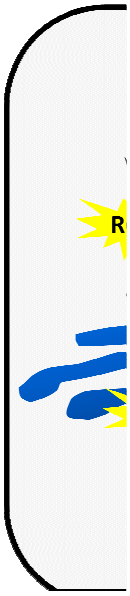

Figure 1.2. Lipotoxicity

Endothelial cells are not
Therefore, exposure to e
or catabolise lipid. As a p
lipid droplets, resulting i
can be generated throug
mitochondrial ROS throu
palmitate is rapidly in
membrane integrity and
of ER stress. Oxidative a
of apoptosis. However, in
survival during palmitate

mitochondrial membrane, leading to ROS production and subsequent apoptosis (Ostrander et al., 2001). Although it has not been confirmed in EC, data from skeletal muscle indicate that incomplete mitochondrial β-oxidation of palmitate contributes to ROS production and insulin resistance (Koves et al., 2008). Considering the role of the mitochondria in energy regulation via intracellular NAD^+/NADH ratios, therapeutic targeting of dysfunction in mitochondrial NAD^+ metabolism, which can also elicit ROS generation (Adam-Vizi and Chinopoulos, 2006), may be a beneficial intervention in the treatment of vascular complications of metabolic disease.

Based on work in other cell types (Brookheart et al., 2009), direct initiation of endoplasmic reticulum (ER) stress is another mechanism by which palmitate may induce EC dysfunction. Palmitate treatment of CHO cells results in the incorporation of this fatty acid into ER membrane phospholipids, leading to dramatic disruption in membrane integrity and initiation of apoptosis (Borradaile et al., 2006). Increasing β-oxidation can reduce palmitate incorporation into ER phospholipids and attenuate the ER stress response. Recent work by Lu et al. (2013) confirms that ER stress may contribute to EC lipotoxicity in vivo.

Although accumulation of lipid in non-adipose tissues is a characteristic of lipotoxicity (Brookheart et al., 2009), increasing the capacity of cells to process lipid through normal, non-pathological, metabolic pathways, including TG synthesis and β-oxidation, can protect against lipotoxicity. Promoting TG synthesis and storage during palmitate overload via induction of stearoyl-CoA desaturase 1 (SCD1) and diacylglycerol acyltransferase (DGAT) has been shown to protect cells, including human primary EC, from lipotoxicity (Listenberger et al., 2003; Peter et al., 2008). Similarly, enhancing mitochondrial β-oxidation via 5-aminoimidazole-4-carboxamide-1-β-4-ribofuranoside (AICAR)-mediated activation of AMPK protects EC from palmitate induced cell dysfunction (Dagher et al., 2001; Kim et al., 2008).

1.4 Regulation of Metabolism and Endothelial Cell Function by Sirtuins

1.4.1 Sirtuins

Mammalian silent information regulators, or sirtuins, are a seven-member family of energy-sensing proteins (SIRT1-7), all of which are expressed in human vascular EC (Potente et al., 2007). Sirtuins are NAD^+-dependent protein deacetylases and/or *O*-ADP-ribosyltransferases that regulate gene expression by deacetylating lysine residues of histones, transcription factors, and coregulators (Blander and Guarente, 2004; Michan and Sinclair, 2007; Yamamoto et al., 2007). Sirtuins also have the ability to directly modulate the activity of enzymes and structural proteins independent of their influence on transcriptional regulation, contributing to the maintenance of whole-body metabolic homeostasis.

As histone acetylation is strongly associated with gene activation, the deacetylase activity of sirtuins is typically related to gene silencing (Jenuwein and Allis, 2001). Relevant to this thesis, SIRT1-3 all possess a conserved deacetylase domain, although only SIRT1 and SIRT2 have biologically significant histone deacetylation functions (Michan and Sinclair, 2007; Scher et al., 2007; Yamamoto et al., 2007). The ADP-ribosylation activities of SIRT1-3 are limited.

Subcellular localization of sirtuins influences their actions (Scher et al., 2007; Tanno et al., 2007). SIRT1 and SIRT2 can be nuclear or cytoplasmic proteins, whereas SIRT3 is generally localized to the mitochondria (Finkel et al., 2009; Jing et al., 2007; Onyango et al., 2002; Schwer et al., 2002). In keeping with their predominant subcellular locations, SIRT1 has a strong role in regulating chromatin structure and gene expression, while SIRT3 causes global deacetylation of mitochondrial proteins (Lombard et al., 2007). SIRT2 is predominantly cytoplasmic, but has the ability to influence nuclear gene expression by deacetylating transcription factors en route to the nucleus, and can alter chromatin structure following nuclear envelope breakdown during mitosis (Jing et al., 2007; Vaquero et al., 2006).

1.4.2 Sirtuin Regulation of Cell Metabolism

SIR2, the yeast ortholog of mammalian SIRT1, was the originally discovered as a factor which extended organismal replicative lifespan (Kaeberlein et al., 1999), although this concept has since been called into question (Burnett et al., 2011). In multicellular organisms, however, lifespan and metabolism have been intricately linked, and sirtuin activation, in particular SIRT1, has been shown to regulate metabolism in multiple tissues (Satoh et al., 2011; Schwer and Verdin, 2008).

During nutrient deprivation in the liver, SIRT1 activates peroxisome proliferator-activated receptor-γ coactivator 1α (PGC-1α) to upregulate gluconeogenesis and inhibit glycogenolysis (Rodgers et al., 2005). Furthermore, in skeletal muscle, liver and brown adipose tissue, SIRT1-mediated deacetlyation of PGC-1α promotes the association between SIRT1 and peroxisome proliferator-activated receptor-α (PPARα), leading to upregulation fatty acid oxidation (Baur et al., 2006; Gerhart-Hines et al., 2007; Lagouge et al., 2006; Purushotham et al., 2009). SIRT3 has also been reported to activate PGC-1α in brown adipose tissue, and consequently improve mitochondrial function and adaptive thermogenesis (Shi et al., 2005).

SIRT1 has been shown to activate nuclear liver X receptors (LXR) both directly, by deacetlyation, and indirectly, through activation of PGC-1α (Li et al., 2007; Rodgers and Puigserver, 2007). While contradictory studies have emerged regarding the effects of LXR activation on cholesterol transport and homeostasis, SIRT-mediated induction of SCD1 has been linked to intermediary LXR activation (Bordone et al., 2007; Chu et al., 2006; Li et al., 2007; Ramsey et al., 2008). SCD1 is the rate-limiting enzyme in triglyceride synthesis from palmitate, catalyzing the Δ9-*cis* desaturation of saturated fatty acyl-CoAs to produce monounsaturated fatty acids (MUFAs). Palmitoleate, the palmitate-derived MUFA, is an excellent substrate for triglyceride synthesis and storage in lipid droplets, and is easily channeled away from lipotoxic pathways (Listenberger et al., 2003). In primary human arterial endothelial cells, treatment with TO-901317, an LXR activator, increases SCD1 mRNA and protein expression, resulting in increased triglyceride synthesis from palmitate and decreased palmitate-induced apoptosis (Peter et al., 2008).

SIRT1 is by far the most extensively studied of the sirtuin family with regards to metabolism, however some evidence has emerged linking SIRT2 and SIRT3 to metabolic disease. As a predominantly cytoplasmic protein, SIRT2 can alter the phosphorylation state of Forkhead Box O1 (FOXO1), resulting in FOXO1 activation and subsequent inhibition of adipogenesis (Jing et al., 2007). In the context of metabolic disease, the prevention of adipocyte differentiation would be detrimental to safe sequestering of excess circulating lipid. The link between SIRT3 and metabolic disease is better studied than SIRT2. SIRT3 regulates mitochondrial fatty acid oxidation via deacetylation of long-chain acyl-CoA dehydrogenase (LCAD) in mouse livers during fasting (Hirschey et al., 2010). Furthermore, Hirschey et al. (2011) demonstrated that ablated SIRT3 expression accelerates the development of metabolic syndrome in mice fed a high fat diet, and identified a single nucleotide polymorphism in human SIRT3 that may be associated with the development of metabolic syndrome.

1.4.3 Sirtuin Regulation of Cell Stress

SIRT1 has been shown to reduce oxidative stress by several mechanisms. For example, SIRT1 overexpression in mice has been shown to decrease high fat diet-induced oxidative stress by inhibition of NF-κB, resulting in reduced hepatic inflammation, glucose intolerance, and NAFLD (Pfluger et al., 2008). In EC, hydrogen peroxide-induced oxidative stress in HUVEC is abrogated by overexpression of SIRT1 through regulation of p53, endothelial nitric oxide synthase (eNOS) and plasminogen activator inhibitor-1 (PAI-1), enzymes which have roles in endothelial dysfunction (Ota et al., 2007). Glucose overload in HAEC increases ROS generation. However, increased SIRT1 activity, induced by modest overexpression of the NAD^{+-} regenerating enzyme, Nampt, decreases cellular ROS accumulation, in part by increasing aerobic glycolysis (Borradaile and Pickering, 2009b). This shift in glucose metabolism may be mediated by SIRT1 suppression of p53 (Bensaad and Vousden, 2007) or of FOXO1 (Borradaile and Pickering, 2009b), which would release the inhibitory influences of these factors on glycolytic metabolism. SIRT3 and SIRT4 have also been implicated in the protection of cells from genotoxic stress and apoptosis during nutrient deprivation - effects which are also dependent on Nampt activity (Yang et al., 2007). Furthermore, SIRT3 has been

implicated in reduced ROS generation through its interactions with mitochondrial proteins (Lombard et al., 2007).

In addition to indirectly reducing apoptosis by reducing oxidative stress, SIRT1 has the ability to directly inhibit apoptosis through several pathways. SIRT1 deacetylates and inhibits FOXO3 and FOXO4, thereby inhibiting FOXO-dependent apoptosis, and increasing cellular resistance to oxidative stress (Brunet et al., 2004; Motta et al., 2004). SIRT1 also deacetylates tumour suppressor p53, inhibiting p53-mediated apoptosis in response to oxidative stress and DNA damage (Cheng et al., 2003; Luo et al., 2001; Vaziri et al., 2001). As demonstrated in HEK-293 cells, SIRT1 inhibits the pro-apoptotic tumour suppressor p73, as well as preventing Bax-dependent apoptosis via deacetylation of Ku70 (Cohen et al., 2004; Dai et al., 2007). Pro-apoptotic transcription factor E2F1 activates SIRT1 transcription, which in turn represses E2F1-driven apoptosis in cancer cell lines U20S and H2199 (Wang et al., 2006). Finally, TGFβ-dependent apoptosis is repressed by SIRT1 through its deactylation of SMAD7 (Kume et al., 2007).

1.4.4 Sirtuin Regulation of Angiogenesis

Sirtuin interactions with Forkhead Box O (FOXO) transcription factors not only have implications for EC stress and survival, but also for angiogenesis. SIRT1-mediated deacetylation of FOXO1 in endothelial cells represses its anti-angiogenic function, thereby promoting vascular growth (Potente et al., 2007). Conflicting reports have emerged regarding the role of SIRT2 in angiogenesis. Bonezzi et al. (2012) found that overexpression of SIRT2 in HUVEC increased cell migration, an important component of angiogenesis. Conversely, Kim et al. (2013) observed that overexpression of SIRT2 in HUVECs decreased lumen area during tube formation in 3D collagen matrices. SIRT3 activity has not yet been linked directly to angiogenesis.

1.5 NAD^+ Biosynthesis and Regulation of SIRT Activity by NAD^+

Nicotinamide adenine dinucleotide, or NAD^+, plays a critical role in energy metabolism in eukaryotic cells. Acting as an acceptor of hydride equivalents during glycolysis and the mitochondrial citric acid cycle, NAD^+ is reduced to NADH. NADH can then be oxidized

to NAD^+, and the freed protons and electrons used to drive ATP generation via the electron transport chain. Intracellular NAD^+ levels therefore fluctuate with its synthesis and consumption, and reflect the nutritional status of an organism (Guarente, 2006; Houtkooper et al., 2010). In particular, NAD^+ levels have been reported to increase during metabolic stress, initiated by prolonged fasting or caloric restriction, and these alterations are closely related to sirtuin activation (Canto et al., 2009; Nisoli et al., 2005).

Due to their dependency on NAD^+, the enzymatic activities of sirtuins are regulated by NAD^+ availability (Imai et al., 2000; Landry et al., 2000b; Smith et al., 2000). In order for the deacetylase reaction to occur, both the acetylated lysine substrate and one molecule of NAD^+ must bind in the catalytic cleft of the sirtuin enzyme (Borra et al., 2005). Thus, NAD^+ content within cell is a main determinant of sirtuin activation.

In addition to the de novo synthesis pathway from tryptophan, NAD^+ is synthesized within the cell through a recycling (salvage) pathway, which is presented schematically in Figure 1.3. The byproducts of sirtuin-mediated deacetylation are 2´-O-acetyl-ADP-ribose and nicotinamide (NAM) (Tanner et al., 2000). NAM inhibits SIRT1 activity (Avalos et al., 2005; Landry et al., 2000a), and is recycled back to NAD^+ via the major salvage pathway. NAM is converted into nicotinamide mononucleotide (NMN) by nicotinamide phosphoribosyltransferase (Nampt), the rate limiting enzyme in the NAD^+ salvage pathway. Overexpression of Nampt leads to increased intracellular NAD^+ and SIRT1 activation in mouse fibroblast cell lines, human vascular smooth muscle cells and HAEC (Borradaile and Pickering, 2009b; Revollo et al., 2004; van der Veer et al., 2007; van der Veer et al., 2005). The final enzyme in the recycling pathway is nicotinamide/nicotinic acid mononucleotide adenylyltransferase (Nmnat), which converts NMN to NAD^+.

Two other pathways exist that are peripheral to the main salvage pathway (Figure 1.3). The substrates for these pathways are nicotinamide riboside (NR) and nicotinic acid (NA), respectively. NR, present as a nutrient in cow's milk, can be derived from the diet (Bieganowski and Brenner, 2004). NR can be converted into either NMN, via activation of nicotinamide riboside kinase (Nrk), or NAM, via catalysis by purine nucleoside

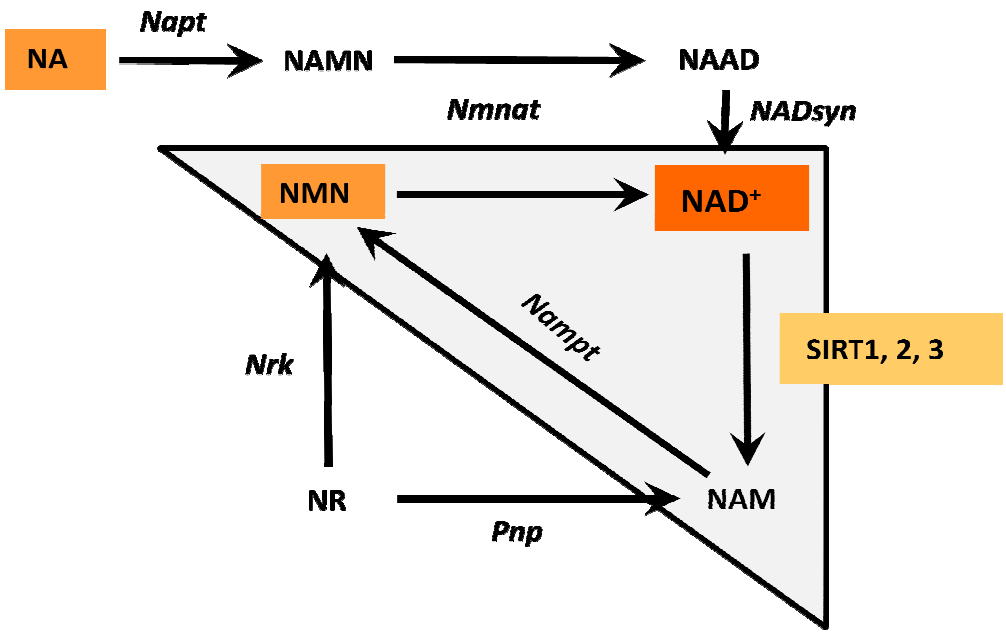

Figure 1.3. Mammalian NAD+ biosynthesis system.

The endogenous NAD^+ salvage pathway (outlined by the triangle) is catalyzed by the rate-limiting conversion of nicotinamide (NAM) to NMN by Nampt. The NAD^+ -dependent sirtuins 1, 2 and 3 generate NAM from NAD^+ as a by-product of protein deacetylase and ADP-ribosyltransferase reactions. NAM exhibits product inhibition over sirtuin activity. Nicotinamide riboside (NR) can generate either NMN or NAM. NAD^+ is also generated from exogenous NA via production of two intermediates. NAMN- nicotinic acid mononucleotide. Napt- nicotinic acid phosphoribosyltransferase. NAAD- nicotinic acid adenine dinucleotide. NADsyn- NAD^+ synthase. Pnp- purine nucleoside phosphorylase. Nrk- nicotinamide riboside kinase. Adapted from Borradaile and Pickering (2009a).

phosphorylase (Pnp) (Belenky et al., 2007). While NR catalysis by either Nrk or Pnp can lead to increased intracellular NAD^+ and SIRT1 and 3 activation in yeast and mammalian models (Belenky et al., 2007; Canto et al., 2012), inhibition of SIRT1 by NAM may limit the therapeutic applications of NR (Landry et al., 2000a). The second peripheral pathway, the Preiss-Handler pathway, utilizes NA as a precursor for NAD^+ synthesis. NA is converted into nicotinic acid mononuleotide (NAMN) by nicotinic acid phosphoribosyltransferase (Napt). Like NMN, NAMN is a substrate for Nmnat, which catalyzes the conversion of NAMN to nicotinic acid adenine dinucleotide (NAAD). NAAD can then be amidated into NAD^+ by NAD^+ synthase (Preiss and Handler, 1958a; Preiss and Handler, 1958b).

Nmnat, the adenylation enzyme with dual specificity to NMN and NAMN, has three isoforms in humans. Nmnat-1 is localized to the nucleus, whereas Nmnat-2 is found in the Golgi, and Nmnat-3 is mitochondrial (Berger et al., 2005; Schweiger et al., 2001). The distribution of these enzymes, which are required for all pathways of NAD^+ biosynthesis, results in stable NAD^+ stores within different subcellular compartments (Di Lisa and Ziegler, 2001).

1.6 Precursors of NAD^+ Biosynthesis

1.6.1 Nicotinic Acid

Nicotinic acid (NA) is one of the oldest lipid-lowering drugs, whose ability to lower serum cholesterol in humans was first documented in 1955 (Altschul et al., 1955). Since its discovery, pharmacological doses of NA have been shown to provide multiple clinical benefits in the setting of metabolic disease, including a reduction of atherogenic lipid species, and increased antiatherogenic high-density lipoprotein fractions. In particular, NA treatment reduces plasma VLDL and LDL cholesterol concentrations, while increasing HDL cholesterol, resulting in improved lipid profiles in dyslipidemic patients (Villines et al., 2012). Clinical use of NA is often hindered by its adverse cutaneous flushing effect, which is not harmful, but limits patient compliance.

As described in section 1.5, mammalian cells have the ability to use NA as a precursor for NAD^+ synthesis through the Preiss-Handler pathway. High-dose dietary niacin

supplementation for a two-week period caused increases in NAD^+ content in rat liver, kidneys, heart and blood plasma (Jackson et al., 1995). At a cellular level, NA has also been shown to elevate NAD^+ levels, increasing intracellular NAD^+ concentrations in the human kidney epithelial cell line, HEK293 cells, after incubation with as little as 1 μM NA (Hara et al., 2007). This augmentation, and the resulting protection from H_2O_2-induced oxidative stress, was dependent on Nampt enzymatic activity. Furthermore, Nampt-dependent increases in total cellular NAD^+ content have increased activation of SIRT1 in mouse fibroblasts (Revollo et al., 2004), implying that NA supplementation has the capacity to activate sirtuins and thereby confer protection from stress to mammalian cells. However, the influence of exogenous NA supplementation on NAD^+ metabolism and subsequent cellular function in EC has not been studied.

NA may elicit some of its effects through a cell surface receptor. GPR109A, a high-affinity NA seven-transmembrane G-protein coupled receptor was first identified in human tissue by Wise et al. (2003). GPR109A, which is endogenously activated by hydroxycarboxylic acids, couples to G_i-type G-proteins, typically resulting in inhibition of adenylyl cyclase (Ahmed et al., 2009). Since its initial discovery, GPR109A has been found to be expressed by several human tissues. With robust expression in adipocytes of both white and brown adipose (Tunaru et al., 2003), GPR109A is also expressed in several immune cell types (Schaub et al., 2001; Yousefi et al., 2000), intestinal epithelium (Thangaraju et al., 2009), and in epidermal Langerhans cells (Maciejewski-Lenoir et al., 2006). Notably, GPR109A activation in Langerhans cells is responsible for the cutaneous flushing side-effect elicited by NA via release of prostaglandins (Benyo et al., 2005). GPR109A expression has never been reported in vascular EC.

Several mechanisms have been proposed for the ability of NA to clinically improve lipid profiles. Carlson and Oro (1962) showed that, within minutes of dosing, NA lowered plasma fatty acids in humans, and observed an in vitro reduction in triglyceride lipolysis in adipose tissue (Carlson, 1963). The observed decrease in plasma fatty acids was followed by a rebound to higher-than-basal levels after 1 h, a time that could be extended by increased and subsequent doses of NA. Based on these and several studies over the following decades, the ability of NA to improve the lipid profile has been attributed to

GPR109A-mediated inhibition of TG lipolysis in adipose, thereby limiting the availability of fatty acids for TG synthesis and release in VLDL by the liver (Carlson, 1960; Carlson, 2005; Eaton et al., 1969; Tunaru et al., 2003). However, a recent study has challenged this hypothesis. Lauring et al. (2012) showed that while mice deficient in GPR109A did not exhibit the acute reduction in plasma fatty acids, they retained the benefits of reduced plasma LDL and TGs, and increased HDL following NA treatment. Furthermore, specific activation of GPR109A in dyslipidemic human subjects did not result in the lipid profile improvements seen with NA treatment despite affecting an acute drop in plasma fatty acids.

Other studies have also suggested GPR109A-independent mechanisms for lipid profile improvements. NA treatment inhibits diacylglycerol aminotransferase 2 (DGAT2) in HepG2 human hepatoma cells, thereby inhibiting the final catalysis step in TG synthesis, as well as increasing the degradation of ApoB, thus decreasing LDL and VLDL flux from the liver (Ganji et al., 2004; Jin et al., 1999). A recent, small uncontrolled clinical study supported to this hypothesis, showing that liver fat content in dyslipidemic patients was significantly reduced after 23 weeks of NA treatment, and that polymorphisms in DGAT2 alleles resulted in smaller decreases in liver fat content during treatment (Hu et al., 2012). Evidence also exists that NA treatment inhibits hepatic PCG-1β expression, leading to a reduction in ApoC3 and a resulting decrease in plasma TG (Hernandez et al., 2010).

The ability of NA to increase HDL cholesterol is still under investigation, and appears to be a multi-faceted process. NA augments reverse cholesterol transport by inhibiting catabolism of hepatic ApoA1, to increase ApoA1 HDL subfractions, as well as increasing expression of PPARγ and the ABCA1 cholesterol transporter on monocytes and macrophages (Rubic et al., 2004; Villines et al., 2012). While NA also seems to inhibit several other hepatic pathways involved in HDL catabolism, the increase in ApoA1 appears to be the primary mechanism for the HDL-raising effect (Villines et al., 2012). Interestingly, single nucleotide polymorphisms of GPR109A were recently identified in a genome-wide association study (GWAS) as being associated with variations in HDL-C

levels, suggesting that GPR109A may be mechanistically associated with NA-induced changes in HDL-C levels (Asselbergs et al., 2012).

Mechanistically independent of its systemic hypolipidemic effects, NA has also been recently linked to vascular improvements. In mice, NA can act through GPR109A on macrophages to reduce the progression of atherosclerosis by inducing the expression of the ABCG1 cholesterol transporter and increased cholesterol efflux to HDL (Lukasova et al., 2011). In vitro effects of NA on monocytes support a GPR109A-mediated anti-inflammatory role that reduces monocyte adhesion to HUVEC that could be antiatherogenic (Digby et al., 2012). Rabbits supplemented with dietary NA showed acute reduction of markers of vascular inflammation and endothelial dysfunction and improved endothelium-mediated vasorelaxation function compared with control animals following vascular injury by periarterial carotid collar (Wu et al., 2010). Ganji et al. (2009) showed that NA treatment of HAEC inhibited markers associated with oxidative stress and atherogenic inflammation independent of effects on lipid concentrations. Additionally, streptozotocin-treated diabetic mice showed improvements in peripheral revascularization of ischemic limbs following treatment with NA, attributed to activation of nitric oxide-related pathways in endothelial progenitor cells (Huang et al., 2012). These results from in vitro and animal models have been supported by human clinical studies. Impaired endothelial-dependent vasodilatory function, measured by forearm blood flow, is improved following NA treatment in patients with T2DM (Hamilton et al., 2010), independent of alterations to the lipid profile. Whether any of these direct vascular benefits are related to activation of sirtuins, through increased NAD^+ availability in cells of the vasculature, is not known.

1.6.2 Nicotinamide Mononucleotide

As described in section 1.5, nicotinamide mononucleotide is produced through the activity of Nampt, as part of the intracellular NAD^+ salvage pathway. NMN has been established as an NAD^+ precursor, readily entering cells and elevating intracellular NAD^+ levels in vitro (Borradaile and Pickering, 2009b; Revollo et al., 2007; Spinnler et al., 2013), and in vivo (Yoshino et al., 2011). Particularly relevant to this thesis, HAEC supplemented with NMN during exposure to high glucose showed significantly improved

growth rate compared with vehicle-treated controls (Borradaile and Pickering, 2009b). This protective effect on EC function was also observed with modest overexpression of Nampt, which resulted in increased SIRT1 activity.

Interestingly, there is evidence that Nampt circulates in the bloodstream of mice and humans (El-Mesallamy et al., 2011; Revollo et al., 2007). In fact, plasma levels of Nampt are increased in patients with T2DM (El-Mesallamy et al., 2011). Although the mechanism for Nampt release from cells is not well understood, these observations may indicate that dysregulation of NAD^+ biosynthesis plays a role in the pathogenesis of T2DM.

In mouse models, treatment with NMN has been shown to have multiple beneficial effects in the context of metabolic disease. NMN supplementation improves glucose-stimulated insulin secretion from islets of mice with Nampt deficits (Revollo et al., 2007), as well as in aged beta-cell specific SIRT1 overexpressing (BESTO) mice (Ramsey et al., 2008). Furthermore, high fat diet-induced T2DM mice show improved glucose tolerance and hepatic insulin sensitivity upon NMN administration, as well as alterations in oxidative stress and inflammatory gene expression related to SIRT1 activation (Yoshino et al., 2011). There is some evidence that these results can also be extended to humans, as NMN supplementation acutely increases glucose-stimulated insulin secretion from primary cultured human islets (Spinnler et al., 2013). These data suggest a role for NMN in improving complications of metabolic syndrome via regulation of NAD^+ metabolism. Whether NMN has direct beneficial effects on the vasculature is not known.

1.7 Objectives and Hypothesis

Rationale

Recent studies indicate that NA has beneficial effects on vascular function, and vascular regeneration after injury, which are independent of its ability to improve plasma lipids (Hamilton et al., 2010; Huang et al., 2012; Wu et al., 2010). Since NA has been reported as a biosynthetic precursor for NAD+ (Belenky et al., 2007; Hara et al., 2007), it is possible that it may activate sirtuin-mediated NAD^+-dependent responses in the vasculature to improve function. In comparison, NMN is a known NAD^+ precursor whose effects in HAEC mimic those of SIRT1 activation during glucose overload (Borradaile and Pickering, 2009b; Spinnler et al., 2013). SIRTs (particularly 1, 2 and 3) are known to improve cell survival under conditions of stress, and to improve glucose and lipid metabolism in many cell types, including those of the vasculature (Bonezzi et al., 2012; Borradaile and Pickering, 2009b; Hirschey et al., 2010; Peter et al., 2008; Potente et al., 2007; Rodgers and Puigserver, 2007; Yang et al., 2007). Whether NA can improve angiogenic function of HMVEC or HAEC under conditions of saturated fatty acid excess and lipotoxicity, and whether this may involve NAD^+-dependent or other pathways, is unknown.

NA is currently approved for clinical use for improving dyslipidemic lipid profiles, though research is currently underway to identify other applications (Villines et al., 2012). The studies in this thesis extend the findings of NA-mediated vascular benefits and identify a novel mechanism by which NA may exert its protective effects on endothelial cell function during palmitate overload.

Hypothesis

Nicotinic acid (NA) improves endothelial cell function under conditions of lipotoxicity through NAD^+-dependent pathways.

Objectives

The specific objectives of this research project are to:

1. Determine whether NA improves in vitro EC angiogenic function and/or survival in the presence of excess saturated fatty acids.
2. Determine whether supplementation with NA is associated with increased cellular NAD+, SIRT activation, and altered fatty acid metabolism.
3. Determine whether HMVEC express the NA receptor, and whether specific activation of this receptor mimics the effects of NA on angiogenic function.
4. Determine global changes in gene expression induced by NA in HMVEC, to confirm or refute involvement of SIRT activation, and to potentially identify new targets.

Relevance to Disease

As described in section 1.2, EC damage is an important initial step in the development of vascular complications during obesity and metabolic disease, and the maintenance of EC function opposes the development of vascular disease (Verma et al., 2003; Xu and Zou, 2009). In light of recent reports linking NA to improvements in vascular function, independent of systemic lipid lowering, determining whether NA can improve human microvascular EC function during lipotoxicity, and by what mechanism(s), may be important steps in determining further clinical applications of this drug. The work described in this thesis could have implications for the use of NA as a treatment for microvascular complications during obesity and metabolic disease.

Chapter 2

2 Materials and Methods

2.1 Cell Culture and Treatments

Primary HMVEC and HAEC cells were obtained from Lonza and grown on 100 mm culture dishes at 37°C and 5% CO_2. Cells were maintained in Medium 199 (Invitrogen) supplemented with EGM-2 MV SingleQuots (HMVEC; Lonza) or EGM-2 SingleQuots (HAEC; Lonza). The medium was changed every 2-3 days. Upon reaching 80% confluence, cells were subcultured at ratios of 1:4 (HMVEC) or 1:5 (HAEC) using trypsin-EDTA solution. Cells were used between passage 5 and passage 12. For experiments, cells were plated in 100 mm dishes, 6-well (35 mm), or 24-well culture plates (Falcon).

For fatty acid treatments, the medium was supplemented with 0.5 mM palmitate, oleate or a combination of palmitate and oleate (1:1 ratio). The concentrations of fatty acids used reflect high physiological to pathophysiological concentrations, as would be observed during obesity, metabolic syndrome, and type 2 diabetes (Gordon, 1960; Soriguer et al., 2009). The 1:1 ratio of palmitate to oleate is similar to the saturated to unsaturated fatty acid composition of North American (Westernized) diets, and is maintained in postprandial compositions of serum free fatty acids (Staiger et al., 2004). For preparation of fatty acids, a 20 mM solution of either palmitate or oleate in 0.01 M NaOH was heated to 70°C for 30 min. 1 N NaOH was added dropwise to facilitate solubilization. Fatty acids were complexed to 30% fatty acid-free bovine serum albumin (BSA) (Sigma) at a fatty acid to BSA ratio of 2:1. The complexed fatty acids were added to cell culture medium to achieve a fatty acid concentration of 0.5 mM (Borradaile et al., 2006). BSA-supplemented medium was used for control conditions.

For NA or NMN treatments, experimental media were supplemented with 10 μM NA or 1 μM NMN. NA (Fluka BioChemika) and NMN (Sigma) were solubilized in cell culture grade water at room temperature. Water was used as the vehicle control. The concentration of NA used reflects plasma levels of NA following pharmaceutical dosing

(Menon et al., 2007). Although not yet studied in humans, NMN has been reported to circulate endogenously in mouse plasma at concentrations around 90 μM (Revollo et al., 2007). However, previous work determined that NMN concentrations above 1 μM are toxic to human EC cultures (N. Borradaile, unpublished data).

For acifran treatments, the medium was supplemented with 1 μM acifran. At this concentration, acifran is highly selective for GPR109A (Jung et al., 2007). Acifran (Tocris Bioscience) was solubilized in DMSO at room temperature. 0.2% DMSO was used as the vehicle control.

2.2 Tube Formation Assay

Cells were plated at 80-90% confluence into a 6-well plate and pre-treated for 24 h with various treatments. Immediately prior to cell harvesting, a 24-well plate was coated with 200 μL/ well of growth factor-replete Matrigel basement membrane (BD Biosciences), and allowed to solidify for 30 min at 37°C. Cells were harvested with trypsin-EDTA solution and resuspended in fatty acid-supplemented medium to a concentration of 3.75-5.0 x 10^5 cells/ mL. Cells were re-treated with corresponding pre-treatment compounds, and 200 μL (7.5-10 x 10^4 cells) of each condition were seeded onto the Matrigel-coated 24-well plate. For any given experiment, the number of cells plated for each condition was identical. Cells were incubated at 37°C and 5% CO_2 for a further 18 h to allow tube assembly. After 18 h, tubes were visualized by light microscopy using an Olympus IX71 inverted microscope. For each well, three fields of view were imaged. Branch points, total tube length, and average tube width per field of view were quantified in Image J. A tube was defined as an apparently 3-dimensional (tube-like), elongated structure stretching between branch points, with a width large enough along its entire length to permit the passage of an erythrocyte. Modified from (Borradaile and Pickering, 2009b).

2.3 Cell Migration

EC were plated in 6-well plates at 100% confluence. Following 24 h preincubations with various treatments, monolayers were scratched using a 200 μl pipette tip. Scratches were imaged by light microscopy at 0, 4 and 8 h using an Olympus IX71 inverted microscope.

Scratch image location was marked by indelible marker on the base of each well, ensuring that image location remained consistent between timepoints. Scratch areas were determined using Image J, and cell migration areas were determined by subtracting scratch areas at 4 h and 8 h from those at 0 h. Modified from (Liang et al., 2007).

2.4 Growth Rate Assay

EC were plated at a density of 1000 cells / cm^2. Cells were grown to 80% confluence in medium containing various treatments, then harvested by trypsinization, and counted using a hemocytometer. The number of population doublings was calculated according to the formula [$\log_{10}$(number of cells harvested) - $\log_{10}$(number of cells seeded)] * [$\log_{10}(2)]^{-1}$ (Borradaile and Pickering, 2009b).

2.5 Cell Death

Apoptosis and cell death were assessed by Alexa Fluor 488 annexin V staining and membrane permeability to propidium iodide, respectively, using the Dead Cell Apoptosis Kit, based on the manufacturer's protocol (Molecular Probes). Following 24 h of incubations with various treatments, cells were washed in cold phosphate-buffered saline (PBS) and harvested by trypsinization. 1X annexin-binding buffer was prepared by adding 1 mL 5X annexin binding buffer to 4 mL deionized water, and 100 µg/mL working solution of propidium iodide (PI) was prepared by diluting 5 µL of 1 mg/mL PI stock solution in 45 µL 1X annexin-binding buffer. Cells were centrifuged and suspended in 200 µL 1X annexin-binding buffer at a density of 1 x 10^6 cells/mL. After adding 2.5 µL Alexa Fluor 488 annexin V and 2 µL PI to each 200 µL of cell suspension, cells were incubated at room temperature for 15 minutes protected from light. Samples were analyzed by flow cytometry with quantification of 10^4 cells/sample. Apoptotic cells were defined as annexin V positive and PI negative, indicating an intact plasma membrane. Late apoptotic and necrotic cells were defined as annexin V positive and PI positive or PI positive alone, while live cells were negative for both annexin V and PI. Fluorescence emission was measured at 530 nm and >575 nm using 488 nm excitation. Cell populations were gated on an unstained control sample to remove debris, and voltages were set using single stained controls.

2.6 NAD^+ Assay

EC were plated in 6-well plates and two wells were combined per treatment condition. Cellular [NAD^+]/[NADH] ratio was assessed using a colorimetric kit (BioVision). Kit components were reconstituted according to the manufacturer's protocol, and kept on ice protected from light. Following treatment, cells were harvested with trypsin and counted. Four hundred thousand cells were resuspended in cold NADH/NAD Extraction Buffer. Cells were homogenized by aspiration through a 25G needle and vortexed for 10 s. Samples were centrifuged at 14000 rpm for 5 min. Supernatant was spin-filtered through a 10 kDa cut-off filter (BioVision) at 11200 rpm for 20 min. Each sample was split into two aliquots. NAD^+ was decomposed in one aliquot of each sample by 30 min incubation at 60°C. All samples were cooled on ice. The NAD^+ Cycling Mix and standard curve solutions were prepared prior to each use, according to the manufacturer's protocol. Fifty µL aliquots of each sample were pipetted in duplicate into a 96-well cell culture plate, followed by 100 µL of the NAD^+ Cycling Mix and thorough mixing. The plate was incubated at room temperature for 5 min to convert NAD^+ to NADH, followed by addition of 10 µL of NAD^+ Developer. The plate was again incubated at room temperature, protected from light for 1 h. Absorbance was quantified spectrophometrically at a wavelength of 450 nm. Cellular [NAD^+]/[NADH] ratio was calculated according to the formula $[NAD^+]/[NADH] = ([NAD^+_{total}] - [NADH]) * ([NADH])^{-1}$. Modified from (Borradaile and Pickering, 2009b).

2.7 SIRT Activation Assay

SIRT1 and SIRT2/3 activation were assessed using a fluorimetric kit (BIOMOL). Kit components were reconstituted according to the manufacturer's protocol, and kept on ice protected from light. EC were plated in duplicate at 5×10^4 cells/well into a 24-well plate and allowed to seed overnight. Two wells with medium but no cells were also included to account for background fluorescence. Following treatment, cells were washed with PBS. Two hundred µL of Opti-MEM Reduced Serum Medium (Invitrogen) supplemented with 1 µM Trichostatin A were added to each well. The use of Opti-MEM ensures that measurements will not be confounded by fluorescence from serum or phenol red. Trichostatin A (TSA) is a potent inhibitor of non-sirtuin histone deacetylases (Dali-

Youcef et al., 2007). Twenty-five μM of acetylated Fluor de Lys SIRT1 or SIRT2/3 substrate was added to each treatment condition, negative control and background well. Twenty-five μM of deacetylated Fluor de Lys substrate was added to each positive control well. The plate was incubated at 37°C for 2 h. Following incubation, 5X Developer II solution was diluted to 1X (300 μL 5X Developer II solution in 1.2 mL SIRT Assay Buffer). Fifty μL aliquots of each sample were aliquoted in duplicate into a black 96-well plate (VWR), followed by 50 μL of 1X Developer II solution. The 96-well plate was incubated at room temperature for 30 min, protected from light. Fluorescence was measured at an excitation wavelength of 360 nm and an emission wavelength of 460 nm. Higher fluorescence values represented increased conversion of the acetylated Fluor de Lys substrate to its fluorescent, deacetylated product. Modified from (de Boer et al., 2006).

Protein was harvested overnight at 4 °C with 50 μL RIPA buffer (150 mM NaCl, 1.0% IGEPAL® CA-630, 0.5% sodium deoxycholate, 0.1% SDS, and 50 mM Tris-HCl, pH 8.0) (Sigma). Total cellular protein was quantified using the Pierce Bicinchoninic Acid (BCA) Protein Assay Kit (Thermo Scientific, Rockford, IL), and fluorescence values were normalized to total protein.

2.8 Lipid Droplet Analysis

Endothelial cells were seeded onto cover glass slides in 6-well plates and allowed to adhere overnight. Once at 80-90% confluence, cells were pre-treated with growth medium containing either NA or NMN for 20 h, followed by a 6 h treatment with the addition of fatty acids. Cells were fixed in 4% paraformaldehyde for 10 min at room temperature. To visualize lipid droplets, cells were stained for 10 min with Oil Red O (Sigma Aldrich). Staining solution was prepared fresh on day of use by dissolving 0.2 g of Oil Red O powder into 40 mL isopropanol. Working solution was prepared by mixing 30 mL stock solution with 20 mL PBS and filter sterilizing using a 0.22 μm syringe filter. All coverslips were mounted onto glass slides with mounting media containing DAPI to visualize nuclei (ProLong Gold Antifade Reagent with DAPI, Molecular Probes). Cells were imaged by fluorescence microscopy on an Olympus BX51 microscope. Lipid

droplet content was analyzed in Image J by quantification of red (Oil Red O) and blue (DAPI) pixel densities. Modified from (Assini et al., 2013).

2.9 ^{3}H-Palmitate Oxidation Assay

HMVEC were plated in duplicate into a 24-well plated at 7.5 x 10^4 cells/well, including two wells without cells for background radioactivity measurements. Following treatment with NA or NMN for 20 h, cells were washed with PBS. Cells were then incubated for 1 h at 37°C and 5% CO_2 with 200 µL growth medium containing 2.0 µCi/ mL [9, 10-^{3}H(N)]palmitic acid (PerkinElmer) in 100 µM palmitate conjugated to BSA. Prior to addition of ^{3}H-palmitate, control wells were treated with growth medium supplemented with either 2 mM AICAR (positive control) or 200 µM etomoxir (negative control). AICAR has been reported to increase palmitate oxidation in EC via AMPK activation (Dagher et al., 1999). Etomoxir impairs palmitate oxidation by inhibiting carnitine palmitoyltransferase 1 (Lopaschuk et al., 1988). Following incubation with ^{3}H-palmitate, media was collected in 1.5 mL microfuge tubes and cells were washed with 200 µL/well of PBS, which was also added to the microfuge tubes. To dissolve cellular proteins, 25 µL of 1 N NaOH was added to each well and incubated at 37°C for 30 min. NaOH was subsequently neutralized by addition of 25 µL of 1 N HCl, and 10 µL aliquots in duplicate for each sample were removed for total protein quantification. Media samples were precipitated with 400 µL 10% trichloroacetic acid (TCA) on ice for 30 min. Remaining cellular protein samples and TCA precipitates were combined and centrifuged for 10 min at 2200 rcf at 4°C. Unreacted fatty acids were extracted from supernatants by washing 4 times with hexane. The aqueous layer was sampled and prepared for scintillation counting. Counts measured represented the amount of ^{3}H-palmitate oxidized to $^{3}H_2O$, and were expressed relative to total protein for each sample. Modified from (Borradaile and Pickering, 2009b).

2.10 Immunoblot Analyses

Whole cell lysates were prepared using RIPA buffer (150 mM NaCl, 1.0% IGEPAL® CA-630, 0.5% sodium deoxycholate, 0.1% SDS, and 50 mM Tris-HCl, pH 8.0) (Sigma) supplemented with protease inhibitors and total cellular protein was quantified using the

Pierce Bicinchoninic Acid (BCA) Protein Assay Kit (Thermo Scientific, Rockford, IL). Lysates were centrifuged for 2 min at 14 000 rpm to eliminate insoluble material. 10, 20 or 40 µg of whole cell lysate protein was diluted 1:1 with 2X Laemmli sample buffer (LSB) containing β- mercaptoethanol and heated to 100°C for 5 minutes. Samples were resolved by 10% SDS-polyacrylamide gel electrophoresis (PAGE) and transferred to a 0.45 µm PVDF membrane using a semi-dry transfer apparatus. Membranes were incubated in 1% blocking buffer for 1 h. GPR109A was detected following an overnight incubation at 4°C with a 1:600 dilution of anti-GPR109A rabbit polyclonal antibody (Abcam), and a 1 h incubation with a 1:5000 dilution of a horseradish peroxidase (HRP)-conjugated polyclonal anti-rabbit antibody (Santa Cruz Biotechnology). GAPDH was detected following a 3 h incubation with a 1:5000 dilution of anti-GAPDH mouse polyclonal antibody (Enzo) and a 1 h incubation with a 1:5000 dilution of HRP-conjugated polyclonal anti-mouse antibody (Santa Cruz Biotechnology). Membranes were washed 3 times for 5 min with Tris-buffered saline and 0.1% Tween-20 (TBS-T) following incubation with primary and secondary antibodies. Blots were incubated with Enhanced Chemilumniscence Reagents (Thermo Scientific, Rockford, IL) for 1 min and exposed on film. Bands corresponding to both GPR109A and GAPDH ran between the 37 and 50 kD reference bands of the Precision Plus Protein All Blue Standards (Biorad), with GAPDH running closer to 37 kD. Bands were quantified by densitometry using Quantity One 1-D Analysis Software (Biorad) and normalized to GAPDH.

2.11 Microarray Analysis

Total RNA was isolated using the RNeasy Mini Kit (QIAGEN). Kit components were reconstituted according to the manufacturer's protocol. HMVEC were grown to 80-90% confluence in 100 mm dishes. Cells were treated for 24 h, with two dishes combined per treatment condition. Following treatment, cells were harvested using trypsin, counted and pelleted. Cells were resuspended in 350 µL Buffer RLT and lysed using QIAshredders (QIAGEN). 350 µL of 70% ethanol was added to each sample and mixed well. Samples were transferred to an RNeasy Mini spin column and centrifuged for 15 s at 8000 rcf. Flow through was discarded and 700 µL of Buffer RW1 was added. Samples were again centrifuged for 15 s at ≥8000 rcf and flow through discarded. 500 µL of Buffer RPE was

added. Samples were again centrifuged for 15 s at ≥8000 rcf and flow through discarded. Again, 500 µL of Buffer RPE was added, and samples were centrifuged for 2 min at ≥8000 rcf. Spin column membrane was dried by a 1 min spin at full speed. RNA was the eluted with a 30 µL rinse with nuclease-free water followed by centrifuging for 1 min at ≥8000 rcf.

Total RNA concentration of each sample was measured by NanoDrop (Thermo Scientific). Samples were diluted in nuclease-free water to a concentration of 200 ng/µL, and concentrations and quality were again confirmed by NanoDrop. Samples were stored at -80 °C until transfer to the London Regional Genomics Centre.

All sample labeling and GeneChip processing was performed at the London Regional Genomics Centre (Robarts Research Institute, London, Ontario, Canada; http://www.lrgc.ca)

RNA quality was assessed using the Agilent 2100 Bioanalyzer (Agilent Technologies Inc., Palo Alto, CA) and the RNA 6000 Nano kit (Caliper Life Sciences, Mountain View, CA).

Single stranded complementary DNA (sscDNA) was prepared from 200 ng of total RNA as per the Ambion WT Expression Kit for Affymetrix GeneChip Whole Transcript WT Expression Arrays (http://tools.invitrogen.com/content/sfs/manuals/cms_064619.pdf, Applied Biosystems, Carlsbad, CA) and the Affymetrix GeneChip WT Terminal Labeling kit and Hybridization User Manual (http://media.affymetrix.com/support/downloads/manuals/wt_term_label_ambion_user_manual.pdf, Affymetrix, Santa Clara, CA). Total RNA was first converted to cDNA, followed by in vitro transcription to make cRNA. 5.5 ug of single stranded cDNA was synthesized, end labeled and hybridized, for 16 hours at 45°C, to Human Gene 1.0 ST arrays.

All liquid handling steps were performed by a GeneChip Fluidics Station 450 and GeneChips were scanned with the GeneChip Scanner 3000 7G (Affymetrix, Santa Clara, CA) using Command Console v3.2.4.

Probe level (.CEL file) data was generated using Affymetrix Command Console v3.2.4. Probes were summarized to gene level data in Partek Genomics Suite v6.6 (Partek, St. Louis, MO) using the RMA algorithm (Irizarry et al., 2003).

Partek was used to determine gene level ANOVA p-values and fold changes. Genes changing at least 1.3 fold and having a p-value less than 0.05 underwent GO (Gene Ontology) and Pathway Enrichment, both using a Fisher's Exact Test. Modified from (Borradaile and Pickering, 2010).

2.12 qRT-PCR

cDNA was synthesized from RNA samples using a High Capacity RNA-to-cDNA kit (Applied Biosystems). Kit components were thawed on ice prior to use. Kit components and RNA samples were mixed in microfuge tubes according to the manufacturer's protocol. To reverse transcribe RNA, samples were incubated at 37 °C for 1 h. Reverse transcription reaction was stopped by heating samples to 95 °C for 5 min, followed by cooling to 4 °C. cDNA content was quantified by NanoDrop.

qRT-PCR was performed using reagents from Applied Biosystems. TaqMan primers for GAPDH control, CYP4Z1 (Clone ID: Hs01045187_m1), EFCAB4B (Hs01592234_m1), NAP1L2 (Hs01114608_s1), OR13C8 (Hs01104244_s1), and SIGLEC5 (Hs00174659_m1) were obtained from Applied Biosystems. Samples were diluted with nuclease-free water to a concentration of 25 ng/µL. Reaction components were mixed according to the TaqMan Gene Expression Assays Reference Card. Twenty µL of each sample was plated in triplicate into a 384-well reaction plate. The plate was sealed and briefly centrifuged before loading into the 7900 HT Fast Real-Time PCR System (Applied Biosystems). The qRT-PCR plate was run for 40 cycles with a 15 s denature at 95 °C followed by a 1 min anneal/ extend step at 60 °C. Following completion, cycle threshold (Ct) values were used to calculate relative quantification (RQ) for each sample. Modified from (Borradaile and Pickering, 2010).

2.13 Statistical Analysis

Statistical analyses were performed using either Student's t-Test or a one-way ANOVA followed by Tukey's post hoc test. Differences in means were considered statistically significant at $p < 0.05$. Immunoblots were quantified by densitometry using Quantity One 1-D Analysis Software (Biorad) and normalized to GAPDH. GraphPad Prism version 5.0 software was used for all statistical analyses and generation of graphs.

Chapter 3

3 Results

3.1 Endothelial cell angiogenic function during fatty acid overload is improved by NA or NMN

Previous studies demonstrated that improvements in HAEC angiogenic function during the stress of glucose overload can be achieved via modest overexpression of Nampt, in association with increased cellular NAD^+ content and activation of SIRT1 (Borradaile and Pickering, 2009b). Activation of sirtuins, particularly SIRT1 and SIRT3, is known to improve cellular response to stress and enhance fatty acid metabolism in many cell types (Nogueiras et al., 2012). Since increases in cellular NAD^+ content can also be induced in human aortic endothelial cells by supplementation with 1 μM NMN, and since concentrations of NA as low as 1 μM have been shown to increase NAD^+ content in other cell types (Borradaile and Pickering, 2009b; Hara et al., 2007), we determined whether these compounds would confer similar benefits to endothelial cells during fatty acid overload.

For the present study, we used two primary human endothelial cell types as in vitro models of small (HMVEC) and large vessels (HAEC), distinct vessel types that are both detrimentally affected during metabolic disease. Both HMVEC (Figure 3.1) and HAEC (Figure 3.2) exhibited characteristics of impaired tube formation on Matrigel after 18 h of treatment with growth medium containing the saturated fatty acid, palmitate (0.5 mM). Although no direct comparisons were performed, HMVEC appeared to be more sensitive to exposure to fatty acid excess than HAEC. This may reflect differences in the in vivo physiology and function of the source vessels of these cells (Aird, 2007). Pre-treatment for 24 h with culture medium supplemented with either NA (10 μM) or NMN (1 μM) improved HMVEC tube branch points and total tube length (Figure 3.1B and C, respectively), and HAEC average tube width (Figure 3.2D) to control levels. Although no statistically significant impairments in tube formation in either cell type were observed following treatment with oleate (0.5 mM) or palmitate plus oleate (1:1, 0.5 mM), trends

were observed, particularly in HMVEC. These data are consistent with the known limited toxicity of unsaturated fatty acids such as oleate.

Figure 3.1. NA and NMN improve HMVEC tube formation during palmitate overload.

(A) Following pre-treatment for 24 h in culture medium supplemented with either vehicle (0.2% water), 10 μM NA or 1 μM NMN, HMVEC were seeded onto growth factor replete Matrigel and incubated with medium containing BSA, 0.5 mM oleate, 0.5 mM palmitate, or palmitate + oleate (1:1, 0.5 mM) conjugated to BSA (molar ratio 2:1). HMVEC were again supplemented with either vehicle, 10 μM NA or 1 μM NMN, and resulting tube networks were analysed by light microscopy after 18 h. Representative photomicrographs of capillary tubes indicate impaired network formation during palmitate overload, which is improved following NA and NMN pre-treatment. Scale bar represents 100 μm. **(B-D)** For quantification, three random fields of view per condition were assessed for **(B)** tube branch points, **(C)** total tube length, and **(D)** average tube width. Data are expressed as mean ± SEM for 5 independent experiments. * $p < 0.05$ vs. BSA.

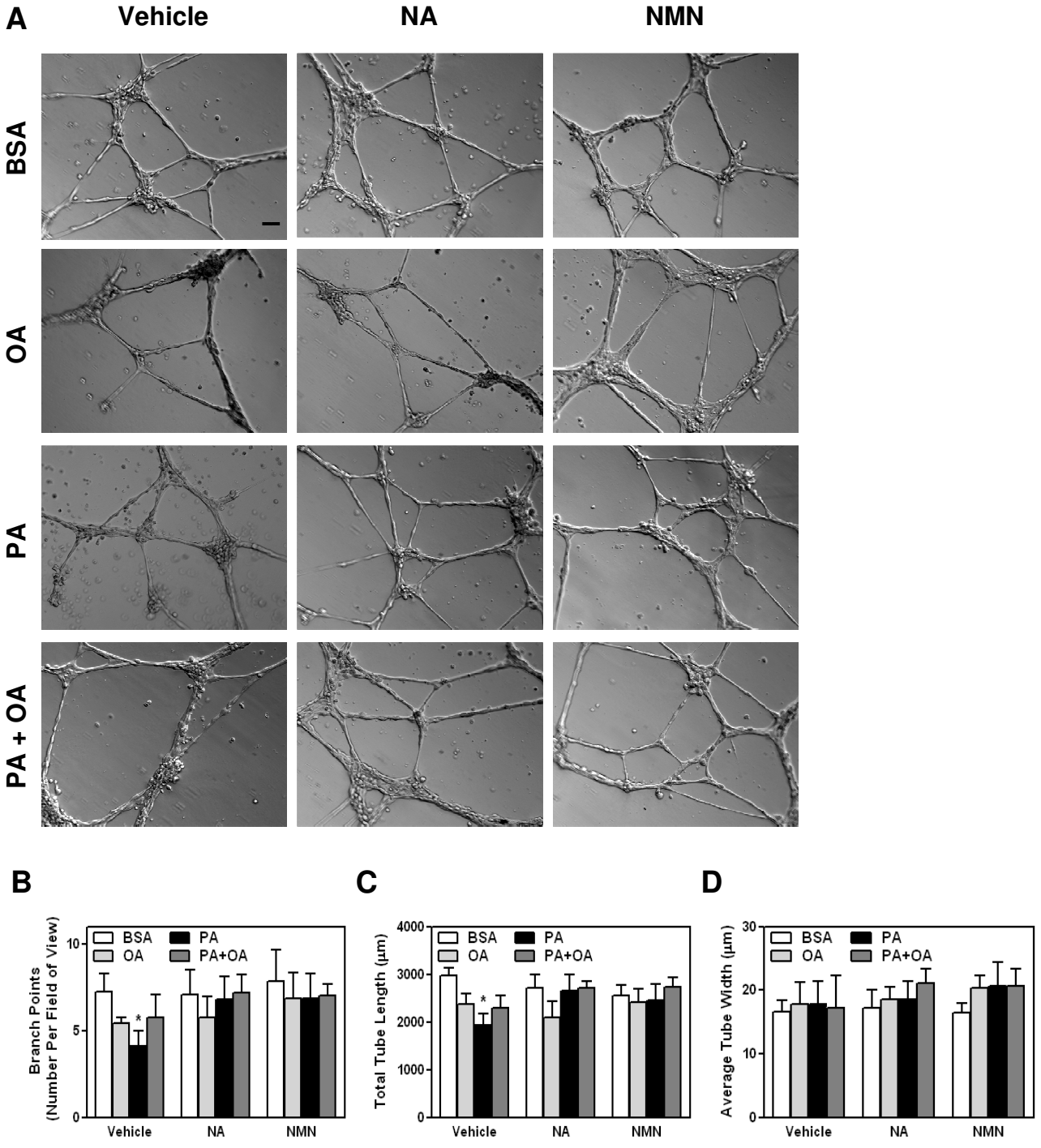
A
Vehicle
NA
NMN
BSA
OA
PA
PA + OA
B
Branch Points (Number Per Field of View)
BSA
OA
PA
PA+OA
Vehicle
NA
NMN
C
Total Tube Length (μm)
D
Average Tube Width (μm)

Figure 3.2. NA and NMN improve HAEC tube width during palmitate overload.

(A) Following pre-treatment for 24 h in culture medium supplemented with either vehicle (0.2% water), 10 μM NA or 1 μM NMN, HAEC were seeded onto growth factor replete Matrigel and incubated with medium containing BSA, 0.5 mM oleate, 0.5 mM palmitate, or palmitate + oleate (1:1, 0.5 mM) conjugated to BSA (molar ratio 2:1). HAEC were again supplemented with either vehicle, 10 μM NA or 1 μM NMN, and resulting tube networks were analysed by light microscopy after 18 h. Representative photomicrographs of capillary tubes indicate impaired network formation during palmitate overload, which is improved following NA and NMN pre-treatment. Scale bar represents 100 μm. **(B-D)** For quantification, three random fields of view per condition were assessed for **(B)** tube branch points, **(C)** total tube length, and **(D)** average tube width. Data are expressed as mean ± SEM for 4 independent experiments. * $p < 0.05$ vs. BSA.

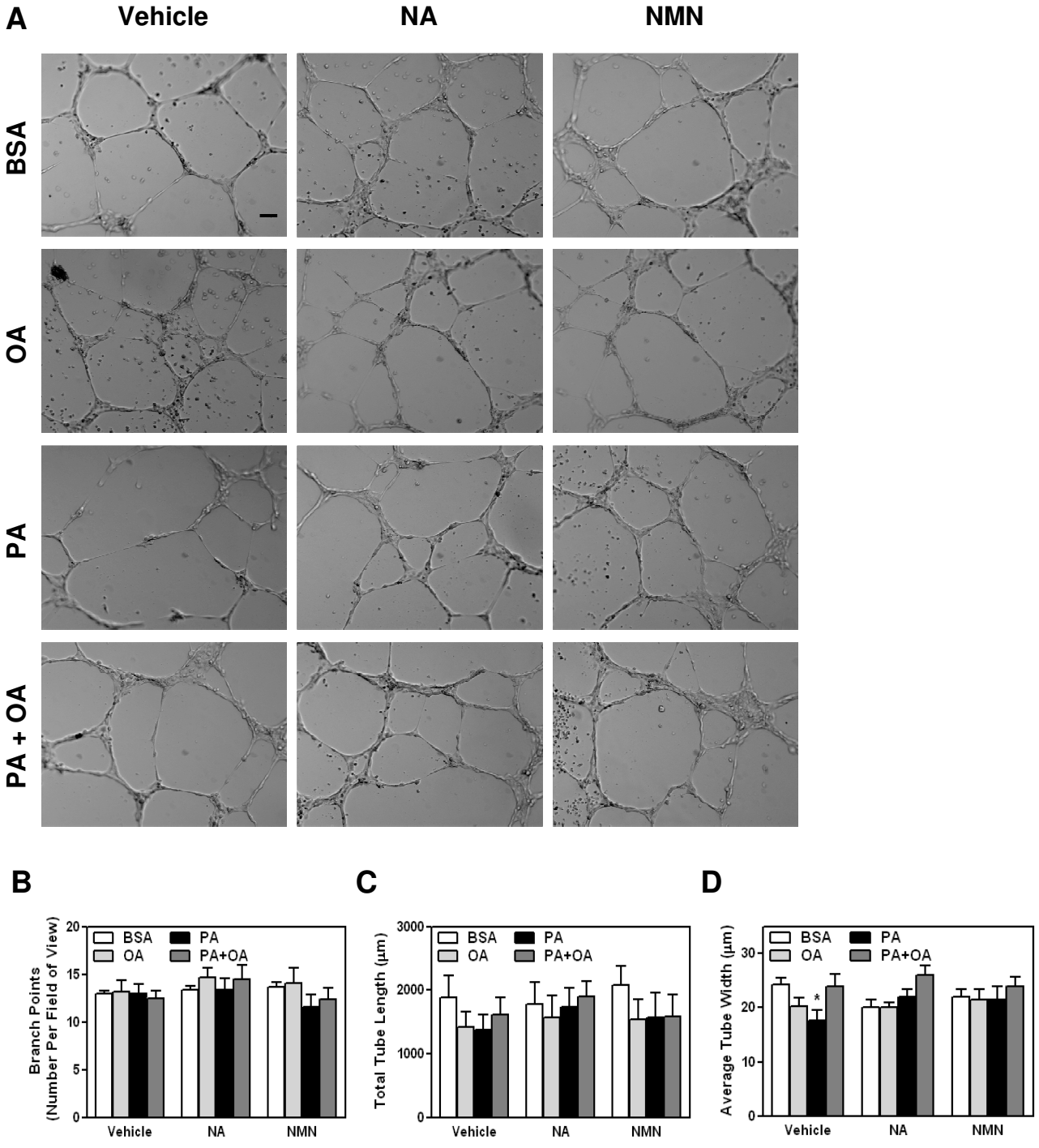
A
Vehicle
NA
NMN
BSA
OA
PA
PA + OA
B
Branch Points (Number Per Field of View)
BSA
OA
PA
PA+OA
Vehicle
NA
NMN
C
Total Tube Length (μm)
D
Average Tube Width (μm)
*

3.2 Endothelial cell migration and cell survival during fatty acid overload are not improved by NA or NMN

The in vitro tube-forming capacity of endothelial cells is a dynamic process that can initially involve cell migration, and cell proliferation. Activation of SIRT1 has been shown to induce endothelial cell proliferation and migration (Potente et al., 2007). To determine whether the improved tube formation observed in the presence of NA or NMN during palmitate overload was related to enhanced early endothelial cell migration, scratch assays were performed. While cell migration occurred over time in both cell types, neither HMVEC (Figure 3.3) nor HAEC (Figure 3.4) showed significant changes in cell migration after 4 h and 8 h of treatment with oleate, palmitate or palmitate plus oleate compared to BSA alone. Moreover, migration was unaffected following 24 h pre-treatment with NA or NMN (Figure 3.3 and 3.3 B-E). Cell proliferation rates were also unaffected by NA or NMN. Basal growth rates of both cell types were unaltered in the presence of NA or NMN treatment, with HMVEC population doublings occurring approximately every 4 days (Figure 3.3F), and HAEC population doublings occurring approximately every 2 days (Figure 3.4F). Together, these data suggest that NA and NMN do not improve angiogenic function during palmitate overload through early changes in cell migration and proliferation.

SIRT1 and SIRT3 activation have been shown to decrease stress-induced apoptosis in several cell types (Nogueiras et al., 2012). To determine whether NA or NMN increased cell survival during fatty acid overload, flow cytometric analyses of cell death were performed. Annexin V (apoptosis) and propidium iodide (late apoptosis and necrosis) staining showed a doubling of total cell death following 20 h treatment with palmitate in both HMVEC (Figure 3.5D) and HAEC (Figure 3.6D), which was not improved by 24 h pre-treatment with NA or NMN. Similar to the differential effects of fatty acids on HMVEC and HAEC tube formation, each cell type appears to react differently to fatty acid treatment in terms of cell survival. Although total cell death was increased during palmitate overload, we observed increased apoptosis (annexin V staining) in HAEC, but not HMVEC. These data indicate that NA and NMN do not improve EC angiogenic function during fatty acid overload through increased cell survival.

Figure 3.3. NA and NMN do not affect early HMVEC migration or proliferation.

(A-E) HMVEC were grown to 100% confluence. Following pre-treatment for 24 h in culture medium supplemented with either vehicle (0.2% water), 10 μM NA or 1 μM NMN, HMVEC were incubated with medium containing BSA, 0.5 mM oleate, 0.5 mM palmitate, or palmitate + oleate (1:1, 0.5 mM) conjugated to BSA (molar ratio 2:1). HMVEC were again supplemented with either vehicle, 10 μM NA or 1 μM NMN, and cell monolayers were scratched with a pipet tip. Scratches were imaged by light microscopy at 0 h, 4 h, and 8 h following fatty acid treatment. **(A)** Representative photomicrographs of vehicle pre-treated HMVEC under BSA and palmitate conditions at each time point. Scale bar represents 100 μm. Migration area for each treatment was quantified using ImageJ by calculating scratch area at each time point and subtracting 4 h and 8 h areas from the 0 h time point. Migration area is shown for each condition following incubation with **(B)** BSA, **(C)** oleate, **(D)** palmitate, and **(E)** palmitate + oleate. Data are expressed as mean ± SEM for 4 independent experiments. **(F)** Endothelial cells were plated at a density of 1000 cells / cm^2, and grown in medium containing water (vehicle), 10 μM NA or 1 μM NMN. At 80% confluence, cells were harvested and counted, and population doublings per day were calculated. Data are expressed as mean ± SEM for 5 independent experiments.

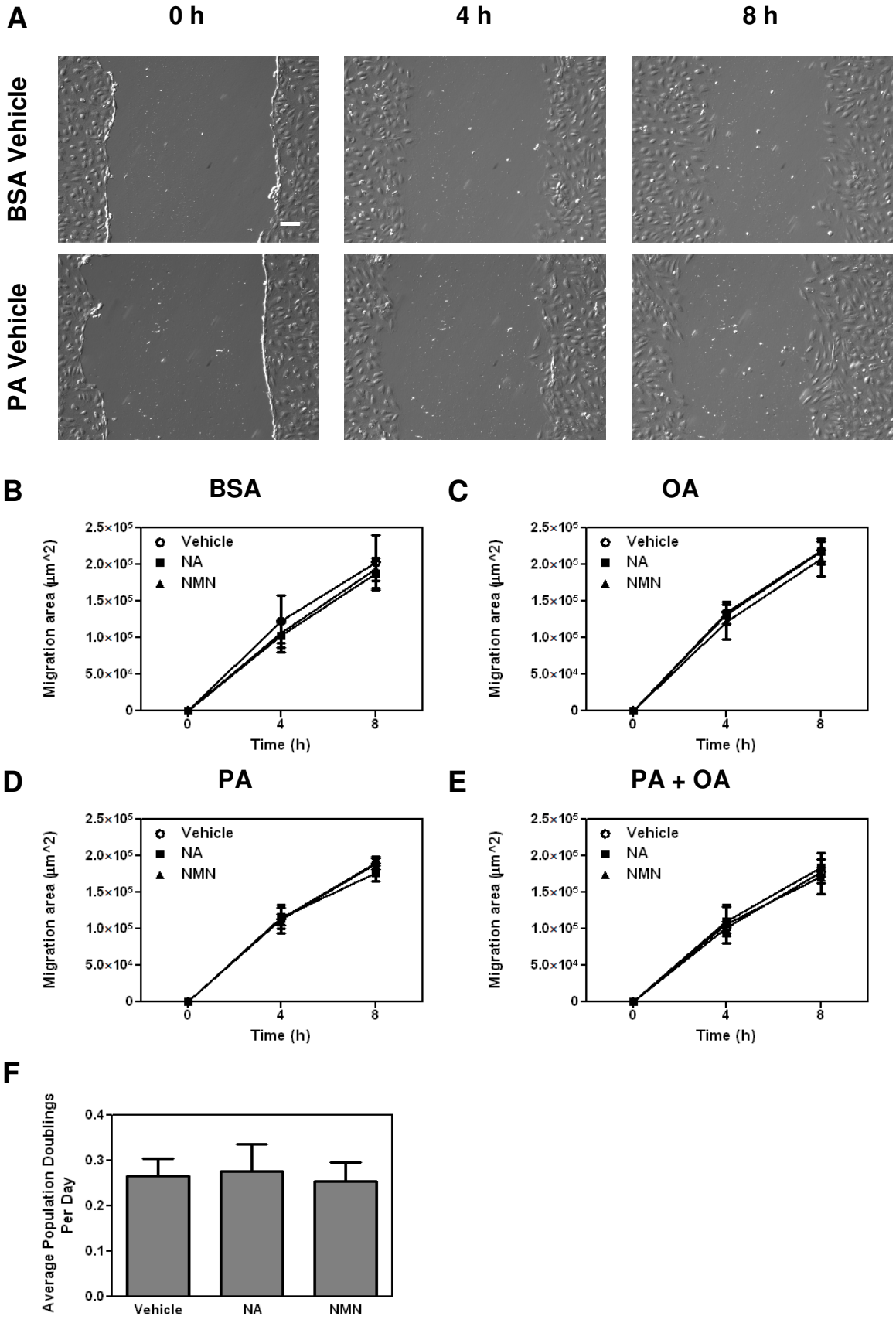
A
0 h
4 h
8 h
BSA Vehicle
PA Vehicle
B
BSA
C
OA
D
PA
E
PA + OA
Vehicle
NA
NMN
Migration area (μm^2)
Time (h)
F
Average Population Doublings Per Day
Vehicle
NA
NMN

Figure 3.4. NA and NMN do not affect early HAEC migration or proliferation.

(A-E) HAEC were grown to 100% confluence. Following pre-treatment for 24 h in culture medium supplemented with either vehicle (0.2% water), 10 μM NA or 1 μM NMN, HAEC were incubated with medium containing BSA, 0.5 mM oleate, 0.5 mM palmitate, or palmitate + oleate (1:1, 0.5 mM) conjugated to BSA (molar ratio 2:1). HAEC were again supplemented with either vehicle, 10 μM NA or 1 μM NMN, and cell monolayers were scratched with a P200 pipet tip. Scratches were imaged by light microscopy at 0 h, 4 h, and 8 h following fatty acid treatment. **(A)** Representative photomicrographs of vehicle pre-treated HAEC under BSA and palmitate conditions at each timepoint. Scale bar represents 100 μm. Migration area for each treatment was quantified using ImageJ by calculating scratch area at each timepoint and subtracting 4 h and 8 h areas from the 0 h timepoint. Migration area is shown for each condition following incubation with **(B)** BSA, **(C)** oleate, **(D)** palmitate, and **(E)** palmitate + oleate. Data are expressed as mean ± SEM for 3 independent experiments. **(F)** Endothelial cells were plated at a density of 1000 cells / cm^2, and grown in medium containing water (vehicle), 10 μM NA or 1 μM NMN. At 80% confluence, cells were harvested and counted, and population doublings per day were calculated. Data are expressed as mean ± SEM for 3 independent experiments.

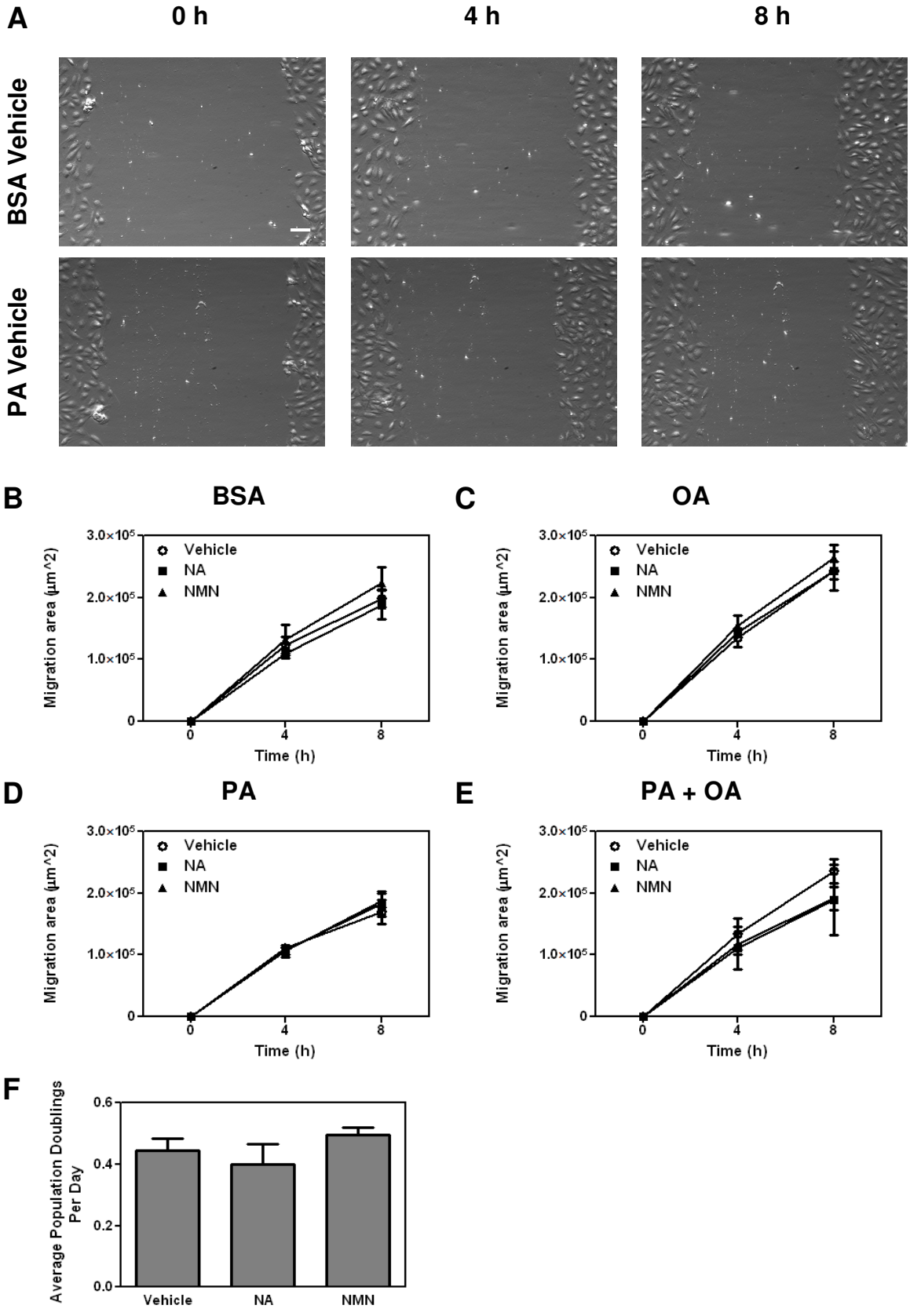
A
0 h
4 h
8 h
BSA Vehicle
PA Vehicle
B
BSA
C
OA
D
PA
E
PA + OA
Vehicle
NA
NMN
Migration area (μm^2)
Time (h)
3.0×10^5
2.0×10^5
1.0×10^5
0
4
8
F
Average Population Doublings Per Day
0.6
0.4
0.2
0.0
Vehicle
NA
NMN

Figure 3.5. Palmitate-induced HMVEC death is not improved by supplementation with NA and NMN.

(A-D) Following a 24 h pre-treatment with medium containing vehicle (0.2% water), 10 μM NA or 1 μM NMN, endothelial cells were incubated for 20 h with medium containing 0.5 mM oleate, 0.5 mM palmitate, or palmitate + oleate (1:1, 0.5 mM) conjugated to BSA (molar ratio, 2:1). Cell survival was assessed by staining with annexin V (AnnV) and propidium iodide (PI), with quantification by flow cytometry. **(A)** Representative dot plots for vehicle-treated microvascular endothelial cells are shown. Quadrant analysis was performed to determine **(B)** percent apoptotic (AnnV+) cells, **(C)** percent late apoptotic/ necrotic (AnnV+ PI+) cells, and **(D)** total cell death. Data are expressed as mean ± SEM for 4 independent experiments. * $p < 0.05$ vs. BSA, OA, PA+OA.

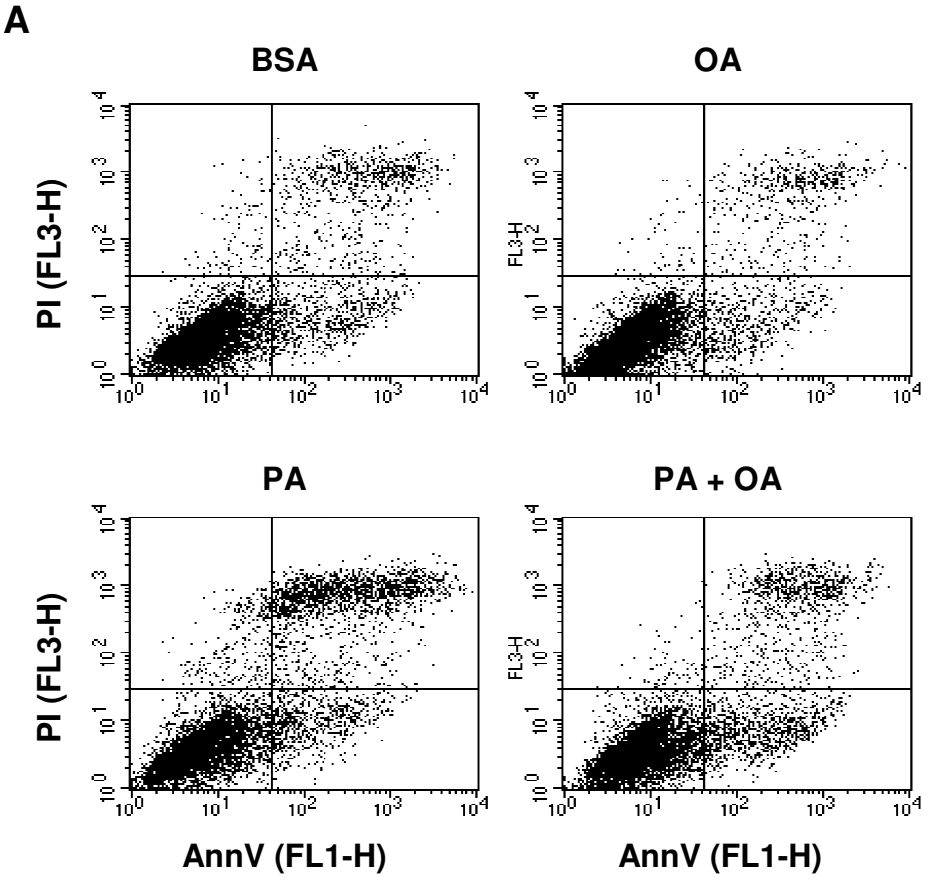
A
BSA
OA
PA
PA + OA
PI (FL3-H)
FL3-H
AnnV (FL1-H)

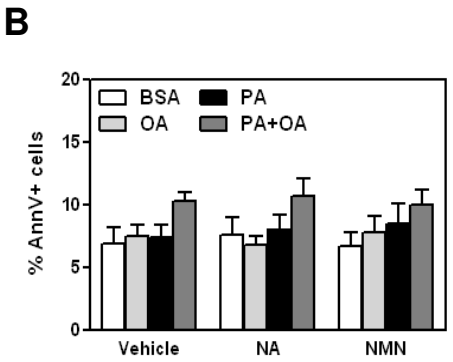
B
BSA
OA
PA
PA+OA
% AnnV+ cells
Vehicle
NA
NMN

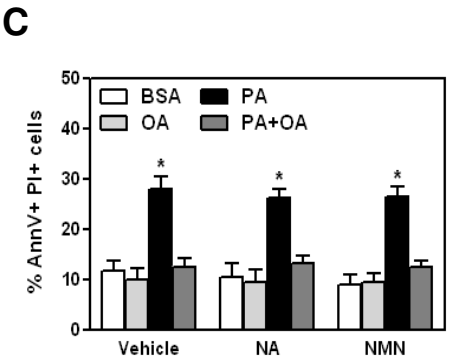
C
BSA
OA
PA
PA+OA
% AnnV+ PI+ cells
Vehicle
NA
NMN

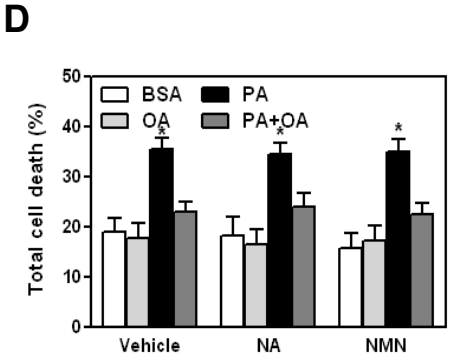
D
BSA
OA
PA
PA+OA
Total cell death (%)
Vehicle
NA
NMN

Figure 3.6. Palmitate-induced HAEC death is not improved by supplementation with NA and NMN.

(A-D) Following a 24 h pre-treatment with medium containing vehicle (0.2% water), 10 μM NA or 1 μM NMN, endothelial cells were incubated for 20 h with medium containing 0.5 mM oleate, 0.5 mM palmitate, or palmitate + oleate (1:1, 0.5 mM) conjugated to BSA (molar ratio, 2:1). Cell survival was assessed by staining with annexin V (AnnV) and propidium iodide (PI), with quantification by flow cytometry. **(A)** Representative dot plots for HAEC are shown. Quadrant analysis was performed to determine **(B)** percent apoptotic (AnnV+) cells (* $p < 0.05$ vs. BSA, OA), **(C)** percent late apoptotic/ necrotic (AnnV+ PI+) cells, and **(D)** total cell death. Data are expressed as mean ± SEM for 4 independent experiments. * $p < 0.05$ vs. BSA, OA, PA+OA.

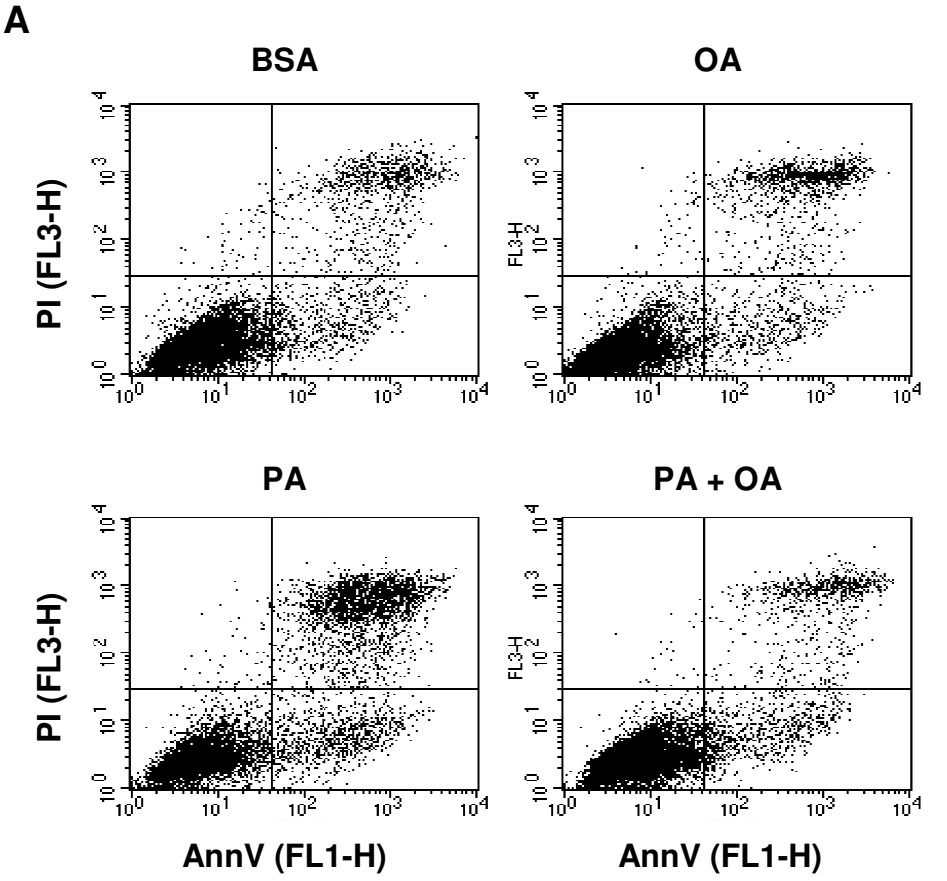
A
BSA
OA
PA
PA + OA
PI (FL3-H)
FL3-H
AnnV (FL1-H)

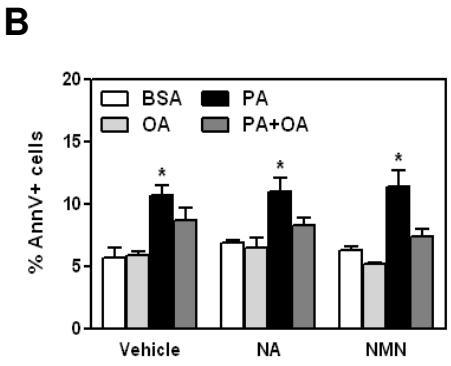
B
BSA
OA
PA
PA+OA
% AnnV+ cells
Vehicle
NA
NMN

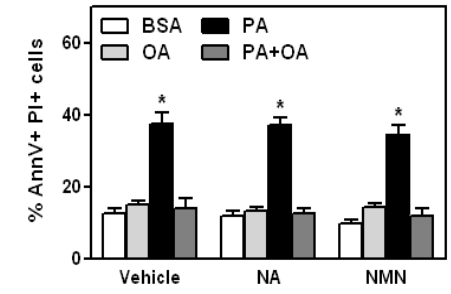
C
BSA
OA
PA
PA+OA
% AnnV+ PI+ cells
Vehicle
NA
NMN

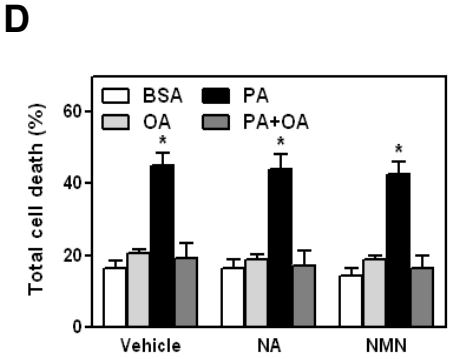
D
BSA
OA
PA
PA+OA
Total cell death (%)
Vehicle
NA
NMN

3.3 NMN efficiently increases cellular NAD^+/NADH ratio, SIRT1 activity, and SIRT2/3 activity

NA and NMN are biosynthetic precursors for NAD^+ synthesis, and supplementation with these molecules has been linked to NAD^+-dependent sirtuin activation in various cell types (Hara et al., 2007; Revollo et al., 2004; Yoshino et al., 2011). We therefore determined whether NA and NMN augmented cellular NAD^+/NADH ratios and activated NAD^+-dependent sirtuins 1 and 2/3 in vascular endothelial cells. SIRT1, 2, and 3 have been associated with improved endothelial function and/or protection from oxidative stress (Bonezzi et al., 2012; Potente et al., 2007; Sundaresan et al., 2008). Having determined that a 2 h incubation with NA and NMN showed the clearest changes in NAD^+/NADH ratio and sirtuin activation, we proceeded with analysis at this timepoint. Intracellular NAD^+/NADH ratio was significantly increased in HMVEC following 2 h treatment with NMN (1 μM) (Figure 3.7A). This was associated with a trend towards increased activation of SIRT1 and activation of SIRT2/3, as assessed by deacetylation of substrate peptides specific for SIRT1 and SIRT2/3, respectively (Figure 3.7B, C). These data are consistent with previous work showing an increase in intracellular NAD^+ content in HAEC within 2 h of supplementation with 1 μM NMN (Borradaile and Pickering, 2009b). In contrast, NA did not alter cellular NAD^+/NADH ratio (Figure 3.7A), and activated only SIRT2/3, (Figure 3.7C). These data differ from the work of Hara et al. (2007) which showed increased intracellular NAD^+ content in HEK293 cells following 6 h treatment with as little as 1 μM NA. It is possible that expression of nicotinic acid phosphoribosyltransferase (Napt) is limited in HMVEC, limiting NAD^+ generation from NA. Taken together, these results suggest that NMN may exert its beneficial effects on HMVEC angiogenic function through increased NAD^+-dependent activation of SIRT1 and SIRT2/3, but that NA likely acts though a different, NAD^+- and SIRT1-independent mechanism.

Figure 3.7. NMN, but not NA, efficiently increases cellular NAD^+/NADH ratio and activates sirtuins.

(A-C) HMVEC were pre-treated for 2 h with medium containing vehicle (0.2% water), 10 μM NA or 1 μM NMN. **(A)** Intracellular NAD^+/NADH ratio for each condition was quantified using a colorimetric enzyme cycling assay. **(B)** SIRT1 and **(C)** SIRT2/3 activation were quantified by measuring conversion of acetylated Flour-de-Lys substrates to a fluorescent product. Data are expressed as mean ± SEM for 3-4 independent experiments. * $p < 0.05$ vs. Vehicle.

A

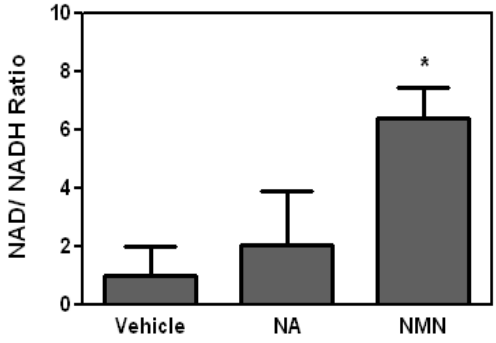
NAD/ NADH Ratio
10
8
6
4
2
0
*
Vehicle
NA
NMN

B

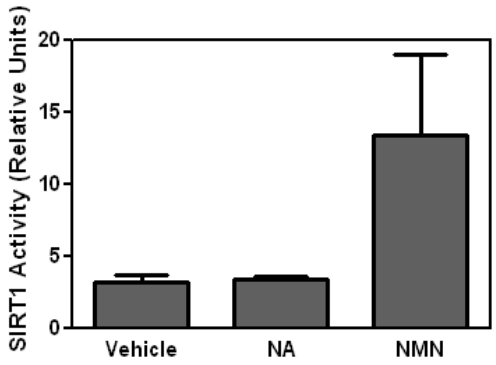
SIRT1 Activity (Relative Units)
20
15
10
5
0
Vehicle
NA
NMN

C

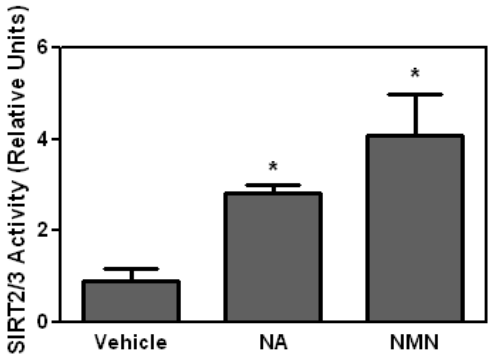
SIRT2/3 Activity (Relative Units)
6
4
2
0
*
*
Vehicle
NA
NMN

3.4 HMVEC fatty acid metabolism is unaltered by NA or NMN supplementation

Activation of SIRT1 and SIRT3 has been linked to alterations in glucose and lipid metabolism in several cell types, including those of the vasculature (Borradaile and Pickering, 2009b; Feige et al., 2008; Hirschey et al., 2010). As some sirtuin activation was observed with supplementation of both NA and NMN (Figure 3.7B, C), we determined whether neutral lipid accumulation and palmitate oxidation rates were also altered. Neutral lipid droplet content was significantly increased in HMVEC exposed to oleate (4.2-fold; $p<0.05$), as has been previously reported (Peter et al., 2008) (Figure 3.8A). However, pre-treatment with NA or NMN did not alter lipid droplets in the presence of palmitate, as assessed by Oil Red O staining (Figure 3.8B). Furthermore, no differences in palmitate oxidation were observed following HMVEC treatment with NA or NMN (Figure 3.8C). These data are consistent with the lack of activation of SIRT1, and suggest that the improved angiogenic function observed with NA and NMN during palmitate overload are not related to SIRT1 mediated changes in fatty acid metabolism.

Figure 3.8. Neither lipid droplet formation nor palmitate oxidation in HMVEC is significantly affected by supplementation with NA or NMN.

(A) Following a 20 h pre-treatment with medium containing vehicle (0.2% water), 10 μM NA or 1 μM NMN, endothelial cells seeded onto coverslips were incubated for a further 6 h with medium containing 0.5 mM oleate, 0.5 mM palmitate, or palmitate + oleate (1:1, 0.5 mM) conjugated to BSA (molar ratio, 2:1). Cells were then fixed and stained with Oil Red O. Representative micrographs of microvascular endothelial cells stained with Oil Red O (red) and DAPI (blue) are shown. Scale bar represents 50 μm. **(B)** Relative lipid droplet contents were assessed for each condition. Three random fields of view were analyzed using ImageJ to calculate the ratio of red (lipid droplet) to blue (nuclei) pixel densities. **(C)** After a 20 h pre-treatment with medium containing water (vehicle), 10 μM NA or 1 μM NMM, rate of palmitate oxidation was determined following a 1 h-incubation with ^{3}H-palmitate. Etomoxir (Eto) was used as a negative control, and AICAR was used as a positive control. Cell lysates were washed with hexane and radioactive counts in the aqueous fraction were quantified by liquid scintillation. Data are expressed as mean ± SEM for 4 independent experiments. * $p < 0.05$ vs. BSA.

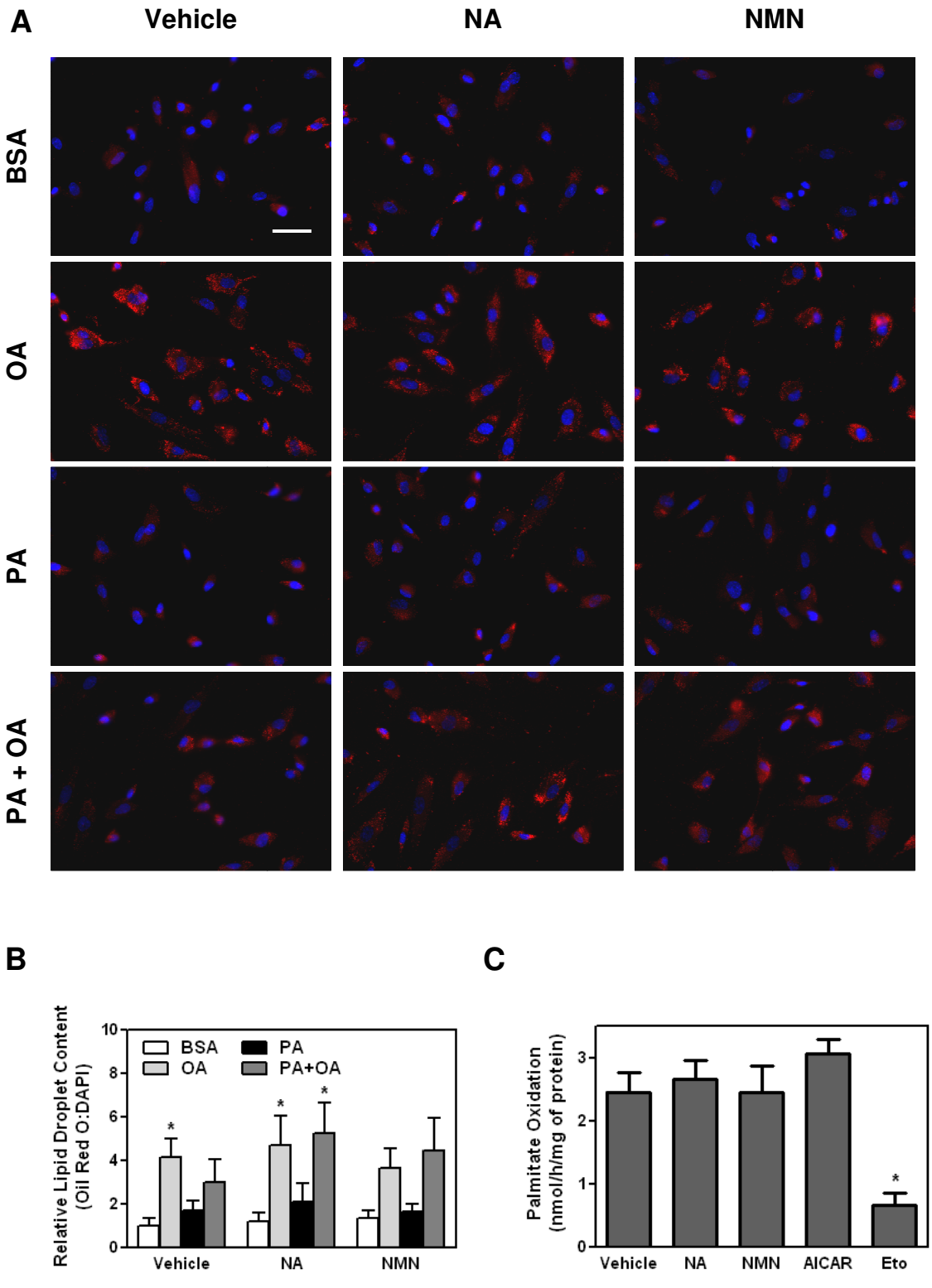
A
Vehicle
NA
NMN
BSA
OA
PA
PA + OA
B
Relative Lipid Droplet Content
(Oil Red O:DAPI)
BSA
OA
PA
PA+OA
Vehicle
NA
NMN
C
Palmitate Oxidation
(nmol/h/mg of protein)
Vehicle
NA
NMN
AICAR
Eto

3.5 HMVEC express the NA receptor, GPR109A, and selective GPR109A activation improves angiogenic function during palmitate overload

Niacin has been used clinically for decades to treat hypertriglyceridemia (Kamanna et al., 2013). The concept that the lipid lowering effects of NA are mediated through its cell surface receptor, GPR109A, is controversial (Lauring et al., 2012; Tunaru et al., 2003). However, the cutaneous flushing observed with pharmaceutical doses of niacin is believed to be mediated by GPR109A (Benyo et al., 2005). Expression of GPR109A, the niacin receptor, has been established in several tissue and cell types, including adipose tissue, epidermis, and various immune cells, but not in endothelial cells (Hanson et al., 2010; Tunaru et al., 2003; Yousefi et al., 2000). Whether the recently reported effects of niacin on revascularization (Huang et al., 2012) involve activation of this receptor in vascular cells is unknown. Thus, we determined whether GPR109A is expressed on HMVEC and whether this receptor could be involved in mediating the beneficial effect of NA on angiogenic function during palmitate overload. Compared to HepG2 cells which are known to express low basal levels of GPR109A (Li et al., 2010), HMVEC exhibited robust expression of GPR109A, independent of NA treatment (Figure 3.9A and B).

Having established that HMVEC express the niacin receptor, we determined whether GRP109A activation with a selective agonist improved tube formation in the presence of palmitate, as we observed for NA. Acifran is a highly selective agonist for GPR109A at concentrations of approximately 1 μM (Jung et al., 2007). Similar to our previous tube formation assays with NA, exposure of HMVEC to excess palmitate significantly reduced total tube length per field of view, but total tube length was maintained at control levels in cells treated with 1 μM acifran prior to exposure to palmitate (Figure 3.10C and 3.1C). In contrast to the earlier tube formation assays, however, palmitate did not impair branch point formation (Figure 3.10B). This may be because total tube length per field of view for HMVEC was markedly decreased (by approximately 1000 μm) following exposure to DMSO, as compared to earlier assays using water as a vehicle (Figure 3.10C and 3.1C). By a direct comparison between DMSO treatment and culture medium alone, we observed that DMSO impaired HMVEC tube formation, even at the low

concentrations used in this study. Nonetheless, we were able to assess the effect of acifran on tube formation during palmitate overload in these experiments. These data suggest that NA may act through its receptor to improve HMVEC angiogenic function during exposure to palmitate.

Figure 3.9. HMVEC exhibit abundant expression of the niacin receptor GPR109A.

(A) GPR109A protein content in HMVEC lysates grown under basal conditions was assessed by immunoblotting. HepG2 human hepatoma cells are known to express low basal levels of GPR109A. For each cell type, 40 μg, 20 μg, or 10 μg of total cell protein were loaded in each lane, as indicated. **(B)** HMVEC were pre-treated for 24 h with medium containing vehicle (0.2% water), 10 μM NA or 1 μM NMN, followed by immunoblotting, as described for **(A)**. Bands corresponding to GPR109A (41 kD) were analyzed by densitometry and normalized to GAPDH (37 kD). Data are expressed as mean ± SEM for 4 independent experiments.

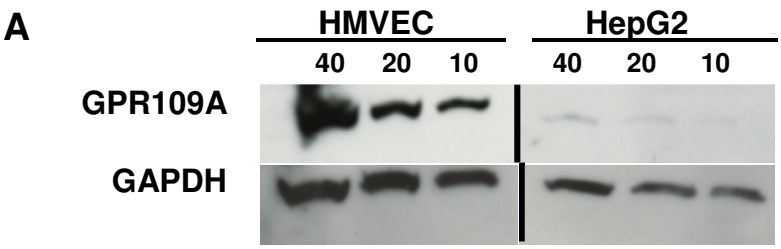
A
HMVEC
HepG2
40
20
10
40
20
10
GPR109A
GAPDH

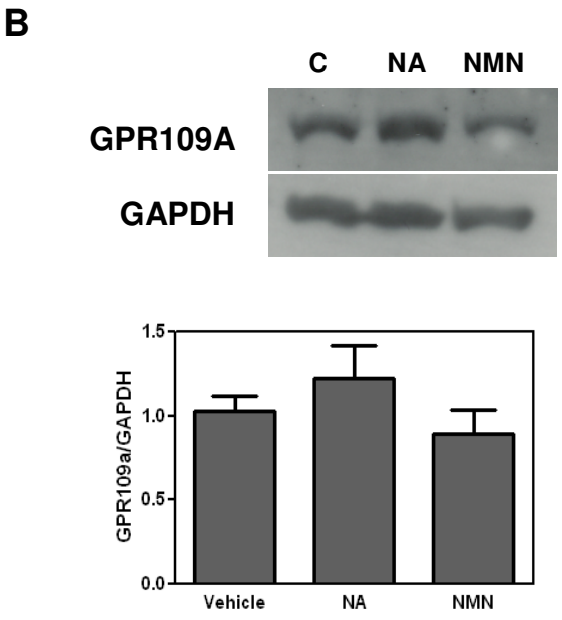
B
C
NA
NMN
GPR109A
GAPDH
GPR109a/GAPDH
1.5
1.0
0.5
0.0
Vehicle
NA
NMN

Figure 3.10. Acifran, a selective GPR109A agonist, improves HMVEC tube formation during palmitate overload.

(A) Following pre-treatment for 24 h in culture medium supplemented with either vehicle (0.2% DMSO) or 1 μM acifran, HMVEC were seeded onto growth factor replete Matrigel and incubated with medium containing BSA or 0.5 mM palmitate conjugated to BSA (molar ratio 2:1). HMVEC were again supplemented with either vehicle or 1 μM acifran, and resulting tube networks were imaged by light microscopy after 18 h. Representative photomicrographs of capillary tubes indicate impaired network formation during palmitate overload, which is improved in the presence of acifran. Scale bar represents 100 μm. **(B, C)** For quantification, three random fields of view per condition were assessed for **(B)** tube branch points, and **(C)** total tube length. Data are expressed as mean ± SEM for 4 independent experiments. * $p < 0.05$ vs. BSA.

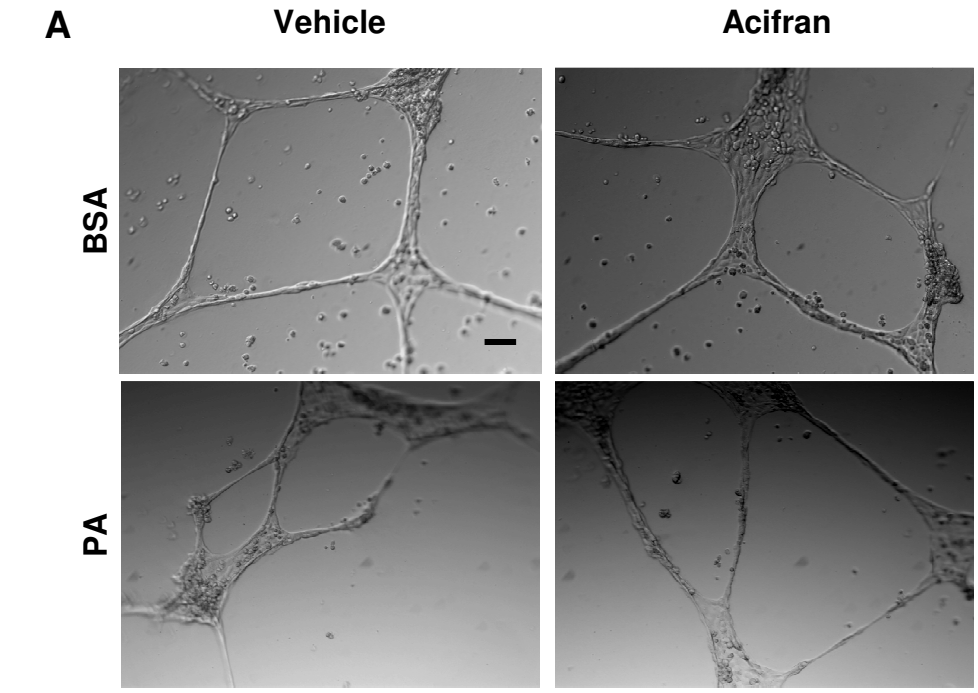
A
Vehicle
Acifran
BSA
PA

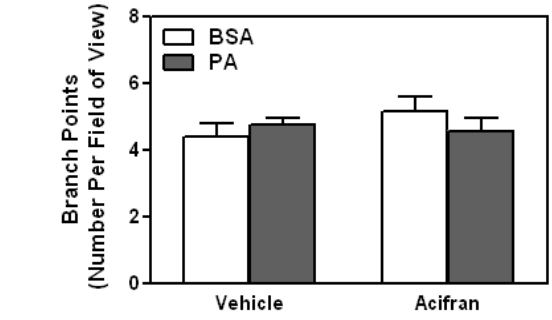
B
Branch Points
(Number Per Field of View)
BSA
PA
0
2
4
6
8
Vehicle
Acifran

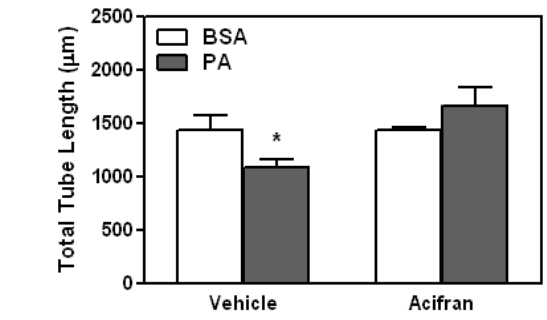
C
Total Tube Length (µm)
BSA
PA
*
0
500
1000
1500
2000
2500
Vehicle
Acifran

3.6 NA supplementation alters expression of a small number of genes in HMVEC

To determine whether niacin supplementation alters expression of sirtuin-related genes, and to identify other potential gene targets, RNA microarray analysis was performed on HMVEC following 24 h pre-treatment with medium containing either vehicle (water) or 10 μM NA. In total, niacin supplementation significantly altered expression of five protein-coding genes at a fold change of > 1.3 (Table 1). Downregulation of EFCAB4B and NAP1L2 in response to niacin treatment were confirmed by qRT-PCR, whereas SIGLEC5, OR13C8 and CYP4Z1 appeared to be below the limits of accurate detection by qRT-PCR. SNORD13P1 is a small nucleolar RNA with unknown function. Reagents for this gene product are not currently commercially available. Although the RNA extraction protocol used was not optimized for small non-coding sequences, an additional thirteen non-coding RNAs with altered expression were detected on the microarray. Functions of the five identified protein-coding genes have been recently studied. EF-Hand Calcium Binding Domain 4B (EFCAB4B) has been associated with inflammation, mediating Ca^{2+} entry into T-cells and contributing to lobular inflammation of the liver during non-alcoholic fatty liver disease (NAFLD) (Chalasani et al., 2010; Srikanth et al., 2010). Nucleosome assembly protein 1 like 2 (NAP1L2) appears to have roles in neural tube formation during embryonic development, and in chromatin modification (Attia et al., 2011). Sialic acid-binding IgG-like lectin 5 (SIGLEC5) has been linked to cell-cell interactions, especially in neutrophils, and has been noted to have roles in angiogenesis in mice (Cornish et al., 1998; Rubinstein et al., 2011). CYP4Z1, a member of the cytochrome P450 enzyme family, is associated with tumour angiogenesis in breast cancer, as well as saturated fatty acid hydroxylation (Yu et al., 2012; Zollner et al., 2009). Olfactory receptor 13C8 (OR13C8) has not yet been studied. Interestingly, none of the identified gene targets have been linked to sirtuin activation, again suggesting that the mechanism of action of NA in endothelial cells is not primarily mediated by sirtuins. In summary, our combined data (Sections 3.1 through 3.6) suggest that niacin has the ability to improve angiogenic function in human endothelial cells during palmitate overload, a process which may be mediated through its receptor, GPR109A, and is likely unrelated to NAD^+-dependent sirtuin activation.

Table 3.1. Altered gene expression in HMVEC treated with NA.

HMVEC were pre-treated for 24 h with growth medium containing either vehicle (0.2% water), or 10 μM NA. Total RNA was extracted and microarray analysis was performed. Transcripts with a fold change > 1.3 (NA vs. vehicle) for 3 independent experiments are shown, $p < 0.05$. Changes in expression were confirmed by qRT-PCR where indicated. No reagents currently exist for SNORD13P1 (N/A, not applicable).

Direction of Gene Regulation	Gene Symbol	Function	p-value	Fold Change (microarray)	Fold Change (qRT-PCR)
Downregulated	NAP1L2	Chromatin modification	0.0048098	-1.34332	-35.0
	EFCAB4B	Ca^{2+} regulation during inflammation	0.0016518	-1.3193	-24.7
Upregulated	SIGLEC5	Cell-cell interactions	0.0234212	1.32142	—
	CYP4Z1	Tumour angiogenesis	0.0257688	1.35765	—
	OR13C8	Unknown	0.0186962	1.35805	—
	SNORD13P1	Unknown	0.0082109	1.43638	N/A

Chapter 4

4 Discussion

4.1 Summary of Results

The vascular complications associated with obesity and metabolic disease result in a large proportion of the morbidity and mortality that accompanies excessive weight gain. EC dysfunction, characterized by impaired functional capacity of the endothelium, precedes the development of vascular disease (Campia et al., 2012). Thus, improving EC function may be a viable target for improving clinical outcomes during obesity. NA has been reported to have vascular benefits that are independent of its role in improving clinical lipid profiles. Since NA has been reported to increase cellular NAD^+ levels (Hara et al., 2007), and since activation of NAD^+-dependent SIRT1 in HAEC improves angiogenic function in high glucose (Borradaile and Pickering, 2009b), it is possible that NA may activate sirtuin pathways in ECs to attenuate dysfunction. However, whether NA can improve EC angiogenic function during saturated fatty acid overload, as is seen in obesity, and by what mechanism this might occur, is unknown. We hypothesized that NA improves vascular EC angiogenic function during lipotoxicity, potentially through NAD^+-dependent pathways.

The major findings of this thesis are as follows. 1) Both NA and NMN improve HMVEC tube formation during palmitate overload. 2) Only NMN efficiently increases cellular NAD^+ levels and activates SIRT1 and SIRT2/3, while NA activates only SIRT2/3. These observations suggest that NA likely improves EC function through an NAD^+- and SIRT1-independent mechanism. 3) HMVEC exhibit robust expression of the NA receptor GPR109A. Selective activation of this receptor recapitulates the effect of NA on tube formation in excess palmitate, suggesting that NA may improve angiogenic function through its endogenous receptor in HMVEC. 4) NA alters gene expression of a small number of genes in HMVEC, which have not been linked previously to NA treatment. These genes may be novel targets of NA action on the vasculature.

4.2 Modulation of EC Function by Activation of Sirtuins

Both NA and NMN can be biosynthetic precursors for NAD^+, and have the potential to activate the NAD^+-dependent sirtuin family of protein deacetylases (Figure 1.3). Although only NMN activated SIRT1, we found that both NA and NMN significantly activated SIRT2/3. Remarkably, NA did not increase cellular NAD^+/NADH ratio in our experiments. However, it is possible that NA selectively increased NAD^+ content in a subcellular compartment without a detectable change in total cellular levels. The mitochondrial Nmnat isoform, Nmnat-3 (Berger et al., 2005), has been shown to contribute to the conversion of NA to NAD^+ within the mitochondria. Further supporting this concept, Di Lisa and Ziegler (2001) showed that mitochondrial NAD^+ stores do not readily leak across mitochondrial membranes, and could therefore locally activate mitochondrial SIRT3. We are currently unable to test this possibility because of a lack of available reagents to measure either SIRT2 activity or SIRT3 activity independently.

In contrast to NA, it appears likely that NMN improves HMVEC angiogenic function through a SIRT1-dependent mechanism. As expected based on previous reports of NMN as an NAD^+ precursor, NMN increased HMVEC intracellular NAD^+/NADH ratio, and activated both SIRT1 and SIRT2/3. Consistent with our observations of improved EC angiogenic function with NMN pre-treatment, other studies have shown that SIRT1 activity in ECs is critical to angiogenic function (Borradaile and Pickering, 2009b; Potente et al., 2007). SIRT1 inhibits the transcription factor FOXO1 in HUVEC, repressing its anti-angiogenic activity on several genes involved in vascular growth, maturation, and remodeling (Potente et al., 2007). SIRT1 activation by NMN could also improve EC function through reduction of oxidative stress (Ota et al., 2007).

SIRT2 activation, though largely unstudied, has been implicated in the promotion of EC migration (Bonezzi et al., 2012), but also in the inhibition of tumour angiogenesis (Kim et al., 2013). With regard to cell survival, selective inhibition of SIRT2 in HUVEC decreases H_2O_2-induced oxidative stress, improving cell viability (Liu et al., 2013). Based on our findings, neither NA nor NMN increased EC migration under any condition. Furthermore, no known SIRT2-regulated genes were identified in our gene

expression microarray analysis of NA treated cells. Taken together, our data are inconsistent with SIRT2 activation.

Similar to our conclusions regarding NA activation of SIRT1 and SIRT2, our gene expression microarray data does not support the concept of robust NA activation of SIRT3, as no known SIRT3 targets were identified. However, this does not preclude SIRT3 activation as a possible mechanism whereby NA improves HMVEC tube formation during lipotoxicity. Although SIRT3 has been implicated in increased fatty acid oxidation (Hirschey et al., 2010), and protection from genotoxic stress and apoptosis (Yang et al., 2007), we observed neither of these effects in our experiments. Rather, the most likely role of SIRT3 would be in the reduction of ROS generation, resulting in a functional improvement during palmitate overload. As a mitochondrial sirtuin, SIRT3 regulates the activities of several mitochondrial proteins, resulting decreased in ROS production (Lombard et al., 2007). Through its deacetylase activity, SIRT3 has been shown to modulate activity of the ROS scavenger superoxide dismutase, as well as several components of the electron transport chain and the citric acid cycle (Greer et al., 2012). Since increased EC ROS production during palmitate overload appears to be a key mechanism in the development of lipotoxicity (Chinen et al., 2007), SIRT3-mediated decreases in ROS could improve EC function. Further experiments are required to determine whether palmitate-induced ROS accumulation and oxidative stress are diminished in NA-treated EC.

4.3 Modulation of EC Function by Activation of GPR109A

GPR109A activation has been implicated in several beneficial effects of NA treatment. In particular, GPR109A activation by NA has anti-inflammatory and antiatherogenic effects (Digby et al., 2012; Lukasova et al., 2011). However, these effects appear to be mediated through GPR109A activation in monocytes and macrophages. Despite acknowledgment of the potential for the direct involvement of the endothelium in NA-mediated antiatherogenic and anti-inflammatory effects, EC have been thought not to express GPR109A (Offermanns, 2012). Here we report for the first time that HMVEC robustly express GPR109A and that the beneficial effects of NA on in vitro angiogenic function during lipotoxicity could be partly due to GPR109A activation.

As a G_i-class G-protein, GPR109A activation inhibits adenylyl cyclase (AC), resulting in decreased cellular cAMP levels and decreased protein kinase A (PKA) activity. Activation of this signalling pathway has been shown to affect cells in the vasculature. GPR109A-mediated AC inhibition in neutrophils increases apoptosis, potentially impacting the atherogenic inflammatory response (Kostylina et al., 2008). Although the mechanism for GPR109A-mediated cholesterol efflux from macrophages, via upregulation of ABCA1 and ABCG1, has yet to be fully elucidated, it appears that cAMP may also be suppressed in this cell type, (Chai et al., 2013). GPR109A signaling has not yet been studied in cell types that comprise the vessel wall (EC and vascular smooth muscle cells).

GPR109A expression at the cell surface is regulated by β-arrestin-mediated internalization and recycling in response to ligand binding (Krupnick and Benovic, 1998). In addition to receptor desensitization, β-arrestins have been shown to activate separate cell signaling pathways following GPCR activation. Both β-arrestin 1 and 2 can interact with $I_\kappa B\alpha$, leading to decreased NF-κB activity and modulation of the associated inflammatory pathway (Gao et al., 2004; Witherow et al., 2004). Additionally, β-arrestin 1 has the ability to translocate to the nucleus following GPCR activation and directly act on promoters to alter gene transcription (Kang et al., 2005). Although these pathways have not been directly studied in relation to GPR109A, they could contribute to some of the observed effects of receptor activation.

Although GPR109A activation has not been studied in EC, activation of GPR109A-associated pathways in other cell types have been linked to improved angiogenic potential. del Valle-Perez et al. (2004) showed that cAMP analogs and activators of AC inhibited transforming growth factor-β (TGFβ)-induced in vitro angiogenesis in HUVEC, without affecting cell viability. In addition, prostaglandin E_2 (PGE_2), a product of GPR109A-mediated cyclooxygenase activation, has been shown to induce in vitro tube formation in HMVEC, via upregulation of chemokine receptor 4 (CXCR4) (Salcedo et al., 2003). Interestingly, and in contrast to del Valle-Perez et al. (2004), activation of adeylyl cyclase in this HMVEC model also increased tube formation. β-arrestin-mediated inhibition of NF-κB could also play a role in improving EC function. As a master

regulator of inflammation, NF-κB has been linked to the inflammatory state during obesity-associated vascular disease, and to the development of oxidative stress and ROS generation (Rahman and Fazal, 2011). Thus, suppression of NF-κB via GPR109A activation represents a possible pathway by which NA could improve HMVEC angiogenic function. Although the known targets of these pathways can result in alterations in gene transcription that were not observed in our microarray analysis, we cannot exclude their potential involvement without further investigation.

4.4 NA- Induced Changes in EC Gene Expression

Few studies have been conducted regarding the alterations in EC gene expression following NA treatment. Ganji et al. (2009) demonstrated that NA treatment of HAEC resulted in decreased protein expression of vascular cell adhesion molecule-1 (VCAM-1), and impairment of several other pathways involved in inflammation, but the doses of NA used were 25-100X pharmacological levels observed in plasma. Lukasova et al. (2011) also demonstrated a decrease in VCAM-1 and P-selectin expression in aortic vessel walls of mice treated with NA, that contributed to the antiatherogenic benefits of NA treatment. However, these changes in expression were not specifically attributed to endothelial cells. This thesis is the first report of gene expression analysis following exposure of HMVEC to a pharmacologically relevant concentration of NA.

Remarkably, of the five coding RNAs identified by our microarray screen as altered by NA treatment, EFCAB4B, SIGLEC5 and CYP4Z1 all have documented roles in metabolic disease or angiogenesis. Studies by Srikanth et al. (2010) suggest that downregulation of EFCAB4B, as we observed with NA treatment in HMVEC, decreases store-operated Ca^{2+} entry and subsequent activation of T-cells, thereby reducing the inflammatory response. A recent genome-wide association study also recently identified variants of EFCAB4B in non-alcoholic fatty liver disease (NAFLD) patients with lobular inflammation (Chalasani et al., 2010). Presumably, downregulation or impairment of EFCAB4B would also reduce inflammation in the setting of NAFLD. Since inflammation plays a key role in the development and progression of endothelial dysfunction and damage, and vascular disease, it is possible that NA-mediated downregulation of EFCAB4B could improve EC function in vivo during metabolic disease. In fact, Ca^{2+}

influx in EC during metabolic disease contributes to cell dysfunction and apoptosis (Smith and Schnellmann, 2012), and the clinical use of calcium channel blockers has been demonstrated to improve EC dysfunction during fatty acid overload (Yasu et al., 2013). Increased expression of the sialic acid binding Ig-like lectin, SIGLEC5, and the cytochrome P450, CYP4Z1, have both been linked to increased angiogenesis (Rubinstein et al., 2011; Yu et al., 2012), providing two other possible downstream effectors of NA in HMVEC.

Small nucleolar RNAs (snoRNA) are non-coding RNAs (ncRNA) of 60-300 base pairs which function as components of small nucleolar ribonucleoproteins to post-transcriptionally modify ribosomal RNAs (Esteller, 2011). Although SNORD13P1 and the other ncRNAs identified in our microarray analysis have not been studied, accumulating evidence indicates that altered expression of ncRNAs contributes to metabolic and vascular disease (Esteller, 2011). MicroRNAs (miRNAs), in particular, have important identified roles in the regulation of glucose and lipid metabolism (Fernandez-Hernando et al., 2013) and in the control of angiogenesis (Dang et al., 2013). Moreover, three snoRNAs were recently implicated in cellular response to fatty acid-induced oxidative stress (Michel et al., 2011). Given the reported roles of ncRNAs in metabolic disease and angiogenesis to date, it is plausible that some of our observations with NA may be a result of altered ncRNA expression.

Figure 4.1. Working model for the effects of NA, compared to NMN, on EC lipotoxicity.

(A) Consistent with previous reports, NMN augmented HMVEC cellular NAD^+ content, and activated SIRT2/3 and perhaps SIRT1. Although no alterations in cell survival, palmitate β-oxidation, or cytosolic lipid droplet formation were observed with NMN, HMVEC angiogenic function may be improved through SIRT1 and SIRT3-mediated ROS reduction, or through direct SIRT1-mediated effects on angiogenesis. **(B)** In contrast, NA-induced improvements in HMVEC angiogenic function in excess palmitate may be in part mediated by GPR109A. The mechanism by which GPR109A might improve angiogenic function requires further investigation, as does the potential involvement of decreased expression of EFCAB4B and NAP1L2, which may improve HMVEC response to palmitate through novel pathways. The activation of SIRT2/3 by NA may also improve HMVEC function, although our data is not entirely consistent with this mechanism.

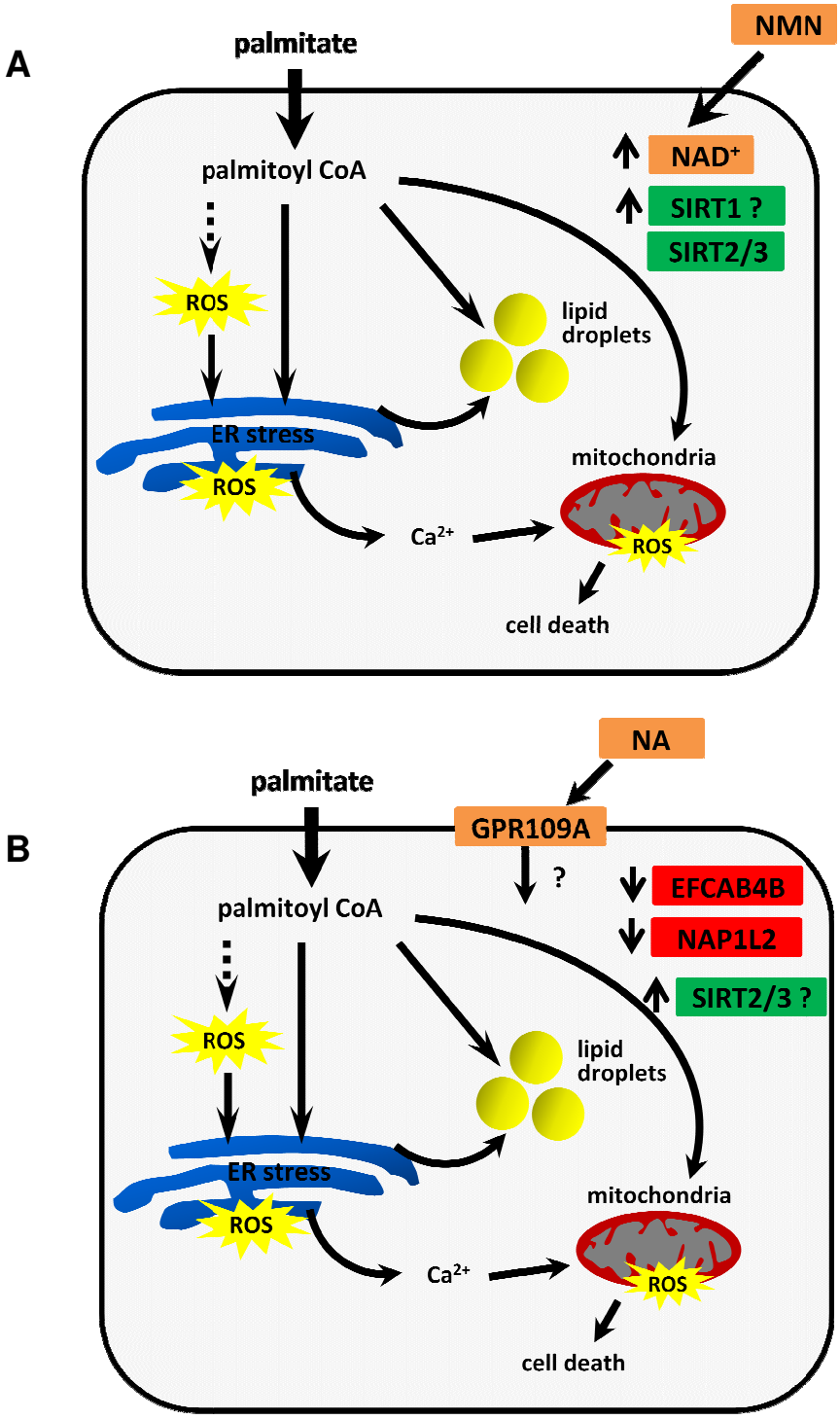
A
palmitate
NMN
palmitoyl CoA
NAD+
SIRT1 ?
SIRT2/3
ROS
lipid
droplets
ER stress
ROS
mitochondria
Ca2+
ROS
cell death
B
NA
palmitate
GPR109A
?
palmitoyl CoA
EFCAB4B
NAP1L2
SIRT2/3 ?
ROS
lipid
droplets
ER stress
ROS
mitochondria
Ca2+
ROS
cell death

4.5 Future Directions

Our working model for the effects of NA and NMN supplementation on HMVEC during saturated fatty acid excess is summarized in Figure 4.1. Based on this model, and our evidence of NA-mediated gene expression alterations in HMVEC, several future experiments are warranted.

In light the heterogeneity of EC from different tissues and vessel types (Aird, 2007), I would like to extend these findings to other vascular EC. In particular, I would like to determine whether GPR109A is expressed on other EC types, including HAEC and human coronary artery EC (HCAEC), by immunoblotting.

Based on our tube formation assays with acifran, it appears that GPR109A activation is at least partly responsible for the observed benefits of NA in HMVEC. However, to further confirm the role of GPR109A in vascular improvements under fatty acid overload, I would like to use a GPR109A antagonist to block receptor activation in HMVEC, followed by NA treatment and the tube formation assay as described earlier. Since no GPR109A antagonists currently exist, inhibiting GPR109A via transfection of small interfering RNA (siRNA) against the mRNA would be an alternate approach.

Our microarray analysis identified several genes with altered expression in HMVEC following NA treatment. Confirmation of whether these gene targets are biologically relevant in the protection of EC from fatty acid overload induced dysfunction will be important follow-up experiments. Knockdown or overexpression of these genes in EC, followed by in vitro analysis of angiogenesis by tube formation assay, with and without NA treatment, could determine whether these genes play a role.

Although our RNA extraction protocol was not optimized for the isolation of ncRNAs, our microarray analysis revealed that several ncRNAs were altered by NA treatment of HMVEC. Considering the documented roles of ncRNAs in metabolic disease (Esteller, 2011), a miRNA gene array of NA-treated HMVEC could be useful in identifying other non-coding gene products that may contribute to improved EC function with NA treatment.

Our data indicate that NA can improve in vitro EC tube formation during palmitate overload. I would like to extend these findings in vivo. A hind limb ischemia model can be used to assess vascular regeneration and angiogenesis in mice (Frontini et al., 2008). Following induction of obesity by a high fat diet to mimic the onset of human metabolic syndrome, a femoral artery ligation to induce ischemia can be performed in a single hind limb. Vascular regeneration, assessed by histology and functional recovery of blood flow and limb use, can be compared between mice treated with NA versus vehicle. GPR109A is known to be expressed in murine tissues (Tunaru et al., 2003). I would like to determine by immunoblotting whether GPR109A (also known as PUMA-G in mice) is expressed in mouse endothelium. Furthermore, to elucidate whether any observed benefits conferred by NA to murine vascular regeneration in obese mice are mediated by GPR109A, hind limb ischemia studies could be performed in a GPR109A$^{-/-}$ mouse model.

References

Abularrage, C.J., A.N. Sidawy, G. Aidinian, N. Singh, J.M. Weiswasser, and S. Arora. 2005. Evaluation of the microcirculation in vascular disease. *Journal of vascular surgery*. 42:574-581.

Adam-Vizi, V., and C. Chinopoulos. 2006. Bioenergetics and the formation of mitochondrial reactive oxygen species. *Trends in pharmacological sciences*. 27:639-645.

Ahmed, K., S. Tunaru, and S. Offermanns. 2009. GPR109A, GPR109B and GPR81, a family of hydroxy-carboxylic acid receptors. *Trends in pharmacological sciences*. 30:557-562.

Aird, W.C. 2007. Phenotypic heterogeneity of the endothelium: I. Structure, function, and mechanisms. *Circulation research*. 100:158-173.

Alberti, K.G., R.H. Eckel, S.M. Grundy, P.Z. Zimmet, J.I. Cleeman, K.A. Donato, J.C. Fruchart, W.P. James, C.M. Loria, S.C. Smith, Jr., E. International Diabetes Federation Task Force on, Prevention, L. Hational Heart, I. Blood, A. American Heart, F. World Heart, S. International Atherosclerosis, and O. International Association for the Study of. 2009. Harmonizing the metabolic syndrome: a joint interim statement of the International Diabetes Federation Task Force on Epidemiology and Prevention; National Heart, Lung, and Blood Institute; American Heart Association; World Heart Federation; International Atherosclerosis Society; and International Association for the Study of Obesity. *Circulation*. 120:1640-1645.

Altschul, R., A. Hoffer, and J.D. Stephen. 1955. Influence of nicotinic acid on serum cholesterol in man. *Archives of biochemistry and biophysics*. 54:558-559.

Asselbergs, F.W., Y. Guo, E.P. van Iperen, S. Sivapalaratnam, V. Tragante, M.B. Lanktree, L.A. Lange, B. Almoguera, Y.E. Appelman, J. Barnard, J. Baumert, A.L. Beitelshees, T.R. Bhangale, Y.D. Chen, T.R. Gaunt, Y. Gong, J.C. Hopewell, T. Johnson, M.E. Kleber, T.Y. Langaee, M. Li, Y.R. Li, K. Liu, C.W. McDonough, M.F. Meijs, R.P. Middelberg, K. Musunuru, C.P. Nelson, J.R. O'Connell, S. Padmanabhan, J.S. Pankow, N. Pankratz, S. Rafelt, R. Rajagopalan, S.P. Romaine, N.J. Schork, J. Shaffer, H. Shen, E.N. Smith, S.E. Tischfield, P.J. van der Most, J.V. van Vliet-Ostaptchouk, N. Verweij, K.A. Volcik, L. Zhang, K.R. Bailey, K.M. Bailey, F. Bauer, J.M. Boer, P.S. Braund, A. Burt, P.R. Burton, S.G. Buxbaum, W. Chen, R.M. Cooper-Dehoff, L.A. Cupples, J.S. deJong, C. Delles, D. Duggan, M. Fornage, C.E. Furlong, N. Glazer, J.G. Gums, C. Hastie, M.V. Holmes, T. Illig, S.A. Kirkland, M. Kivimaki, R. Klein, B.E. Klein, C. Kooperberg, K. Kottke-Marchant, M. Kumari, A.Z. LaCroix, L. Mallela, G. Murugesan, J. Ordovas, W.H. Ouwehand, W.S. Post, R. Saxena, H. Scharnagl, P.J. Schreiner, T. Shah, D.C. Shields, D. Shimbo, S.R. Srinivasan, R.P. Stolk, D.I.

Swerdlow, H.A. Taylor, Jr., E.J. Topol, E. Toskala, J.L. van Pelt, J. van Setten, S. Yusuf, J.C. Whittaker, A.H. Zwinderman, S. LifeLines Cohort, S.S. Anand, A.J. Balmforth, G.S. Berenson, et al. 2012. Large-scale gene-centric meta-analysis across 32 studies identifies multiple lipid loci. *American journal of human genetics*. 91:823-838.

Assini, J.M., E.E. Mulvihill, B.G. Sutherland, D.E. Telford, C.G. Sawyez, S.L. Felder, S. Chhoker, J.Y. Edwards, R. Gros, and M.W. Huff. 2013. Naringenin prevents cholesterol-induced systemic inflammation, metabolic dysregulation, and atherosclerosis in Ldlr(-)/(-) mice. *Journal of lipid research*. 54:711-724.

Attia, M., A. Forster, C. Rachez, P. Freemont, P. Avner, and U.C. Rogner. 2011. Interaction between nucleosome assembly protein 1-like family members. *Journal of molecular biology*. 407:647-660.

Avalos, J.L., K.M. Bever, and C. Wolberger. 2005. Mechanism of sirtuin inhibition by nicotinamide: altering the NAD(+) cosubstrate specificity of a Sir2 enzyme. *Molecular cell*. 17:855-868.

Baur, J.A., K.J. Pearson, N.L. Price, H.A. Jamieson, C. Lerin, A. Kalra, V.V. Prabhu, J.S. Allard, G. Lopez-Lluch, K. Lewis, P.J. Pistell, S. Poosala, K.G. Becker, O. Boss, D. Gwinn, M. Wang, S. Ramaswamy, K.W. Fishbein, R.G. Spencer, E.G. Lakatta, D. Le Couteur, R.J. Shaw, P. Navas, P. Puigserver, D.K. Ingram, R. de Cabo, and D.A. Sinclair. 2006. Resveratrol improves health and survival of mice on a high-calorie diet. *Nature*. 444:337-342.

Bays, H.E., J.M. Gonzalez-Campoy, G.A. Bray, A.E. Kitabchi, D.A. Bergman, A.B. Schorr, H.W. Rodbard, and R.R. Henry. 2008. Pathogenic potential of adipose tissue and metabolic consequences of adipocyte hypertrophy and increased visceral adiposity. *Expert review of cardiovascular therapy*. 6:343-368.

Belenky, P., F.G. Racette, K.L. Bogan, J.M. McClure, J.S. Smith, and C. Brenner. 2007. Nicotinamide riboside promotes Sir2 silencing and extends lifespan via Nrk and Urh1/Pnp1/Meu1 pathways to NAD+. *Cell*. 129:473-484.

Bensaad, K., and K.H. Vousden. 2007. p53: new roles in metabolism. *Trends in cell biology*. 17:286-291.

Benyo, Z., A. Gille, J. Kero, M. Csiky, M.C. Suchankova, R.M. Nusing, A. Moers, K. Pfeffer, and S. Offermanns. 2005. GPR109A (PUMA-G/HM74A) mediates nicotinic acid-induced flushing. *The Journal of clinical investigation*. 115:3634-3640.

Berger, F., C. Lau, M. Dahlmann, and M. Ziegler. 2005. Subcellular compartmentation and differential catalytic properties of the three human nicotinamide mononucleotide adenylyltransferase isoforms. *The Journal of biological chemistry*. 280:36334-36341.

Bieganowski, P., and C. Brenner. 2004. Discoveries of nicotinamide riboside as a nutrient and conserved NRK genes establish a Preiss-Handler independent route to NAD+ in fungi and humans. *Cell*. 117:495-502.

Bigornia, S.J., M.M. Mott, D.T. Hess, C.M. Apovian, M.E. McDonnell, M.A. Duess, M.A. Kluge, A.J. Fiscale, J.A. Vita, and N. Gokce. 2010. Long-term successful weight loss improves vascular endothelial function in severely obese individuals. *Obesity*. 18:754-759.

Blander, G., and L. Guarente. 2004. The Sir2 family of protein deacetylases. *Annual review of biochemistry*. 73:417-435.

Bocci, G., A. Fioravanti, P. Orlandi, T. Di Desidero, G. Natale, G. Fanelli, P. Viacava, A.G. Naccarato, G. Francia, and R. Danesi. 2012. Metronomic ceramide analogs inhibit angiogenesis in pancreatic cancer through up-regulation of caveolin-1 and thrombospondin-1 and down-regulation of cyclin D1. *Neoplasia*. 14:833-845.

Bonezzi, K., D. Belotti, B.J. North, C. Ghilardi, P. Borsotti, A. Resovi, P. Ubezio, A. Riva, R. Giavazzi, E. Verdin, and G. Taraboletti. 2012. Inhibition of SIRT2 potentiates the anti-motility activity of taxanes: implications for antineoplastic combination therapies. *Neoplasia*. 14:846-854.

Bordone, L., D. Cohen, A. Robinson, M.C. Motta, E. van Veen, A. Czopik, A.D. Steele, H. Crowe, S. Marmor, J. Luo, W. Gu, and L. Guarente. 2007. SIRT1 transgenic mice show phenotypes resembling calorie restriction. *Aging cell*. 6:759-767.

Borra, M.T., B.C. Smith, and J.M. Denu. 2005. Mechanism of human SIRT1 activation by resveratrol. *The Journal of biological chemistry*. 280:17187-17195.

Borradaile, N.M., X. Han, J.D. Harp, S.E. Gale, D.S. Ory, and J.E. Schaffer. 2006. Disruption of endoplasmic reticulum structure and integrity in lipotoxic cell death. *Journal of lipid research*. 47:2726-2737.

Borradaile, N.M., and J.G. Pickering. 2009a. NAD(+), sirtuins, and cardiovascular disease. *Current pharmaceutical design*. 15:110-117.

Borradaile, N.M., and J.G. Pickering. 2009b. Nicotinamide phosphoribosyltransferase imparts human endothelial cells with extended replicative lifespan and enhanced angiogenic capacity in a high glucose environment. *Aging cell*. 8:100-112.

Borradaile, N.M., and J.G. Pickering. 2010. Polyploidy impairs human aortic endothelial cell function and is prevented by nicotinamide phosphoribosyltransferase. *American journal of physiology. Cell physiology*. 298:C66-74.

Breslow, J.L. 1996. Mouse models of atherosclerosis. *Science*. 272:685-688.

Brookheart, R.T., C.I. Michel, and J.E. Schaffer. 2009. As a matter of fat. *Cell metabolism*. 10:9-12.

Brunet, A., L.B. Sweeney, J.F. Sturgill, K.F. Chua, P.L. Greer, Y. Lin, H. Tran, S.E. Ross, R. Mostoslavsky, H.Y. Cohen, L.S. Hu, H.L. Cheng, M.P. Jedrychowski, S.P. Gygi, D.A. Sinclair, F.W. Alt, and M.E. Greenberg. 2004. Stress-dependent regulation of FOXO transcription factors by the SIRT1 deacetylase. *Science*. 303:2011-2015.

Burnett, C., S. Valentini, F. Cabreiro, M. Goss, M. Somogyvari, M.D. Piper, M. Hoddinott, G.L. Sutphin, V. Leko, J.J. McElwee, R.P. Vazquez-Manrique, A.M. Orfila, D. Ackerman, C. Au, G. Vinti, M. Riesen, K. Howard, C. Neri, A. Bedalov, M. Kaeberlein, C. Soti, L. Partridge, and D. Gems. 2011. Absence of effects of Sir2 overexpression on lifespan in C. elegans and Drosophila. *Nature*. 477:482-485.

Campia, U., M. Tesauro, and C. Cardillo. 2012. Human obesity and endothelium-dependent responsiveness. *British journal of pharmacology*. 165:561-573.

Canto, C., Z. Gerhart-Hines, J.N. Feige, M. Lagouge, L. Noriega, J.C. Milne, P.J. Elliott, P. Puigserver, and J. Auwerx. 2009. AMPK regulates energy expenditure by modulating NAD+ metabolism and SIRT1 activity. *Nature*. 458:1056-1060.

Canto, C., R.H. Houtkooper, E. Pirinen, D.Y. Youn, M.H. Oosterveer, Y. Cen, P.J. Fernandez-Marcos, H. Yamamoto, P.A. Andreux, P. Cettour-Rose, K. Gademann, C. Rinsch, K. Schoonjans, A.A. Sauve, and J. Auwerx. 2012. The NAD(+) precursor nicotinamide riboside enhances oxidative metabolism and protects against high-fat diet-induced obesity. *Cell metabolism*. 15:838-847.

Carlson, L.A. 1960. Studies on the incorporation of injected palmitic acid-I-C into liver and plasma lipids in man. *Acta Societatis Medicorum Upsaliensis*. 65:85-90.

Carlson, L.A. 1963. Studies on the effect of nicotinic acid on catecholamine stimulated lipolysis in adipose tissue in vitro. *Acta medica Scandinavica*. 173:719-722.

Carlson, L.A. 2005. Nicotinic acid: the broad-spectrum lipid drug. A 50th anniversary review. *Journal of internal medicine*. 258:94-114.

Carlson, L.A., and L. Oro. 1962. The effect of nicotinic acid on the plasma free fatty acid; demonstration of a metabolic type of sympathicolysis. *Acta medica Scandinavica*. 172:641-645.

Carrero, J.J., and R.F. Grimble. 2006. Does nutrition have a role in peripheral vascular disease? *The British journal of nutrition*. 95:217-229.

Chai, J.T., J.E. Digby, and R.P. Choudhury. 2013. GPR109A and vascular inflammation. *Current atherosclerosis reports*. 15:325.

Chalasani, N., X. Guo, R. Loomba, M.O. Goodarzi, T. Haritunians, S. Kwon, J. Cui, K.D. Taylor, L. Wilson, O.W. Cummings, Y.D. Chen, J.I. Rotter, and N. Nonalcoholic Steatohepatitis Clinical Research. 2010. Genome-wide association study identifies

variants associated with histologic features of nonalcoholic Fatty liver disease. *Gastroenterology*. 139:1567-1576, 1576 e1561-1566.

Cheng, H.L., R. Mostoslavsky, S. Saito, J.P. Manis, Y. Gu, P. Patel, R. Bronson, E. Appella, F.W. Alt, and K.F. Chua. 2003. Developmental defects and p53 hyperacetylation in Sir2 homolog (SIRT1)-deficient mice. *Proceedings of the National Academy of Sciences of the United States of America*. 100:10794-10799.

Chinen, I., M. Shimabukuro, K. Yamakawa, N. Higa, T. Matsuzaki, K. Noguchi, S. Ueda, M. Sakanashi, and N. Takasu. 2007. Vascular lipotoxicity: endothelial dysfunction via fatty-acid-induced reactive oxygen species overproduction in obese Zucker diabetic fatty rats. *Endocrinology*. 148:160-165.

Chu, K., M. Miyazaki, W.C. Man, and J.M. Ntambi. 2006. Stearoyl-coenzyme A desaturase 1 deficiency protects against hypertriglyceridemia and increases plasma high-density lipoprotein cholesterol induced by liver X receptor activation. *Molecular and cellular biology*. 26:6786-6798.

Ciapaite, J., J. van Bezu, G. van Eikenhorst, S.J. Bakker, T. Teerlink, M. Diamant, R.J. Heine, K. Krab, H.V. Westerhoff, and C.G. Schalkwijk. 2007. Palmitate and oleate have distinct effects on the inflammatory phenotype of human endothelial cells. *Biochimica et biophysica acta*. 1771:147-154.

Claria, J. 2006. Regulation of cell proliferation and apoptosis by bioactive lipid mediators. *Recent patents on anti-cancer drug discovery*. 1:369-382.

Cohen, H.Y., C. Miller, K.J. Bitterman, N.R. Wall, B. Hekking, B. Kessler, K.T. Howitz, M. Gorospe, R. de Cabo, and D.A. Sinclair. 2004. Calorie restriction promotes mammalian cell survival by inducing the SIRT1 deacetylase. *Science*. 305:390-392.

Cornish, A.L., S. Freeman, G. Forbes, J. Ni, M. Zhang, M. Cepeda, R. Gentz, M. Augustus, K.C. Carter, and P.R. Crocker. 1998. Characterization of siglec-5, a novel glycoprotein expressed on myeloid cells related to CD33. *Blood*. 92:2123-2132.

Dagher, Z., N. Ruderman, K. Tornheim, and Y. Ido. 1999. The effect of AMP-activated protein kinase and its activator AICAR on the metabolism of human umbilical vein endothelial cells. *Biochemical and biophysical research communications*. 265:112-115.

Dagher, Z., N. Ruderman, K. Tornheim, and Y. Ido. 2001. Acute regulation of fatty acid oxidation and amp-activated protein kinase in human umbilical vein endothelial cells. *Circulation research*. 88:1276-1282.

Dai, J.M., Z.Y. Wang, D.C. Sun, R.X. Lin, and S.Q. Wang. 2007. SIRT1 interacts with p73 and suppresses p73-dependent transcriptional activity. *Journal of cellular physiology*. 210:161-166.

Dali-Youcef, N., M. Lagouge, S. Froelich, C. Koehl, K. Schoonjans, and J. Auwerx. 2007. Sirtuins: the 'magnificent seven', function, metabolism and longevity. *Annals of medicine*. 39:335-345.

Dang, L.T., N.D. Lawson, and J.E. Fish. 2013. MicroRNA control of vascular endothelial growth factor signaling output during vascular development. *Arteriosclerosis, thrombosis, and vascular biology*. 33:193-200.

de Boer, V.C., M.C. de Goffau, I.C. Arts, P.C. Hollman, and J. Keijer. 2006. SIRT1 stimulation by polyphenols is affected by their stability and metabolism. *Mechanisms of ageing and development*. 127:618-627.

del Valle-Perez, B., O.M. Martinez-Estrada, S. Vilaro, F. Ventura, and F. Vinals. 2004. cAMP inhibits TGFbeta1-induced in vitro angiogenesis. *FEBS letters*. 569:105-111.

Di Lisa, F., and M. Ziegler. 2001. Pathophysiological relevance of mitochondria in NAD(+) metabolism. *FEBS letters*. 492:4-8.

Digby, J.E., F. Martinez, A. Jefferson, N. Ruparelia, J. Chai, M. Wamil, D.R. Greaves, and R.P. Choudhury. 2012. Anti-inflammatory effects of nicotinic acid in human monocytes are mediated by GPR109A dependent mechanisms. *Arteriosclerosis, thrombosis, and vascular biology*. 32:669-676.

Eaton, R.P., M. Berman, and D. Steinberg. 1969. Kinetic studies of plasma free fatty acid and triglyceride metabolism in man. *The Journal of clinical investigation*. 48:1560-1579.

El-Mesallamy, H.O., D.H. Kassem, E. El-Demerdash, and A.I. Amin. 2011. Vaspin and visfatin/Nampt are interesting interrelated adipokines playing a role in the pathogenesis of type 2 diabetes mellitus. *Metabolism: clinical and experimental*. 60:63-70.

Esteller, M. 2011. Non-coding RNAs in human disease. *Nature reviews. Genetics*. 12:861-874.

Feige, J.N., M. Lagouge, C. Canto, A. Strehle, S.M. Houten, J.C. Milne, P.D. Lambert, C. Mataki, P.J. Elliott, and J. Auwerx. 2008. Specific SIRT1 activation mimics low energy levels and protects against diet-induced metabolic disorders by enhancing fat oxidation. *Cell metabolism*. 8:347-358.

Fernandez-Hernando, C., C.M. Ramirez, L. Goedeke, and Y. Suarez. 2013. MicroRNAs in metabolic disease. *Arteriosclerosis, thrombosis, and vascular biology*. 33:178-185.

Finkel, T., C.X. Deng, and R. Mostoslavsky. 2009. Recent progress in the biology and physiology of sirtuins. *Nature*. 460:587-591.

Frontini, M., Z.X. Nong, M. Drangova, R. Gros, and J.G. Pickering. 2008. Fibroblast Growth Factor-9 Stabilizes Angiogenesis and Generates Vasoresponsive Microvessels. *Circulation*. 118:S449-S449.

Ganji, S.H., S. Qin, L. Zhang, V.S. Kamanna, and M.L. Kashyap. 2009. Niacin inhibits vascular oxidative stress, redox-sensitive genes, and monocyte adhesion to human aortic endothelial cells. *Atherosclerosis*. 202:68-75.

Ganji, S.H., S. Tavintharan, D. Zhu, Y. Xing, V.S. Kamanna, and M.L. Kashyap. 2004. Niacin noncompetitively inhibits DGAT2 but not DGAT1 activity in HepG2 cells. *Journal of lipid research*. 45:1835-1845.

Gao, H., Y. Sun, Y. Wu, B. Luan, Y. Wang, B. Qu, and G. Pei. 2004. Identification of beta-arrestin2 as a G protein-coupled receptor-stimulated regulator of NF-kappaB pathways. *Molecular cell*. 14:303-317.

Gerhart-Hines, Z., J.T. Rodgers, O. Bare, C. Lerin, S.H. Kim, R. Mostoslavsky, F.W. Alt, Z. Wu, and P. Puigserver. 2007. Metabolic control of muscle mitochondrial function and fatty acid oxidation through SIRT1/PGC-1alpha. *The EMBO journal*. 26:1913-1923.

Gordon, E.S. 1960. Non-Esterified Fatty Acids in the Blood of Obese and Lean Subjects. *American Journal of Clinical Nutrition*. 8:740-747.

Greer, S.N., J.L. Metcalf, Y. Wang, and M. Ohh. 2012. The updated biology of hypoxia-inducible factor. *The EMBO journal*. 31:2448-2460.

Guarente, L. 2006. Sirtuins as potential targets for metabolic syndrome. *Nature*. 444:868-874.

Hamilton, S.J., G.T. Chew, T.M. Davis, and G.F. Watts. 2010. Niacin improves small artery vasodilatory function and compliance in statin-treated type 2 diabetic patients. *Diabetes & vascular disease research : official journal of the International Society of Diabetes and Vascular Disease*. 7:296-299.

Hanson, J., A. Gille, S. Zwykiel, M. Lukasova, B.E. Clausen, K. Ahmed, S. Tunaru, A. Wirth, and S. Offermanns. 2010. Nicotinic acid- and monomethyl fumarate-induced flushing involves GPR109A expressed by keratinocytes and COX-2-dependent prostanoid formation in mice. *The Journal of clinical investigation*. 120:2910-2919.

Hara, N., K. Yamada, T. Shibata, H. Osago, T. Hashimoto, and M. Tsuchiya. 2007. Elevation of cellular NAD levels by nicotinic acid and involvement of nicotinic acid phosphoribosyltransferase in human cells. *The Journal of biological chemistry*. 282:24574-24582.

Helies-Toussaint, C., S. Gambert, P. Roller, S. Tricot, B. Lacour, and A. Grynberg. 2006. Lipid metabolism in human endothelial cells. *Biochimica et biophysica acta*. 1761:765-774.

Hernandez, C., M. Molusky, Y. Li, S. Li, and J.D. Lin. 2010. Regulation of hepatic ApoC3 expression by PGC-1beta mediates hypolipidemic effect of nicotinic acid. *Cell metabolism*. 12:411-419.

Hirschey, M.D., T. Shimazu, E. Goetzman, E. Jing, B. Schwer, D.B. Lombard, C.A. Grueter, C. Harris, S. Biddinger, O.R. Ilkayeva, R.D. Stevens, Y. Li, A.K. Saha, N.B. Ruderman, J.R. Bain, C.B. Newgard, R.V. Farese, Jr., F.W. Alt, C.R. Kahn, and E. Verdin. 2010. SIRT3 regulates mitochondrial fatty-acid oxidation by reversible enzyme deacetylation. *Nature*. 464:121-125.

Hirschey, M.D., T. Shimazu, E. Jing, C.A. Grueter, A.M. Collins, B. Aouizerat, A. Stancakova, E. Goetzman, M.M. Lam, B. Schwer, R.D. Stevens, M.J. Muehlbauer, S. Kakar, N.M. Bass, J. Kuusisto, M. Laakso, F.W. Alt, C.B. Newgard, R.V. Farese, Jr., C.R. Kahn, and E. Verdin. 2011. SIRT3 deficiency and mitochondrial protein hyperacetylation accelerate the development of the metabolic syndrome. *Molecular cell*. 44:177-190.

Houtkooper, R.H., C. Canto, R.J. Wanders, and J. Auwerx. 2010. The secret life of NAD+: an old metabolite controlling new metabolic signaling pathways. *Endocrine reviews*. 31:194-223.

Hu, M., W.C. Chu, S. Yamashita, D.K. Yeung, L. Shi, D. Wang, D. Masuda, Y. Yang, and B. Tomlinson. 2012. Liver fat reduction with niacin is influenced by DGAT-2 polymorphisms in hypertriglyceridemic patients. *Journal of lipid research*. 53:802-809.

Huang, P.H., C.P. Lin, C.H. Wang, C.H. Chiang, H.Y. Tsai, J.S. Chen, F.Y. Lin, H.B. Leu, T.C. Wu, J.W. Chen, and S.J. Lin. 2012. Niacin improves ischemia-induced neovascularization in diabetic mice by enhancement of endothelial progenitor cell functions independent of changes in plasma lipids. *Angiogenesis*. 15:377-389.

Imai, S., C.M. Armstrong, M. Kaeberlein, and L. Guarente. 2000. Transcriptional silencing and longevity protein Sir2 is an NAD-dependent histone deacetylase. *Nature*. 403:795-800.

Inoguchi, T., P. Li, F. Umeda, H.Y. Yu, M. Kakimoto, M. Imamura, T. Aoki, T. Etoh, T. Hashimoto, M. Naruse, H. Sano, H. Utsumi, and H. Nawata. 2000. High glucose level and free fatty acid stimulate reactive oxygen species production through protein kinase C--dependent activation of NAD(P)H oxidase in cultured vascular cells. *Diabetes*. 49:1939-1945.

Irizarry, R.A., B.M. Bolstad, F. Collin, L.M. Cope, B. Hobbs, and T.P. Speed. 2003. Summaries of Affymetrix GeneChip probe level data. *Nucleic acids research*. 31:e15.

Jackson, T.M., J.M. Rawling, B.D. Roebuck, and J.B. Kirkland. 1995. Large supplements of nicotinic acid and nicotinamide increase tissue NAD+ and poly(ADP-ribose) levels but do not affect diethylnitrosamine-induced altered hepatic foci in Fischer-344 rats. *The Journal of nutrition*. 125:1455-1461.

Jenuwein, T., and C.D. Allis. 2001. Translating the histone code. *Science*. 293:1074-1080.

Jin, F.Y., V.S. Kamanna, and M.L. Kashyap. 1999. Niacin accelerates intracellular ApoB degradation by inhibiting triacylglycerol synthesis in human hepatoblastoma (HepG2) cells. *Arteriosclerosis, thrombosis, and vascular biology*. 19:1051-1059.

Jing, E., S. Gesta, and C.R. Kahn. 2007. SIRT2 regulates adipocyte differentiation through FoxO1 acetylation/deacetylation. *Cell metabolism*. 6:105-114.

Jung, J.K., B.R. Johnson, T. Duong, M. Decaire, J. Uy, T. Gharbaoui, P.D. Boatman, C.R. Sage, R. Chen, J.G. Richman, D.T. Connolly, and G. Semple. 2007. Analogues of acifran: agonists of the high and low affinity niacin receptors, GPR109a and GPR109b. *Journal of medicinal chemistry*. 50:1445-1448.

Kaeberlein, M., M. McVey, and L. Guarente. 1999. The SIR2/3/4 complex and SIR2 alone promote longevity in Saccharomyces cerevisiae by two different mechanisms. *Genes & development*. 13:2570-2580.

Kamanna, V.S., S.H. Ganji, and M.L. Kashyap. 2013. Recent advances in niacin and lipid metabolism. *Current opinion in lipidology*. 24:239-245.

Kang, J., Y. Shi, B. Xiang, B. Qu, W. Su, M. Zhu, M. Zhang, G. Bao, F. Wang, X. Zhang, R. Yang, F. Fan, X. Chen, G. Pei, and L. Ma. 2005. A nuclear function of beta-arrestin1 in GPCR signaling: regulation of histone acetylation and gene transcription. *Cell*. 123:833-847.

Kim, D.J., L.A. Martinez-Lemus, and G.E. Davis. 2013. EB1, p150Glued, and Clasp1 control endothelial tubulogenesis through microtubule assembly, acetylation, and apical polarization. *Blood*. 121:3521-3530.

Kim, J.E., Y.W. Kim, I.K. Lee, J.Y. Kim, Y.J. Kang, and S.Y. Park. 2008. AMP-activated protein kinase activation by 5-aminoimidazole-4-carboxamide-1-beta-D-ribofuranoside (AICAR) inhibits palmitate-induced endothelial cell apoptosis through reactive oxygen species suppression. *Journal of pharmacological sciences*. 106:394-403.

Kostylina, G., D. Simon, M.F. Fey, S. Yousefi, and H.U. Simon. 2008. Neutrophil apoptosis mediated by nicotinic acid receptors (GPR109A). *Cell death and differentiation*. 15:134-142.

Koves, T.R., J.R. Ussher, R.C. Noland, D. Slentz, M. Mosedale, O. Ilkayeva, J. Bain, R. Stevens, J.R. Dyck, C.B. Newgard, G.D. Lopaschuk, and D.M. Muoio. 2008.

Mitochondrial overload and incomplete fatty acid oxidation contribute to skeletal muscle insulin resistance. *Cell metabolism*. 7:45-56.

Kris-Etherton, P.M., and S. Yu. 1997. Individual fatty acid effects on plasma lipids and lipoproteins: human studies. *The American journal of clinical nutrition*. 65:1628S-1644S.

Krupnick, J.G., and J.L. Benovic. 1998. The role of receptor kinases and arrestins in G protein-coupled receptor regulation. *Annual review of pharmacology and toxicology*. 38:289-319.

Kume, S., M. Haneda, K. Kanasaki, T. Sugimoto, S. Araki, K. Isshiki, M. Isono, T. Uzu, L. Guarente, A. Kashiwagi, and D. Koya. 2007. SIRT1 inhibits transforming growth factor beta-induced apoptosis in glomerular mesangial cells via Smad7 deacetylation. *The Journal of biological chemistry*. 282:151-158.

Lagouge, M., C. Argmann, Z. Gerhart-Hines, H. Meziane, C. Lerin, F. Daussin, N. Messadeq, J. Milne, P. Lambert, P. Elliott, B. Geny, M. Laakso, P. Puigserver, and J. Auwerx. 2006. Resveratrol improves mitochondrial function and protects against metabolic disease by activating SIRT1 and PGC-1alpha. *Cell*. 127:1109-1122.

Landry, J., J.T. Slama, and R. Sternglanz. 2000a. Role of NAD(+) in the deacetylase activity of the SIR2-like proteins. *Biochemical and biophysical research communications*. 278:685-690.

Landry, J., A. Sutton, S.T. Tafrov, R.C. Heller, J. Stebbins, L. Pillus, and R. Sternglanz. 2000b. The silencing protein SIR2 and its homologs are NAD-dependent protein deacetylases. *Proceedings of the National Academy of Sciences of the United States of America*. 97:5807-5811.

Lauring, B., A.K. Taggart, J.R. Tata, R. Dunbar, L. Caro, K. Cheng, J. Chin, S.L. Colletti, J. Cote, S. Khalilieh, J. Liu, W.L. Luo, A.A. Maclean, L.B. Peterson, A.B. Polis, W. Sirah, T.J. Wu, X. Liu, L. Jin, K. Wu, P.D. Boatman, G. Semple, D.P. Behan, D.T. Connolly, E. Lai, J.A. Wagner, S.D. Wright, C. Cuffie, Y.B. Mitchel, D.J. Rader, J.F. Paolini, M.G. Waters, and A. Plump. 2012. Niacin lipid efficacy is independent of both the niacin receptor GPR109A and free fatty acid suppression. *Science translational medicine*. 4:148ra115.

Levine, G.N., J.F. Keaney, Jr., and J.A. Vita. 1995. Cholesterol reduction in cardiovascular disease. Clinical benefits and possible mechanisms. *The New England journal of medicine*. 332:512-521.

Li, X., J.S. Millar, N. Brownell, F. Briand, and D.J. Rader. 2010. Modulation of HDL metabolism by the niacin receptor GPR109A in mouse hepatocytes. *Biochemical pharmacology*. 80:1450-1457.

Li, X., S. Zhang, G. Blander, J.G. Tse, M. Krieger, and L. Guarente. 2007. SIRT1 deacetylates and positively regulates the nuclear receptor LXR. *Molecular cell*. 28:91-106.

Liang, C.C., A.Y. Park, and J.L. Guan. 2007. In vitro scratch assay: a convenient and inexpensive method for analysis of cell migration in vitro. *Nature protocols*. 2:329-333.

Lim, S.S., R.J. Norman, M.J. Davies, and L.J. Moran. 2013. The effect of obesity on polycystic ovary syndrome: a systematic review and meta-analysis. *Obesity reviews : an official journal of the International Association for the Study of Obesity*. 14:95-109.

Listenberger, L.L., X. Han, S.E. Lewis, S. Cases, R.V. Farese, Jr., D.S. Ory, and J.E. Schaffer. 2003. Triglyceride accumulation protects against fatty acid-induced lipotoxicity. *Proceedings of the National Academy of Sciences of the United States of America*. 100:3077-3082.

Listenberger, L.L., D.S. Ory, and J.E. Schaffer. 2001. Palmitate-induced apoptosis can occur through a ceramide-independent pathway. *The Journal of biological chemistry*. 276:14890-14895.

Liu, J., X. Wu, X. Wang, Y. Zhang, P. Bu, Q. Zhang, and F. Jiang. 2013. Global Gene Expression Profiling Reveals Functional Importance of Sirt2 in Endothelial Cells under Oxidative Stress. *International journal of molecular sciences*. 14:5633-5649.

Lombard, D.B., F.W. Alt, H.L. Cheng, J. Bunkenborg, R.S. Streeper, R. Mostoslavsky, J. Kim, G. Yancopoulos, D. Valenzuela, A. Murphy, Y. Yang, Y. Chen, M.D. Hirschey, R.T. Bronson, M. Haigis, L.P. Guarente, R.V. Farese, Jr., S. Weissman, E. Verdin, and B. Schwer. 2007. Mammalian Sir2 homolog SIRT3 regulates global mitochondrial lysine acetylation. *Molecular and cellular biology*. 27:8807-8814.

Lopaschuk, G.D., S.R. Wall, P.M. Olley, and N.J. Davies. 1988. Etomoxir, a carnitine palmitoyltransferase I inhibitor, protects hearts from fatty acid-induced ischemic injury independent of changes in long chain acylcarnitine. *Circulation research*. 63:1036-1043.

Lu, Y., L. Qian, Q. Zhang, B. Chen, L. Gui, D. Huang, G. Chen, and L. Chen. 2013. Palmitate induces apoptosis in mouse aortic endothelial cells and endothelial dysfunction in mice fed high-calorie and high-cholesterol diets. *Life sciences*.

Lukasova, M., C. Malaval, A. Gille, J. Kero, and S. Offermanns. 2011. Nicotinic acid inhibits progression of atherosclerosis in mice through its receptor GPR109A expressed by immune cells. *The Journal of clinical investigation*. 121:1163-1173.

Luo, J., A.Y. Nikolaev, S. Imai, D. Chen, F. Su, A. Shiloh, L. Guarente, and W. Gu. 2001. Negative control of p53 by Sir2alpha promotes cell survival under stress. *Cell*. 107:137-148.

Maciejewski-Lenoir, D., J.G. Richman, Y. Hakak, I. Gaidarov, D.P. Behan, and D.T. Connolly. 2006. Langerhans cells release prostaglandin D2 in response to nicotinic acid. *The Journal of investigative dermatology*. 126:2637-2646.

Manduteanu, I., and M. Simionescu. 2012. Inflammation in atherosclerosis: a cause or a result of vascular disorders? *Journal of cellular and molecular medicine*. 16:1978-1990.

Maric, C., and J.E. Hall. 2011. Obesity, metabolic syndrome and diabetic nephropathy. *Contributions to nephrology*. 170:28-35.

Masuoka, H.C., and N. Chalasani. 2013. Nonalcoholic fatty liver disease: an emerging threat to obese and diabetic individuals. *Annals of the New York Academy of Sciences*. 1281:106-122.

Matsen, F.A., 3rd, C.R. Wyss, L.R. Pedegana, R.B. Krugmire, Jr., C.W. Simmons, R.V. King, and E.M. Burgess. 1980. Transcutaneous oxygen tension measurement in peripheral vascular disease. *Surgery, gynecology & obstetrics*. 150:525-528.

Mattu, H.S., and H.S. Randeva. 2013. Role of adipokines in cardiovascular disease. *The Journal of endocrinology*. 216:T17-36.

Menon, R.M., M.H. Adams, M.A. Gonzalez, D.S. Tolbert, J.H. Leu, and E.A. Cefali. 2007. Plasma and urine pharmacokinetics of niacin and its metabolites from an extended-release niacin formulation. *International journal of clinical pharmacology and therapeutics*. 45:448-454.

Michan, S., and D. Sinclair. 2007. Sirtuins in mammals: insights into their biological function. *The Biochemical journal*. 404:1-13.

Michel, C.I., C.L. Holley, B.S. Scruggs, R. Sidhu, R.T. Brookheart, L.L. Listenberger, M.A. Behlke, D.S. Ory, and J.E. Schaffer. 2011. Small nucleolar RNAs U32a, U33, and U35a are critical mediators of metabolic stress. *Cell metabolism*. 14:33-44.

Motta, M.C., N. Divecha, M. Lemieux, C. Kamel, D. Chen, W. Gu, Y. Bultsma, M. McBurney, and L. Guarente. 2004. Mammalian SIRT1 represses forkhead transcription factors. *Cell*. 116:551-563.

Mugabo, Y., Y. Mukaneza, and G. Renier. 2011. Palmitate induces C-reactive protein expression in human aortic endothelial cells. Relevance to fatty acid-induced endothelial dysfunction. *Metabolism: clinical and experimental*. 60:640-648.

Muoio, D.M., and C.B. Newgard. 2006. Obesity-related derangements in metabolic regulation. *Annual review of biochemistry*. 75:367-401.

Nikolopoulou, A., and N.P. Kadoglou. 2012. Obesity and metabolic syndrome as related to cardiovascular disease. *Expert review of cardiovascular therapy*. 10:933-939.

Nishina, P.M., J. Verstuyft, and B. Paigen. 1990. Synthetic low and high fat diets for the study of atherosclerosis in the mouse. *Journal of lipid research*. 31:859-869.

Nisoli, E., C. Tonello, A. Cardile, V. Cozzi, R. Bracale, L. Tedesco, S. Falcone, A. Valerio, O. Cantoni, E. Clementi, S. Moncada, and M.O. Carruba. 2005. Calorie restriction promotes mitochondrial biogenesis by inducing the expression of eNOS. *Science*. 310:314-317.

Nogueiras, R., K.M. Habegger, N. Chaudhary, B. Finan, A.S. Banks, M.O. Dietrich, T.L. Horvath, D.A. Sinclair, P.T. Pfluger, and M.H. Tschop. 2012. Sirtuin 1 and sirtuin 3: physiological modulators of metabolism. *Physiological reviews*. 92:1479-1514.

O'Reilly, J.R., and R.M. Reynolds. 2013. The risk of maternal obesity to the long-term health of the offspring. *Clinical endocrinology*. 78:9-16.

Odegaard, J.I., and A. Chawla. 2013. Pleiotropic actions of insulin resistance and inflammation in metabolic homeostasis. *Science*. 339:172-177.

Offermanns, S. 2012. It ain't over 'til the fat lady sings. *Science translational medicine*. 4:148fs130.

Onyango, P., I. Celic, J.M. McCaffery, J.D. Boeke, and A.P. Feinberg. 2002. SIRT3, a human SIR2 homologue, is an NAD-dependent deacetylase localized to mitochondria. *Proceedings of the National Academy of Sciences of the United States of America*. 99:13653-13658.

Ostrander, D.B., G.C. Sparagna, A.A. Amoscato, J.B. McMillin, and W. Dowhan. 2001. Decreased cardiolipin synthesis corresponds with cytochrome c release in palmitate-induced cardiomyocyte apoptosis. *The Journal of biological chemistry*. 276:38061-38067.

Ota, H., M. Akishita, M. Eto, K. Iijima, M. Kaneki, and Y. Ouchi. 2007. Sirt1 modulates premature senescence-like phenotype in human endothelial cells. *Journal of molecular and cellular cardiology*. 43:571-579.

Peter, A., C. Weigert, H. Staiger, K. Rittig, A. Cegan, P. Lutz, F. Machicao, H.U. Haring, and E. Schleicher. 2008. Induction of stearoyl-CoA desaturase protects human arterial endothelial cells against lipotoxicity. *American journal of physiology. Endocrinology and metabolism*. 295:E339-349.

Pfluger, P.T., D. Herranz, S. Velasco-Miguel, M. Serrano, and M.H. Tschop. 2008. Sirt1 protects against high-fat diet-induced metabolic damage. *Proceedings of the National Academy of Sciences of the United States of America*. 105:9793-9798.

Potente, M., L. Ghaeni, D. Baldessari, R. Mostoslavsky, L. Rossig, F. Dequiedt, J. Haendeler, M. Mione, E. Dejana, F.W. Alt, A.M. Zeiher, and S. Dimmeler. 2007. SIRT1 controls endothelial angiogenic functions during vascular growth. *Genes & development*. 21:2644-2658.

Preiss, J., and P. Handler. 1958a. Biosynthesis of diphosphopyridine nucleotide. I. Identification of intermediates. *The Journal of biological chemistry*. 233:488-492.

Preiss, J., and P. Handler. 1958b. Biosynthesis of diphosphopyridine nucleotide. II. Enzymatic aspects. *The Journal of biological chemistry*. 233:493-500.

Purushotham, A., T.T. Schug, Q. Xu, S. Surapureddi, X. Guo, and X. Li. 2009. Hepatocyte-specific deletion of SIRT1 alters fatty acid metabolism and results in hepatic steatosis and inflammation. *Cell metabolism*. 9:327-338.

Rahman, A., and F. Fazal. 2011. Blocking NF-kappaB: an inflammatory issue. *Proceedings of the American Thoracic Society*. 8:497-503.

Ramsey, K.M., K.F. Mills, A. Satoh, and S. Imai. 2008. Age-associated loss of Sirt1-mediated enhancement of glucose-stimulated insulin secretion in beta cell-specific Sirt1-overexpressing (BESTO) mice. *Aging cell*. 7:78-88.

Revollo, J.R., A.A. Grimm, and S. Imai. 2004. The NAD biosynthesis pathway mediated by nicotinamide phosphoribosyltransferase regulates Sir2 activity in mammalian cells. *The Journal of biological chemistry*. 279:50754-50763.

Revollo, J.R., A. Korner, K.F. Mills, A. Satoh, T. Wang, A. Garten, B. Dasgupta, Y. Sasaki, C. Wolberger, R.R. Townsend, J. Milbrandt, W. Kiess, and S. Imai. 2007. Nampt/PBEF/Visfatin regulates insulin secretion in beta cells as a systemic NAD biosynthetic enzyme. *Cell metabolism*. 6:363-375.

Rodgers, J.T., C. Lerin, W. Haas, S.P. Gygi, B.M. Spiegelman, and P. Puigserver. 2005. Nutrient control of glucose homeostasis through a complex of PGC-1alpha and SIRT1. *Nature*. 434:113-118.

Rodgers, J.T., and P. Puigserver. 2007. Fasting-dependent glucose and lipid metabolic response through hepatic sirtuin 1. *Proceedings of the National Academy of Sciences of the United States of America*. 104:12861-12866.

Rubic, T., M. Trottmann, and R.L. Lorenz. 2004. Stimulation of CD36 and the key effector of reverse cholesterol transport ATP-binding cassette A1 in monocytoid cells by niacin. *Biochemical pharmacology*. 67:411-419.

Rubinstein, E., J.Y. Cho, P. Rosenthal, J. Chao, M. Miller, A. Pham, S.S. Aceves, A. Varki, and D.H. Broide. 2011. Siglec-F inhibition reduces esophageal eosinophilia and angiogenesis in a mouse model of eosinophilic esophagitis. *Journal of pediatric gastroenterology and nutrition*. 53:409-416.

Salcedo, R., X. Zhang, H.A. Young, N. Michael, K. Wasserman, W.H. Ma, M. Martins-Green, W.J. Murphy, and J.J. Oppenheim. 2003. Angiogenic effects of prostaglandin E2 are mediated by up-regulation of CXCR4 on human microvascular endothelial cells. *Blood*. 102:1966-1977.

Satoh, A., L. Stein, and S. Imai. 2011. The role of mammalian sirtuins in the regulation of metabolism, aging, and longevity. *Handbook of experimental pharmacology*. 206:125-162.

Schaub, A., A. Futterer, and K. Pfeffer. 2001. PUMA-G, an IFN-gamma-inducible gene in macrophages is a novel member of the seven transmembrane spanning receptor superfamily. *European journal of immunology*. 31:3714-3725.

Scher, M.B., A. Vaquero, and D. Reinberg. 2007. SirT3 is a nuclear NAD+-dependent histone deacetylase that translocates to the mitochondria upon cellular stress. *Genes & development*. 21:920-928.

Schreyer, S.A., D.L. Wilson, and R.C. LeBoeuf. 1998. C57BL/6 mice fed high fat diets as models for diabetes-accelerated atherosclerosis. *Atherosclerosis*. 136:17-24.

Schweiger, M., K. Hennig, F. Lerner, M. Niere, M. Hirsch-Kauffmann, T. Specht, C. Weise, S.L. Oei, and M. Ziegler. 2001. Characterization of recombinant human nicotinamide mononucleotide adenylyl transferase (NMNAT), a nuclear enzyme essential for NAD synthesis. *FEBS letters*. 492:95-100.

Schwer, B., B.J. North, R.A. Frye, M. Ott, and E. Verdin. 2002. The human silent information regulator (Sir)2 homologue hSIRT3 is a mitochondrial nicotinamide adenine dinucleotide-dependent deacetylase. *The Journal of cell biology*. 158:647-657.

Schwer, B., and E. Verdin. 2008. Conserved metabolic regulatory functions of sirtuins. *Cell metabolism*. 7:104-112.

Shao, S., Y. Yang, G. Yuan, M. Zhang, and X. Yu. 2013. Signaling molecules involved in lipid-induced pancreatic beta-cell dysfunction. *DNA and cell biology*. 32:41-49.

Shi, T., F. Wang, E. Stieren, and Q. Tong. 2005. SIRT3, a mitochondrial sirtuin deacetylase, regulates mitochondrial function and thermogenesis in brown adipocytes. *The Journal of biological chemistry*. 280:13560-13567.

Simionescu, M. 2007. Implications of early structural-functional changes in the endothelium for vascular disease. *Arteriosclerosis, thrombosis, and vascular biology*. 27:266-274.

Simionescu, M., N. Simionescu, and G.E. Palade. 1975. Segmental differentiations of cell junctions in the vascular endothelium. The microvasculature. *The Journal of cell biology*. 67:863-885.

Simionescu, M., N. Simionescu, and G.E. Palade. 1976. Segmental differentiations of cell junctions in the vascular endothelium. Arteries and veins. *The Journal of cell biology*. 68:705-723.

Smith, J.S., C.B. Brachmann, I. Celic, M.A. Kenna, S. Muhammad, V.J. Starai, J.L. Avalos, J.C. Escalante-Semerena, C. Grubmeyer, C. Wolberger, and J.D. Boeke. 2000. A phylogenetically conserved NAD+-dependent protein deacetylase activity in the Sir2 protein family. *Proceedings of the National Academy of Sciences of the United States of America*. 97:6658-6663.

Smith, M.A., and R.G. Schnellmann. 2012. Calpains, mitochondria, and apoptosis. *Cardiovascular research*. 96:32-37.

Soriguer, F., S. Garcia-Serrano, J.M. Garcia-Almeida, L. Garrido-Sanchez, J. Garcia-Arnes, F.J. Tinahones, I. Cardona, J. Rivas-Marin, J.L. Gallego-Perales, and E. Garcia-Fuentes. 2009. Changes in the serum composition of free-fatty acids during an intravenous glucose tolerance test. *Obesity*. 17:10-15.

Sparks, J.D., C.E. Sparks, and K. Adeli. 2012. Selective hepatic insulin resistance, VLDL overproduction, and hypertriglyceridemia. *Arteriosclerosis, thrombosis, and vascular biology*. 32:2104-2112.

Spinnler, R., T. Gorski, K. Stolz, S. Schuster, A. Garten, A.G. Beck-Sickinger, M.A. Engelse, E.J. de Koning, A. Korner, W. Kiess, and K. Maedler. 2013. The adipocytokine Nampt and its product NMN have no effect on beta-cell survival but potentiate glucose stimulated insulin secretion. *PloS one*. 8:e54106.

Srikanth, S., H.J. Jung, K.D. Kim, P. Souda, J. Whitelegge, and Y. Gwack. 2010. A novel EF-hand protein, CRACR2A, is a cytosolic Ca2+ sensor that stabilizes CRAC channels in T cells. *Nature cell biology*. 12:436-446.

Staiger, H., K. Staiger, N. Stefan, H.G. Wahl, F. Machicao, M. Kellerer, and H.U. Haring. 2004. Palmitate-induced interleukin-6 expression in human coronary artery endothelial cells. *Diabetes*. 53:3209-3216.

Staiger, K., H. Staiger, C. Weigert, C. Haas, H.U. Haring, and M. Kellerer. 2006. Saturated, but not unsaturated, fatty acids induce apoptosis of human coronary artery endothelial cells via nuclear factor-kappaB activation. *Diabetes*. 55:3121-3126.

Steinberg, H.O., H. Chaker, R. Leaming, A. Johnson, G. Brechtel, and A.D. Baron. 1996. Obesity/insulin resistance is associated with endothelial dysfunction. Implications for the syndrome of insulin resistance. *The Journal of clinical investigation*. 97:2601-2610.

Sundaresan, N.R., S.A. Samant, V.B. Pillai, S.B. Rajamohan, and M.P. Gupta. 2008. SIRT3 is a stress-responsive deacetylase in cardiomyocytes that protects cells from stress-mediated cell death by deacetylation of Ku70. *Molecular and cellular biology*. 28:6384-6401.

Talayero, B.G., and F.M. Sacks. 2011. The role of triglycerides in atherosclerosis. *Current cardiology reports*. 13:544-552.

Tanner, K.G., J. Landry, R. Sternglanz, and J.M. Denu. 2000. Silent information regulator 2 family of NAD- dependent histone/protein deacetylases generates a unique product, 1-O-acetyl-ADP-ribose. *Proceedings of the National Academy of Sciences of the United States of America*. 97:14178-14182.

Tanno, M., J. Sakamoto, T. Miura, K. Shimamoto, and Y. Horio. 2007. Nucleocytoplasmic shuttling of the NAD+-dependent histone deacetylase SIRT1. *The Journal of biological chemistry*. 282:6823-6832.

Teodorescu, V.J., A.K. Vavra, and M.R. Kibbe. 2013. Peripheral arterial disease in women. *Journal of vascular surgery*. 57:18S-26S.

Thangaraju, M., G.A. Cresci, K. Liu, S. Ananth, J.P. Gnanaprakasam, D.D. Browning, J.D. Mellinger, S.B. Smith, G.J. Digby, N.A. Lambert, P.D. Prasad, and V. Ganapathy. 2009. GPR109A is a G-protein-coupled receptor for the bacterial fermentation product butyrate and functions as a tumor suppressor in colon. *Cancer research*. 69:2826-2832.

Tunaru, S., J. Kero, A. Schaub, C. Wufka, A. Blaukat, K. Pfeffer, and S. Offermanns. 2003. PUMA-G and HM74 are receptors for nicotinic acid and mediate its anti-lipolytic effect. *Nature medicine*. 9:352-355.

Unger, R.H., and P.E. Scherer. 2010. Gluttony, sloth and the metabolic syndrome: a roadmap to lipotoxicity. *Trends in endocrinology and metabolism: TEM*. 21:345-352.

van der Veer, E., C. Ho, C. O'Neil, N. Barbosa, R. Scott, S.P. Cregan, and J.G. Pickering. 2007. Extension of human cell lifespan by nicotinamide phosphoribosyltransferase. *The Journal of biological chemistry*. 282:10841-10845.

van der Veer, E., Z. Nong, C. O'Neil, B. Urquhart, D. Freeman, and J.G. Pickering. 2005. Pre-B-cell colony-enhancing factor regulates NAD+-dependent protein deacetylase activity and promotes vascular smooth muscle cell maturation. *Circulation research*. 97:25-34.

VanderLaan, P.A., C.A. Reardon, and G.S. Getz. 2004. Site specificity of atherosclerosis: site-selective responses to atherosclerotic modulators. *Arteriosclerosis, thrombosis, and vascular biology*. 24:12-22.

Vaquero, A., M.B. Scher, D.H. Lee, A. Sutton, H.L. Cheng, F.W. Alt, L. Serrano, R. Sternglanz, and D. Reinberg. 2006. SirT2 is a histone deacetylase with preference for histone H4 Lys 16 during mitosis. *Genes & development*. 20:1256-1261.

Vaziri, H., S.K. Dessain, E. Ng Eaton, S.I. Imai, R.A. Frye, T.K. Pandita, L. Guarente, and R.A. Weinberg. 2001. hSIR2(SIRT1) functions as an NAD-dependent p53 deacetylase. *Cell*. 107:149-159.

Vecka, M., M. Dusejovska, B. Stankova, M. Zeman, L. Vavrova, J. Kodydkova, A. Slaby, and A. Zak. 2012. N-3 polyunsaturated fatty acids in the treatment of atherogenic dyslipidemia. *Neuro endocrinology letters*. 33 Suppl 2:87-92.

Verma, S., M.R. Buchanan, and T.J. Anderson. 2003. Endothelial function testing as a biomarker of vascular disease. *Circulation*. 108:2054-2059.

Villines, T.C., A.S. Kim, R.S. Gore, and A.J. Taylor. 2012. Niacin: the evidence, clinical use, and future directions. *Current atherosclerosis reports*. 14:49-59.

Vucenik, I., and J.P. Stains. 2012. Obesity and cancer risk: evidence, mechanisms, and recommendations. *Annals of the New York Academy of Sciences*. 1271:37-43.

Wang, C., L. Chen, X. Hou, Z. Li, N. Kabra, Y. Ma, S. Nemoto, T. Finkel, W. Gu, W.D. Cress, and J. Chen. 2006. Interactions between E2F1 and SirT1 regulate apoptotic response to DNA damage. *Nature cell biology*. 8:1025-1031.

Wang, C.Y., H.H. Kim, Y. Hiroi, N. Sawada, S. Salomone, L.E. Benjamin, K. Walsh, M.A. Moskowitz, and J.K. Liao. 2009. Obesity increases vascular senescence and susceptibility to ischemic injury through chronic activation of Akt and mTOR. *Science signaling*. 2:ra11.

Widlansky, M.E., N. Gokce, J.F. Keaney, Jr., and J.A. Vita. 2003. The clinical implications of endothelial dysfunction. *Journal of the American College of Cardiology*. 42:1149-1160.

Wise, A., S.M. Foord, N.J. Fraser, A.A. Barnes, N. Elshourbagy, M. Eilert, D.M. Ignar, P.R. Murdock, K. Steplewski, A. Green, A.J. Brown, S.J. Dowell, P.G. Szekeres, D.G. Hassall, F.H. Marshall, S. Wilson, and N.B. Pike. 2003. Molecular identification of high and low affinity receptors for nicotinic acid. *The Journal of biological chemistry*. 278:9869-9874.

Witherow, D.S., T.R. Garrison, W.E. Miller, and R.J. Lefkowitz. 2004. beta-Arrestin inhibits NF-kappaB activity by means of its interaction with the NF-kappaB inhibitor IkappaBalpha. *Proceedings of the National Academy of Sciences of the United States of America*. 101:8603-8607.

Wu, B.J., L. Yan, F. Charlton, P. Witting, P.J. Barter, and K.A. Rye. 2010. Evidence that niacin inhibits acute vascular inflammation and improves endothelial dysfunction

independent of changes in plasma lipids. *Arteriosclerosis, thrombosis, and vascular biology*. 30:968-975.

Xiao-Yun, X., C. Zhuo-Xiong, L. Min-Xiang, H. Xingxuan, E.H. Schuchman, L. Feng, X. Han-Song, and L. An-Hua. 2009. Ceramide mediates inhibition of the AKT/eNOS signaling pathway by palmitate in human vascular endothelial cells. *Medical science monitor : international medical journal of experimental and clinical research*. 15:BR254-261.

Xu, J., and M.H. Zou. 2009. Molecular insights and therapeutic targets for diabetic endothelial dysfunction. *Circulation*. 120:1266-1286.

Yamamoto, H., K. Schoonjans, and J. Auwerx. 2007. Sirtuin functions in health and disease. *Molecular endocrinology*. 21:1745-1755.

Yang, H., T. Yang, J.A. Baur, E. Perez, T. Matsui, J.J. Carmona, D.W. Lamming, N.C. Souza-Pinto, V.A. Bohr, A. Rosenzweig, R. de Cabo, A.A. Sauve, and D.A. Sinclair. 2007. Nutrient-sensitive mitochondrial NAD+ levels dictate cell survival. *Cell*. 130:1095-1107.

Yasu, T., M. Kobayashi, A. Mutoh, K. Yamakawa, S. Momomura, and S. Ueda. 2013. Dihydropyridine calcium channel blockers inhibit non-esterified-fatty-acid-induced endothelial and rheological dysfunction. *Clinical science*. 125:247-255.

Yoshino, J., K.F. Mills, M.J. Yoon, and S. Imai. 2011. Nicotinamide mononucleotide, a key NAD(+) intermediate, treats the pathophysiology of diet- and age-induced diabetes in mice. *Cell metabolism*. 14:528-536.

Yousefi, S., P.R. Cooper, B. Mueck, S.L. Potter, and G. Jarai. 2000. cDNA representational difference analysis of human neutrophils stimulated by GM-CSF. *Biochemical and biophysical research communications*. 277:401-409.

Yu, W., H. Chai, Y. Li, H. Zhao, X. Xie, H. Zheng, C. Wang, X. Wang, G. Yang, X. Cai, J.R. Falck, and J. Yang. 2012. Increased expression of CYP4Z1 promotes tumor angiogenesis and growth in human breast cancer. *Toxicology and applied pharmacology*. 264:73-83.

Zhuo, Q., W. Yang, J. Chen, and Y. Wang. 2012. Metabolic syndrome meets osteoarthritis. *Nature reviews. Rheumatology*. 8:729-737.

Zollner, A., C.A. Dragan, D. Pistorius, R. Muller, H.B. Bode, F.T. Peters, H.H. Maurer, and M. Bureik. 2009. Human CYP4Z1 catalyzes the in-chain hydroxylation of lauric acid and myristic acid. *Biological chemistry*. 390:313-317.

Curriculum Vitae

JENNIFER HUGHES-LARGE

EDUCATION

September 2011 - Present	MSc Candidate, Physiology Western University London, Ontario, Canada
September 2007 - April 2011	BMSc, Honours Physiology Western University London, Ontario, Canada

ACADEMIC AWARDS

2011- 2013	Western Graduate Research Scholarship
2011/2012	Graduate Thesis Research Award
2007	Western University Scholarship of Excellence

PUBLICATIONS

Bell GI, Meschino MT, **Hughes-Large JM**, Broughton HC, Xenocostas A, Hess DA. Combinatorial human progenitor cell transplantation optimizes islet regeneration through secretion of paracrine factors. Stem Cells and Development (2012) Jul 20; 21(11):1863-76. [Published]

Bell GI, Putman DM, **Hughes-Large JM**, Hess DA. Intra-pancreatic delivery of human umbilical cord blood aldehyde dehydrogenase-producing cells promotes islet regeneration. Diabetologia (2012) Jun; 55(6):1755-60. [Published]

PRESENTATIONS & CONFERENCES

Hughes-Large J, Chan P, Robson D, Borradaile NM. NAD+ biosynthetic precursors improve human vascular endothelial cell angiogenic function during fatty acid overload. Physiology and Pharmacology Research Day. Western University. November 6, 2012. [poster]

Hughes-Large J, Chan P, Robson D, Borradaile NM. NAD+ biosynthetic precursors improve human vascular endothelial cell angiogenic function during fatty acid overload. Frontiers in Lipid Biology. Banff, Alberta. September 6-9, 2012. [poster]

TEACHING EXPERIENCE

September 2011- April 2013	Teaching Assistant Western University, London, ON Department of Physiology and Pharmacology *Physiology 3130Y*